Development of new tools and germplasms for improvement of wheat resistance to *Fusarium* head blight

by

Yaoguang Li

B.E., Anyang Institute of Technology, 2013
M.S., Henan Agricultural University, 2016

AN ABSTRACT OF A DISSERTATION

submitted in partial fulfillment of the requirements for the degree

DOCTOR OF PHILOSOPHY

Department of Agronomy
College of Agriculture

KANSAS STATE UNIVERSITY
Manhattan, Kansas

2019

Abstract

Wheat *Fusarium* head blight (FHB) is a devastating disease of wheat worldwide, which can significantly reduce grain yield and quality. Although the application of fungicides can reduce FHB damage, growing FHB resistant wheat is the most effective and eco-friendly approach to reduce the losses. To develop locally adapted FHB-resistant hard winter wheat germplasm, we transferred three major QTLs: *Fhb1*, *Qfhs.ifa-5A*, and *Qfhb.rwg-5A.2* into two hard winter wheat cultivars, 'Everest' and 'Overland', using marker-assisted backcrossing and multiplex restriction amplicon sequencing (MRASeq). Ten 'Overland' background lines and nine 'Everest' background lines with better FHB resistance, recurrent parent similar agronomic traits were selected. They can be used as FHB resistant bridge parents for hard winter wheat breeding. To identify native FHB resistant sources, a population of 201 U.S. breeding lines and cultivars were genotyped using 90K wheat SNP arrays and phenotyped for the percentage of symptomatic spikelets (PSS), *Fusarium* damaged kernels (FDK) and deoxynivalenol (DON), a toxin produced by the pathogen. Genome-wide association studies (GWAS) identified significant trait associations with single nucleotide polymorphisms (SNPs) on chromosomes 1A, 1D, 2B, 3A, 3B, 4A, 5B and 5D. These marker-trait associations (MTAs) were significant for at least two of the three traits or a single trait in at least two experiments. To accelerate the evaluation of the FDK, we developed an algorithm that can separate FDK from healthy kernels with an accuracy of 90% based on color differences using image processing and unsupervised machine learning methods. Discovery and creation of the new FHB resistant germplasms and development of the fast FDK phenotyping algorithm will accelerate the improvement of U.S. hard winter wheat cultivars for FHB resistance.

Development of new tools and germplasms for improvement of wheat resistance to *Fusarium* head blight

by

Yaoguang Li

B.E., Anyang Institute of Technology, 2013
M.S., Henan Agricultural University, 2016

A DISSERTATION

submitted in partial fulfillment of the requirements for the degree

DOCTOR OF PHILOSOPHY

Department of Agronomy
College of Agriculture

KANSAS STATE UNIVERSITY
Manhattan, Kansas

2019

Approved by:

Co-Major Professor
Dr. Guihua Bai

Approved by:

Co-Major Professor
Dr. Xiaomao Lin

Copyright

Abstract

Wheat *Fusarium* head blight (FHB) is a devastating disease of wheat worldwide, which can significantly reduce grain yield and quality. Although the application of fungicides can reduce FHB damage, growing FHB resistant wheat is the most effective and eco-friendly approach to reduce the losses. To develop locally adapted FHB-resistant hard winter wheat germplasm, we transferred three major QTLs: *Fhb1*, *Qfhs.ifa-5A*, and *Qfhb.rwg-5A.2* into two hard winter wheat cultivars, 'Everest' and 'Overland', using marker-assisted backcrossing and multiplex restriction amplicon sequencing (MRASeq). Ten 'Overland' background lines and nine 'Everest' background lines with better FHB resistance, recurrent parent similar agronomic traits were selected. They can be used as FHB resistant bridge parents for hard winter wheat breeding. To identify native FHB resistant sources, a population of 201 U.S. breeding lines and cultivars were genotyped using 90K wheat SNP arrays and phenotyped for the percentage of symptomatic spikelets (PSS), *Fusarium* damaged kernels (FDK) and deoxynivalenol (DON), a toxin produced by the pathogen. Genome-wide association studies (GWAS) identified significant trait associations with single nucleotide polymorphisms (SNPs) on chromosomes 1A, 1D, 2B, 3A, 3B, 4A, 5B and 5D. These marker-trait associations (MTAs) were significant for at least two of the three traits or a single trait in at least two experiments. To accelerate the evaluation of the FDK, we developed an algorithm that can separate FDK from healthy kernels with an accuracy of 90% based on color differences using image processing and unsupervised machine learning methods. Discovery and creation of the new FHB resistant germplasms and development of the fast FDK phenotyping algorithm will accelerate the improvement of U.S. hard winter wheat cultivars for FHB resistance.

Table of Contents

List of Figures

List of Tables

Acknowledgments

To the nine-year-old girl, who never gives up herself.

I would like to thank my co-major professor Dr. Guihua Bai, who provided me the opportunity to join his lab and supported me for all these years with his patience, motivations, and endless encouragements. I would like to thank my co-major professor Dr. Xiaomao Lin, thesis committee members Dr. Jesse Poland and Dr. Geoffrey Morris, and the outside chair Dr. Carolyn J. Ferguson, without them, I would never have a chance to explore the fantastic new world of wheat genetics, genomics and breeding research.

I would like to thank all the members in our lab, Dr. Paul St. Amand, Dr. Amy Bernardo, Dr. Hui Chen, Dr. Yunfeng Xu, Dr. Zhao Liu, Dr. Lanfei Zhao, Dr. Meng Lin, Dr. Yue Lu, Dr. Jin Cai, Dr. Minqin Shao and Dr. Dadong Zhang, graduate students Ms. Ruolin Bian, Ms. Nida Ghori, Mr. Yuzhou Xu, Mr. Abdulrahman Hashimi and other former members, without their supports, I would never finish all these projects.

I would like to thank my friends, Dr. Katherine Jordan, Ms. Laura Constance, Mr. Jun Huang, Dr. Jianan Wang, Dr. Zhenbin Hu, Ms. Qianli Pan, Ms. Ying Jie, Mr. Hao Zhang, and all other friends in the U.S. and in China, without them, I would never manage my life and work in Manhattan during these years.

I would like to thank my mother Ms. Qiuzhen Du, my father Mr. Fei Li, my husband Dr. Xian Wu and all my family members, without them, I would never be able to see the wonderful world.

I appreciate all the people who loved and helped me all these years from my heart and soul; without you, I would never be who I am today. I love you all.

Chapter 1 - Literature Review

Importance and origin of wheat

Wheat (*Triticum aestivum*) is one of the most important crops and the largest food commodity in the world (FAO, 2013). Wheat provides about 19% of human-available calories globally (Ray et al., 2013), and considered as one of the excellent sources for protein, fiber, and other nutrients (Šramková et al., 2009). About 2.5 billion people consume wheat all around the world as a staple food. Among different types of wheat, bread wheat is the most consumed daily (IWGSC, 2014). The top five wheat-producing countries are China, India, Russia, the U.S., and France. In 2017, the U.S. produced about 47 million tons of wheat (FAO STAT, 2019).

Today's wheat has undergone evolution, hybridization, domestication, and modern wheat breeding, which makes modern wheat become one of the most valuable cereal crops (Nesbitt, 2001). Wheat's ancestry is traced to wild diploids *Triticum Urartu.* Although the and B genome ancestry of B genome remains to be determined, Aegilops speltoides (or a closest extant species of is likely the B genome donor) (Shewry, 2009). When wild species T. urartu hybridized naturally with A. speltoidesthe B genome ancestor, a wild tetraploid T. turgidum was produced with AABB genome and was later domesticated as cultivated Emmer wheat (Matsuoka, 2011). About 10,000 years ago in the Fertile Crescent region, another natural hybridization occurred between tetraploid T. turgidum and T. tauschii (DD) that generated allohexaploid bread wheat (T. aestivum) with A, B and D genomes.

Wheat was estimated to be domesticated 10,000 years ago in the Near-Eastern Fertile Crescent (Matsuoka, 2011; Gustafson et al., 2009; Avni et al., 2017; Piperno et al., 2004). The primary domestication traits in bread wheat include free-threshing, non-shattering, and high yielding. Since the domestication of common wheat, it has spread across the world (Dubcovsky

and Dvorak, 2007). Massive wheat cultivation mainly started in the U.S. in the 16th century during the colonial period, although it was first introduced to the New World in the 15th century (Lupton, 1987; Bell, 1987).

Wheat production and classification in the U.S.

Currently, wheat is planted on more than 18.62 million hectares every year in almost all states in the U.S., with an average yield about 31 metric tons per hectare in the last decade (USDA Wheat Data, 2019 https://www.ers.usda.gov/data-products/wheat-data/). In the U.S., wheat is classified into six classes according to their seed color, hardness, and growth habit, including one tetraploid durum wheat used mainly for pasta, and five hexaploid wheat classes used mainly for bread and other products. These five bread wheat classes are hard red winter (HRW), hard red spring (HRS), soft red winter (SRW), soft white (SW) and hard white (HW) (Vocke and Ali, 2013; U.S. wheat associates https://www.uswheat.org/working-with-buyers/wheat-classes/).

The six classes of wheat are primarily planted in different regions across the states for divergent end-use purposes (Gwirtz et al., 2007). HRW is mainly grown in Montana, South Dakota, Nebraska, Kansas, Oklahoma, Texas, and Colorado, and is known for good milling and baking quality in the U.S. bun production. HRS is grown mostly in the northern Great Plains area such as Minnesota, North Dakota, South Dakota, but also in Pacific Northwest area including Montana, Idaho and Washington. HRS has a high protein content, as well as good milling and baking quality. HW is used in yeast bread, flatbread and noodles, and grown in Kansas, Idaho, Montana, and California and has no subclass designation for different growing seasons. SRW can be found from Missouri to the east coast, and used for crackers, flatbread, noodles, cakes, and other pastries. SW is primarily grown in Washington, Oregon, and Idaho with a similar end-

use as SRW. Although there are spring and winter varieties for SW, it is not classified by growing season. Durum wheat is generally grown in North Dakota and Montana and used for pasta products (Gwirtz et al., 2007; U.S. wheat associates https://www.uswheat.org/working-with-buyers/wheat-classes/). Kansas is one of the largest wheat-producing states in the U.S. for many years. Wheat production in Kansas originally started by the Mennonites, who brought in a hard winter wheat 'Turkey Red' to Kansas farming field. In 2018, about 3.12 million hectares of wheat were planted in Kansas with a total production of 75,386 metric tons (USDA, 2018 https://www.nass.usda.gov/Quick_Stats/Ag_Overview/stateOverview.php?state=KANSAS).

To continuously produce high quality and yielding wheat, use of new wheat cultivars that adapt growing environments is critical (Battenfield et al., 2016; Asseng, 2015; Figueroa et al., 2017; Tabatabaeefar et al., 2009; Zwart and Bastiaanssen, 2004). Dedicated breeders continuously release numerous genetically improved new cultivars for production. In Kansas, wheat breeding started in 1863 by J.S. Hougham (Paulsen, 2001). Since then, breeders have continued releasing high yielding and adapted wheat varieties to growers such as 'Pawnee', 'Wichita', 'Jagger' and 'Everest'. These Kansas wheat cultivars were bred for stable high grain yield and quality, disease and insect resistance, and tolerance to abiotic stresses (Paulsen, 2001). Besides using new improved cultivars, other cultural practices such as applications of herbicides, fungicides, insecticides, and other field management strategies also have been used to improve wheat production (Bergtold et al., 2014). However, plant diseases still caused severe yield and quality losses for wheat growers in the past, thus have been a major obstacle for breeders to overcome (Taheri, 2018).

Wheat *Fusarium* head blight (FHB)

Fusarium head blight (FHB) is a devastating fungal disease for cereal crops worldwide, including bread wheat, barley, and durum wheat (Bai and Shaner 1994; Dweba et al., 2017). In the U.S., FHB is mainly caused by *Fusarium graminearum* Schw. (Bai and Shaner, 2004). *F. graminearum* survives on plant residues of small grain crops under favorable weather conditions (> 90% RH; 59-86 °F), and form spores to start a new disease cycle. Spores travel from the ground to wheat spikes in a field by airflow or water splashes. Wheat spikes are susceptible from the early flowering stage (Feeks 10.5.1) to the soft dough stage (Feeks 11.2) under the warm and humid weather condition. If the injection happens just after the florets' emergence, infected spikelets produce no seeds, or the florets can produce tombstone kernels if the disease occurs later (Naroei and Salari, 2015; McMullen et al., 2012).

FHB can cause not only significant reductions in wheat grain yield, but also a reduction in grain quality (Giancaspro et al., 2016). The FHB infected grains are called *Fusarium* damaged kernels (FDK) which are much lighter in weight than the healthy ones. FDK usually have a pale color, sometimes with pinkish spots on the surface (Malihipour et al., 2016). More importantly, FDK is always contaminated with mycotoxins, especially deoxynivalenol (DON), which is regarded as the most impacted mycotoxin produced by the fungus *F. graminearum* (Jin et al., 2014). DON is stable in high temperatures, which makes it harder to reduce the content during the food and feed processing (Manthey et al., 2004). For livestock, DON provokes the animal to refuse to eat the feed and induces weight loss, which not only slows down animal growth but also lower the quality of animal products. Human consumption of DON can result in immunological and teratogenic problems and may be associated with the symptoms of severe vomiting and diarrhea etc. (Sobrova et al., 2010; McMullen et al., 2012). Many countries,

including the U.S., have maximum thresholds for DON content allowed in food and feed. The Food and Drug Administration (FDA) in the U.S. currently has set the maximum allowed DON level as 1 part per million (ppm) for human consumed products, 10 ppm in feed for cattle older than 4 months, 10 ppm for poultry feed, and 5 ppm for the feed of swine and all other animals (Sobrova et al., 2010; Giménez et al., 2013; Maresca, 2013).

To reduce the loss associated with the disease, many FHB control strategies have been reported, including biological and chemical control, genetic control using host plant resistance, and other cultural practices. The most promising one is the genetic control using host resistance because this method is more environmentally friendly, durable, and easier for growers to manage. (Petersen et al., 2017; Shah et al., 2017; Bai et al., 2018).

Host resistance to FHB can be divided into five different types: Type I, resistance to initial infection, which prevents the pathogen from infecting the florets of plants. Type II, resistance to spread of FHB symptoms within a spike, which prevents the disease from spreading from the initially infected spikelet to others within a spike. Type III, resistance to kernel infection with low FDK. Type IV, tolerance to FHB, which means the yield and quality reduction is still limited even plants are infected by the fungus. Type V, resistance to DON accumulation, in which infected plants have a low level of DON content in the grains (Dweba et al., 2017; Cai, 2016). Among them, Type II resistance is the major type of resistance where researchers have been focused since it is easier to access in the greenhouse experiments and less affected by environments (Bai and Shaner, 2004).

Quantitative trait locus (QTL) for FHB resistance in wheat

Although the host resistance is the most economically effective and environmentally friendly measure for FHB control, wheat cultivars that are entirely immune to the FHB pathogen

have not been found to date (Bai et al., 2018). FHB resistance is a quantitative trait controlled by several major quantitative trait locus (QTL) and some minor QTLs (Cai, 2016). Over the last three decades, numerous researchers have been working on identifying QTLs for FHB resistance in wheat, which has resulted in the discovery of more than 150 QTLs with varied effects on all the wheat chromosomes (Bai et al., 2018; Buerstmayr et al., 2009). Nearly 100 QTLs in 52 papers have been reviewed previously (Buerstmayr et al., 2009). A list of QTLs that have been reported since 2009 in different wheat populations can be found in Table 1.1. Most of the FHB resistance QTLs have been mapped using bi-parental populations for single or combinations of several FHB related traits, including FHB incidence, FDK value and DON content (Bai et al., 2018; Clark et al., 2016; McCartney et al., 2007).

Fhb1 on chromosome arm 3BS from the Chinese cultivars 'Ning7840' and 'Sumai3' was the first mapped QTL for FHB resistance and was validated in several subsequent studies (Waldron et al., 1999; Bai et al., 1999; Anderson et al., 2001; Yang et al., 2005; Liu et al., 2006; Zhou et al., 2002). *Fhb1* is the most widely deployed FHB resistance QTL because it consistently shows moderate to high resistance to a broad spectrum of *Fusarium* in various genetic backgrounds (Bernardo et al., 2014; Brown-Guedira et al., 2008; Lu et al., 2011; Xie et al., 2007).

Since the QTL was mapped, the *Fhb1* gene has been the focus of many wheat researchers and breeders (Cuthbert et al., 2006; Pumphrey et al., 2007; Rawat et al., 2016; Li et al., 2019; Su et al., 2019). Genetic mapping studies identified two flanking markers, Xgwm533 and Xgwm493, for *Fhb1* in 'Sumai 3' related populations, which have been used routinely for marker-assisted selection (MAS) in breeding programs for over a decade (Cuthbert et al., 2006). More recently, a candidate gene for *Fhb1* has been reported (Su et al., 2019; Li et al., 2019), and

diagnostic markers were developed for using in breeding programs (Su et al., 2018). To date, *Fhb1* is the only cloned FHB resistance gene with diagnostic markers.

Several hypotheses on *Fhb1* functions have been proposed to explain the Type II resistance mechanisms (Chrispeels et al., 2007; Rawat et al., 2016; Li et al., 2019; Su et al., 2019). The latest prevailing ones are: 1) that the *Fhb1* gene is a histidine-rich calcium-binding-protein gene (*TaHRC*), which is a susceptible factor for FHB in wheat. A large sequence deletion in the *TaHRC* removes the start codon and in turn reduces the susceptibility by disrupting proper *TaHRC* protein function (Su et al., 2019). 2) The large fragment deletion in *TaHRC* creates a new start codon in the upstream region, which results in new functional alleles for FHB resistance (Li et al., 2019). Currently, convincing evidence is still needed to determine the function and related pathways of the *TaHRC* to fully understand the mechanism of FHB Type II resistance in wheat (He et al., 2018; Lagudah and Krattinger, 2019).

In addition to *Fhb1*, several other QTLs for FHB resistance with relatively large effects were named including *Fhb2* to *Fhb7* (Cainong et al., 2015; Cuthbert et al., 2007; Guo et al., 2015; Xue et al., 2011; Qi et al., 2008; Xue et al., 2010). *Fhb2* was reported on chromosome 6B and explained about 21% of the phenotypic variation in a mapping population (Yang et al., 2003). Genes related to the cell wall reinforcement and DON detoxification were reported in the *Fhb2* QTL region (Dhokane et al., 2016). *Fhb4* and *Fhb5* were reported to show Type I resistance in wheat. *Fhb4* is flanked by the markers Xhbg226 and Xgwm149 in a Chinese germplasm 'Wangshuibai'. The near isogenic line (NIL) carrying *Fhb4* had 60% higher resistance than the susceptible NIL (Xue et al., 2010). *Fhb5*, located on chromosome 5AS is another Type I resistance QTL from 'Wangshuibai', and is flanked by the markers Xgwm304

and Xgwm415. The resistant NIL showed nearly 55% less infection (Xue et al., 2011) than in the susceptible NIL.

Fhb3, *Fhb6,* and *Fhb7* are three resistance QTLs from alien species that were transferred into wheat backgrounds (Bai et al., 2018). *Fhb3* was identified in *Leymus racemosus* and has been transferred onto the wheat 7AL chromosome as a Robertsonian translocation T7AL·7Lr#1S wheat line (Qi et al., 2008). *Fhb6* is from *Elymus tsukushiensis* and was transferred to the sub-terminal region (1Ets#1S of *Elymus tsukushiensis*) of 1AS and showed high resistance with 7% disease severity (Cainong et al., 2015). *Fhb7* is derived from *Thinopyrum ponticum* and transferred through 7DS.7el$_2$L Robertsonian translocation. *Fhb7* is flanked by markers XsdauK66 and Xcfa2240 and explains about 15-32.5% of phenotypic variances for FHB resistance (Guo et al., 2015).

Besides these QTLs, several other QTLs with relatively large effects have also been reported in recent studies. For example, QTLs on long arms of wheat chromosome 5A was reported to show high FHB resistance (Chu et al., 2011). The *Qfhb.rwg-5A.2* on 5AL explained up to 30% of the phenotypic variance for Type II resistance. In addition, durum wheat containing the *Qfhb.rwg-5A.2* demonstrated enhanced resistance to FHB (Zhao et al., 2018).

Conventional breeding for wheat FHB resistance

Since the first report of FHB in 1884, wheat geneticists and breeders have devoted their efforts to develop FHB resistant cultivars (McCartney et al., 2007; McCartney et al., 2004; Steiner et al., 2017; Weguloet al., 2015). Conventional or classical breeding uses Mendelian principles to create variations and select the progenies with desired traits from segregating populations (Acquaah, 2015). Conventional plant breeding programs apply biparental crossing, backcrossing, or top crossing to create segregation populations, single seed descent to advance

progeny, bulk, pedigree, mass, systematic, or recurrent selection methods to select desired genotypes from segregation populations under specific environments to develop new cultivars (Caligari et al., 2001; Mwadzingeni et al., 2016). Most of these classical methods have been successfully applied in wheat FHB resistance breeding programs. Direct phenotypic selection under constant high disease pressure has proven to be critical for FHB resistance cultivar development (Miedaner, 2016; Ma et al., 2008; Rudd et al., 2001).

Using classical breeding, several FHB resistant wheat cultivars have been developed (Mesterházy et al., 1997, 2002; Mergoum et al., 2007; Ma et al., 2008). The FHB resistant cultivar 'Sumai 3' was a good example. 'Sumai 3' was selected from 'Taiwanxiaomai' × 'Funo' using direct phenotypic selection and have been used as FHB resistant parents in several Chinese resistant cultivars including 'Ning 7840' (Bai and Shaner, 1994). Breeders in Hungary then crossed European adapted susceptible lines to resistant lines from Asia. After selecting the progenies with low or no FDK, they have selected several FHB resistant lines that were used in Hungary and the neighboring countries (Mesterházy et al., 1997, 2002). Similarly, North Dakota State University also extensively screened the progenies from crosses between the Asian resistant line 'Sumai3' and locally adapted germplasms for FHB resistance and obtained several FHB resistant hard red spring wheat cultivars (Mergoum et al., 2007). However, classical breeding methods are usually time and labor-consuming and a new cultivar from crossing to cultivar release usually needs ten years.

Modern breeding for wheat FHB resistance

Modern crop breeding techniques add tissue culture and chromosome engineering to transfer desired genes from alien species. Genetic/genomic engineering, proteomics and metabolomics are applied to manipulate specific genes of interest. Marker assisted selection,

genomic selection plus double haploid technique are applied for quick selection of individual or genome-wide beneficial genes/traits or genetic backgrounds to shorten breeding cycles and increase selection efficiency. And bioinformatics, phenomics assist with high-throughput data analysis. All those new breeding technologies can accelerate the genetic gain in a breeding program (Cabrera et al., 2014; Nadeem et al., 2018; Semagn et al., 2006; Tardieu et al., 2017; Xu et al., 2017; Schrag et al., 2018).

Among these modern breeding techniques, molecular markers have wider applications in different breeding programs (Caligari et al., 2001). Generally, there are two types of markers: classical (morphological markers, cytological markers, and biochemical markers) and molecular markers (DNA markers). Genetic markers can be used in studying genetic architecture and diversity of populations, uncovering the domestication of a crop, and helping breeders understand the genetic relationship among plant materials they work with (Varshney et al., 2005, Khan et al., 2014; Rasheed et al., 2017). Genetic markers are also essential for QTL mapping and genome-wide association studies (GWAS), which allows researchers to find genes underlying traits of interests, ultimately assisting breeders in finding and using target genetic variations to breed new varieties (Simons et al., 2006). Specifically, using the marker information, breeders can select the best lines for crossing to improve their parental pools, as well as selecting desired progenies (Semagn et al., 2014; Talukder and Saha, 2017; Varshney et al., 2016). Currently many marker platforms are available (Table 1.2), but the most frequently used marker systems in breeding programs are single nucleotide polymorphism (SNP) and simple sequence repeats (SSR) markers. SSR markers played major role for MAS in last two decades, while SNP is a popular markers platform for breeding currently due to low cost of next generation sequencing

(NGS) technologies for SNP genotyping (Collard and Mackill, 2008; Khan et al., 2014; Nadeem et al., 2018; Thomson, 2014; Varshney et al., 2016).

Using modern breeding methods to breed FHB resistant wheat, genetic markers can be applied in marker-assisted selection (MAS) for transferring novel QTLs into adapted wheat cultivars, and in genomic selection (GS) for genome-wide selections of multiple small effect loci (Eckard et al., 2015; Steiner et al., 2017). Marker-assisted breeding (MAB) uses markers that are tightly linked to QTLs of breeders' interest in breeding processes (Johnson, 2003, Shah et al., 2017) and include: i) fingerprinting breeding materials, ii) marker-assisted backcrossing, iii) pyramiding different genes in one germplasm line or cultivar, iv) early generation selection, and v) genomic selection (Collard et al., 2008; Nadeem et al., 2017). For wheat FHB resistance breeding, several groups around the world have utilized MAB to introduce resistance QTLs into locally adapted lines (Miedaner et al., 2005; McCartney et al., 2007; Guo et al., 2015; Bai et al., 2018). A European group introduced two QTLs from 'CM82036' and one QTL from 'Frontana' into European elite spring wheat lines, which reduced both DON content and FHB severity in the progenies (Miedaner et al., 2005). A Canadian team has transferred different FHB resistance QTLs into three BC_2 populations to evaluate the effects of FHB resistance in elite Canadian lines. They found that the resistance tended to increase with the number of favorable alleles introduced into the lines (McCartney et al., 2007).

Because most of the resistance sources with major QTLs are from China or Japan, it has been hard to transfer these major resistance QTLs from the Asian sources to U.S. adapted backgrounds due to undesired linkage drag in these Asian sources. However, using the marker-assisted backcrossing, resistance QTLs can be transferred to U.S. adapted backgrounds with reduced linkage drag with these undesired traits to develop locally adapted bridge parents. These

bridge parents can then be used as resistant parents in breeding programs. In this way, the resistance QTLs from China and Japan can be easily applied to breed FHB resistant U.S. winter wheat lines (Guo et al., 2015; Bai et al., 2018).

Since FHB resistance is a quantitative trait controlled by multiple genes, researchers are trying to combine multiple genes to increase the FHB resistance through gene pyramiding, which is a useful breeding strategy for quantitative trait improvement in crops (Collard et al., 2008; Kumar et al., 2010; Servin et al., 2004; Tyagi et al., 2014). Gene pyramiding can employ marker-assisted backcrossing to stack the desired QTLs or genes from one or more donor parents into an adapted recurrent parent. Gene pyramiding in general consists of three steps: the selection of donor and recurrent parents, crossing and backcrossing donors to the recurrent parent by the aid of markers, and then selecting homozygous lines with desired alleles (Joshi et al., 2010). For FHB resistance, a group of researchers successfully pyramided resistance QTLs from 'Sumai 3', 'Wangshuibai' and 'Nobeokabouzu' and obtained lines with high Type II resistance (Shi et al., 2008).

For gene pyramiding, background selection in each backcross can significantly reduce the number of backcrossing generations and quickly recover the genome of the recurrent parents (Gopalakrishnan et al., 2008; Leonova, 2013). Using marker-assisted background selection, more than 97% of the recurrent parent genome can be recovered in only two backcrosses, which significantly shortens the breeding cycle, resulting in new favorable germplasms within 5 years (Randhawa et al., 2009). However, background selection needs to use genome-wide markers, which significantly increases the cost. Currently the fast development of next-generation sequencing (NGS) technologies can significantly reduce the cost of sequencing.

Our lab has developed a genome-wide NGS based high-throughput genotyping platform called Multiplex Restriction Amplicon Sequencing (MRAseq) that can be applied for background selection due to its high-throughput and low cost per sample. MRAseq uses simplified procedures with only two steps of polymerase chain reaction (PCR) for library construction, which simplifies library construction procedure and reduces reagent and lab cost compared to the traditional Genotyping-By-Sequencing (GBS) (Elshire et al., 2011; Bernardo et al., 2019). The first PCR step uses an M13-tailed sequence to pool all amplicons from each sample, and the second PCR uses barcodes to pool different samples for NGS (Bernardo et al., 2019).

Genome-wide association studies (GWAS) for wheat FHB resistance

As previously mentioned, the essential requirement for successful MAS is to have markers that tightly link to the QTLs of the target traits (Gopalakrishnan et al., 2008). Mapping QTLs using segregating bi-parental recombinant inbred line (RIL) populations is one of the widely used strategies, and many QTLs were identified using this strategy (Crisp et al., 1988; Holland, 2007; Xu et al., 2017). However, developing such populations can take years. Also, the limitations in detecting variations beyond the biparental difference encouraged researchers to develop new mapping methods for complex quantitative traits (Pascual et al., 2016; Xu et al., 2017; Borevitz et al., 2003; Korte and Farlow, 2013). In the early 2000s, association mapping using linkage disequilibrium (LD), which is a "nonrandom association of alleles at different loci" (Flint-Garcia et al., 2003), was first applied in human genetics to identify genetic variations associated with diseases, which has been later extended to plants for QTL detection (Hirschhorn and Daly, 2005; Visscher et al., 2012).

A genome-wide association study (GWAS) refers to the analysis of statistical associations between the genome-wide markers and phenotypic data for a target trait in a natural population (Rafalski, 2010).(Bush and Moore, 2012; Rafalski, 2010). SNPs, which can be detected using NGS methods covering the whole genome, are usually the genetic markers representing the genetic variations in genomes for GWAS (Ball, 2013). GWAS may produce two possible outcomes: 1) a direct association in which the SNP is within the causal gene; 2) an indirect association in which the SNP is in LD with the causal gene (Bush and Moore, 2012). Both outcomes can lead to significant associations.

GWAS, which relies on the historical combinations and LD, has some advantages over traditional linkage mapping. A natural population can be assembled as the association panel, and in general, effect sizes are like what can be found in nature. There is no need to build mapping populations which can take many years. Additionally, once the diverse panel is genotyped, multiple traits could be analyzed using the same set of marker data (Korte and Farlow, 2013; Xu et al., 2017; Rafalski, 2010). For these merits, numerous GWAS has been published for more than one decade in various species since the first successful one published in 2002 (Ozaki et al. 2002; Guo et al., 2018; Huang and Han, 2014; Visscher et al., 2017; Zhang et al., 2014; Visscher et al., 2012; Zargar et al., 2015). In the plant studies, GWAS is usually used with association panels that were genotyped with markers generated from high-throughput genotyping platforms for multiple trait analysis to discover the associated genetic variation or regions (Nadeem et al., 2017; Zargar et al., 2015). GWAS has also been adopted to dissect the genetic architecture of the valuable plant traits, and to investigate the evolution of crops (Bevan et al., 2017; Huang and Han, 2014; Wang and Qin, 2017; Wen et al., 2019). Currently, GWAS has been successfully implemented in nearly all important crops, including maize, rice, wheat, sorghum, and soybean

to identify genomic regions for traits of interest, associated markers, and finally candidate genes (Crowell et al., 2016; Han et al., 2018; Lin et al., 2016; Boyles et al., 2016; Wen et al., 2019).

Several GWAS have been conducted for FHB resistance using different diverse panels. For example, a wheat germplasm collection from Central Europe was genotyped using genome-wide microsatellite markers and analyzed for the QTLs for FHB resistance, and significant loci were found on all wheat chromosomes except chromosome 6B (Kollers et al., 2013). In a U.S. wheat population, GWAS was conducted for a collection of 273 winter wheat lines, and multiple SNPs were found to be significantly associated with FHB resistance on chromosomes 4A, 6A, 7A, 1D, 4D, 7D, and 3B (*Fhb1*) (Arruda et al., 2016). Using a collection of spring wheat lines developed in the Pacific Northwest and International Maize and Wheat Improvement Center (CIMMYT), significant SNPs were associated with FHB resistance on chromosomes 1B, 2B, 4B, 5A, 5B, and 6A, with the one on 5B as a novel QTL for DON reduction (Wang et al., 2017). Another study analyzed an association panel from China, Japan, America, France, Russia, Argentina, Brazil, Italy, Austria, Ukraine, and CIMMYT , and found 11 significant markers associated with FHB resistance (Li et al., 2016). More recently, a group in China reported that using GWAS, they found a novel FHB resistance locus in Chinese elite lines for FHB severity and DON content (Wu et al., 2019). These studies reveal the genetic architecture of FHB resistance: 1) resistance QTLs can be identified on all wheat chromosomes, 2) QTLs from different sources may be different, 3) most of QTLs are minor QTLs and such QTLs in the same line may not be repeatedly identified in different environments, or these QTLs have genotype and environment interaction, 4) a few QTLs with a major effect are mainly from Chinese resources (Arruda et al., 2016; Kollers et al., 2013; Löffler et al., 2009; Massman et al., 2011). Since most FHB resistance QTLs show minor effects on FHB resistance, GWAS can be an ideal

tool for identification of these QTLs and linked markers for marker-assisted breeding (Miedaner et al., 2011). Coupled with genomic selection and other genomic technologies, GWAS could be used together with other technologies to increase genetic gain, making precise selections, and shortening breeding cycles in wheat FHB resistance breeding (Arruda et al., 2016; Herter et al., 2018; Silva, 2018).

Technologies for FDK evaluation

Along with genotyping, accurate phenotyping is crucial to detection of wheat FHB resistance QTLs, and selection of FHB resistant cultivars. However, it is not easy to score FHB severity in either laboratory or field, even trained evaluators may give wrong FHB scores of wheat materials because disease pressure may vary among testing environments and human eye gets tired after a long time of visual scoring of field plots (Brown-Guedira et al., 2008; Buerstmayr et al., 2009; Alisaac et al., 2018; Mwadzingeni et al., 2016).

FDK are usually decolorized, shriveled, light-weighted, and can significantly lower the quality of wheat kernel and flour (Wiwart et al., 2001; Hatcher et al., 2003). To evaluate FDK along with other wheat seed traits, several methods and devices including visual assessment, near-infrared and hyperspectral image analysis, computer vision techniques have been developed (Saini et al., 2012; Tekauz et al., 2000; Sankaran et al., 2010)

Visual FDK assessment

The visual assessment has been the major method for FDK evaluation in both FHB resistance breeding and research (Jones and Mirocha 1999; Zheng et al., 2006). To determine the percentage of FDK, some researchers directly counted FDK and healthy kernels to calculate the percentage of FDK (McCartney et al., 2007). Others prepare a set of FDK standards, such as <5%, 10%, 15%, 20%, >95% FDK by counting, then compare harvested seed samples with the

standards to estimate FDK percentage for each sample (Cai, 2016). The visual assessment method can be time and labor-consuming for a large number of samples, and sometimes there may be a weak correlation for the same samples set between different evaluators, even for who have been trained to give relatively consistent ratings (Maloney et al., 2014).

Near-infrared and hyperspectral image analysis

In the visible range and near-infrared (NIR) range of electromagnetic spectrum, the reflectance or transmittance spectroscopy can be used for assessing the plant density, nutrition deficiency, grain hardness, protein content, moisture, and characteristics related with plant diseases in multiple crops (Caporaso et al., 2018; Polder et al., 2005; Wang et al., 2004). Many researchers have exploited suitable detection wavelengths using NIR in grain detection and quality evaluation (Delwiche et al., 2011; Menesatti et al., 2013; Singh et al., 2012). In 2004, a group described a semi-automated wheat single kernel FDK scoring system using NIR reflectance (1,000-1,700 nm) and obtained 88-97% accuracy (Delwiche and Hareland, 2004). Then two-wavelengths (one visible at 675 nm and one NIR at 1,480 nm) were used to develop a high-speed optical FDK sorting system for application in *Fusarium*-infected soft red winter wheat (Delwiche et al., 2005). In 2010, an automated single kernel near-infrared spectroscopic method-based machine was built for estimating FDK and DON levels at the very high accuracies of 98.8 and 99.9%, respectively (Peiris et al., 2010).

A hyperspectral image can be viewed as a cube in which the spectral domain represented by hundreds of spectral wavelengths can be regarded as values for the height axis (Chang, 2000). The hyperspectral remote sensing method has been used for specific crops under specific climates, although the cost of acquiring hyperspectral images is typically high (Bajwa et al., 2004; Caporaso et al., 2018). Some previously published studies used hyperspectral image

analysis for FDK detection and evaluation. In 2000, a custom-made hyperspectral imaging system at a wavelength range from 425 to 860 nm was used to detect FDK and achieved an average covariance error between 2-17% (Delwiche and Kim, 2000). Shahin and Symons also built a model to classify FDK and sound kernels using the hyperspectral imaging system in the visible-NIR (400-1000nm) wavelength range for Canadian wheat samples with an overall accuracy of 92% (Shahin and Symons, 2011). Later, another group similarly found that hyperspectral imaging-based analysis in either visible (400-1000 nm) or NIR (1000-1700 nm) wavelength regions were suitable for differentiating sound and FDK with increased average accuracy of approximately 95% (Delwiche et al., 2011). Another group investigated a method for industry-level classification of FDK, yellow berry, and vitreous types of Italian durum wheat kernels. They found that proper classification can be obtained using the entire NIR (1000-1700 nm) wavelength or only three narrowed ranges of wavelengths (1209-1230 nm, 1489-1510 nm, and 1601-1622 nm) (Serranti et al., 2013).

Image processing with computer vision

From the mid-1980s, image processing technology has been used to separate different classes of wheat (Zayas et al., 1986; Ahmad et al., 1999). In 1998, a group used machine vision and a neural network method to estimate FDK and obtained a correlation of 0.97 with visual FDK scores and concluded that the machine network method gave a more accurate result (Ruan et al., 1998). A few years later, another group used digital images and statistical methods to identify FDK and achieved an accuracy of 85% (Jirsa and Polišenská, 2011). In addition, Maloney et al. (2014) evaluated an alternative method for quantifying FDK using a digital image analysis program, ImageJ, and demonstrated that digital image analysis could be a viable

alternative for estimating FDK. More recently, a group applied a deep learning method in FDK evaluation, which resulted in 20% of misclassification (Nicolau et al., 2018).

Besides these phenotyping platforms, other advanced phenotyping technologies have been developed for crop improvement. All the developed and developing phenotyping techniques have potential to be used for future FHB breeding programs (Bolger et al., 2019; Patrício and Rieder, 2018; Sytar et al., 2016).

Integrative breeding for wheat FHB resistance

Feeding the growing population under changing environments with limited available land, water, and other natural resources for farming is a great challenge for humans. One of the proposed solutions is to integrate all the advanced technologies to continuously improve the crop production potential for sustainable food supply (Chiurugwi et al., 2018; Schaart et al., 2016). In crops, quantitative traits are controlled by multiple genes whose expression are affected by the environment. In order to continuously improve wheat lines for important traits such as high yield, drought tolerance and FHB resistance, the integration of the advanced phenotyping, genotyping, gene editing and other innovative biotechnologies is required (Crossa et al., 2017; Mwadzingeni et al., 2016; Song et al., 2017; Tardieu et al., 2017). Considering only breeding for FHB resistance, we need to find new sources and identify novel QTLs for resistance, develop more effective tools and methods for disease evaluation, build practical genomic selection models, understand the mechanisms of different types of FHB resistance, and use gene editing to create new variation and manipulate beneficial alleles in breeding materials (Galiano et al., 2019; Guérard et al., 2018; Steiner et al., 2017).

Our objectives are to: 1) generate resistant germplasm lines with adaptation to the local environments by marker-assisted backcrossing and gene pyramiding, so these lines can be used

directly as parents in the U.S. hard winter wheat breeding programs; 2) discover resistance QTLs through GWAS and develop markers linked to these QTLs for MAS in breeding programs; 3) develop a new computer vision-based, unsupervised clustering algorithm for fast, cost-effective and accurate FDK evaluation.

References

Acquaah, G. (2015). Conventional plant breeding principles and techniques. In Advances in Plant Breeding Strategies: Breeding, Biotechnology and Molecular Tools. Pp. 115-158. Springer, Cham.

Ahmad, I. S., Reid, J. F., Paulsen, M. R., & Sinclair, J. B. (1999). Color classifier for symptomatic soybean seeds using image processing. Plant Disease, 83(4), 320-327.

Alisaac, E., Behmann, J., Kuska, M. T., Dehne, H. W., & Mahlein, A. K. (2018). Hyperspectral quantification of wheat resistance to *Fusarium* head blight: comparison of two *Fusarium* species. European Journal of Plant Pathology, 152(4), 869-884.

Arruda, M. P., Brown, P., Brown-Guedira, G., Krill, A. M., Thurber, C., Merrill, K. R., Foresman, B.J. & Kolb, F. L. (2016). Genome-wide association mapping of *Fusarium* head blight resistance in wheat using genotyping-by-sequencing. The Plant Genome, 9(1). doi:10.3835/plantgenome2015.04.0028.

Arruda, M. P., Lipka, A. E., Brown, P. J., Krill, A. M., Thurber, C., Brown-Guedira, G., Dong, Y., Foresman, Kolb, F. L. (2016). Comparing genomic selection and marker-assisted selection for *Fusarium* head blight resistance in wheat (*Triticum aestivum* L.). Molecular Breeding, 36(7), 84. https://doi.org/10.1007/s11032-016-0508-5.

Asseng, S., Ewert, F., Martre, P., Rötter, R. P., Lobell, D. B., Cammarano, D., Kimball, B.A., Ottman, M.J., Wall, G.W., White, J.W. & Reynolds, M. P. (2015). Rising temperatures reduce global wheat production. Nature Climate Change, 5(2), 143-147.

Avni, R., Nave, M., Barad, O., Baruch, K., Twardziok, S. O., Gundlach, H., Hale, I., Mascher, M., Spannagl, M., Wiebe, K. & Jordan, K. W. (2017). Wild emmer genome architecture and diversity elucidate wheat evolution and domestication. Science, 357(6346), 93-97.

Bai, G., & Shaner, G. (1994). Scab of wheat: prospects for control. Plant Disease, 78(8), 760-766.

Bai, G., & Shaner, G. (2004). Management and resistance in wheat and barley to *Fusarium* head blight. Annual Review of Phytopathology, 42, 135-161.

Bai, G., Kolb, F. L., Shaner, G., & Domier, L. L. (1999). Amplified fragment length polymorphism markers linked to a major quantitative trait locus controlling scab resistance in wheat. Phytopathology, 89(4), 343-348.

Bai, G., Su, Z., & Cai, J. (2018). Wheat resistance to *Fusarium* head blight. Canadian Journal of Plant Pathology, 40(3), 336-346.

Bajwa, S. G., Bajcsy, P., Groves, P., & Tian, L. F. (2004). Hyperspectral image data mining for band selection in agricultural applications. Transactions of the ASAE, 47(3), 895-907.

Ball, R. D. (2013). Designing a GWAS: power, sample size, and data structure. In Genome-Wide Association Studies and Genomic Prediction. Pp. 37-98. Humana Press, Totowa, NJ.

Battenfield, S. D., Guzmán, C., Gaynor, R. C., Singh, R. P., Peña, R. J., Dreisigacker, S., Fritz, A.K. & Poland, J. A. (2016). Genomic selection for processing and end-use quality traits in the CIMMYT spring bread wheat breeding program. The Plant Genome, 9. doi:10.3835/plantgenome2016.01.0005.

Bell, G. D. H. (1987). The history of wheat cultivation. In Wheat Breeding. Pp. 31-49. Springer, Dordrecht.

Barkley, A., Tack, J., Nalley, L. L., Bergtold, J., Bowden, R., & Fritz, A. (2014). Weather, disease, and wheat breeding effects on Kansas wheat varietal yields, 1985 to 2011. Agronomy Journal, 106(1), 227-235.

Bernardo, A., Amand, P. S., Le, H. Q., Su, Z., & Bai, G. (2019). Multiplex Restriction Amplicon Sequencing (MRAS eq), a novel next generation sequencing based marker platform for high-throughput genotyping. Plant Biotechnology Journal, Pp.1-14. https://doi.org/10.1111/pbi.13192.

Bernardo, A., Bai, G., Yu, J., Kolb, F., Bockus, W., & Dong, Y. (2014). Registration of near-isogenic winter wheat germplasm contrasting in *Fhb1* for *Fusarium* head blight resistance. Journal of Plant Registrations, 8(1), 106-108.

Bevan, M. W., Uauy, C., Wulff, B. B., Zhou, J., Krasileva, K., & Clark, M. D. (2017). Genomic innovation for crop improvement. Nature, 543(7645), 346-357.

Bolger, A. M., Poorter, H., Dumschott, K., Bolger, M. E., Arend, D., Osorio, S., Gundlach, H., Mayer, K.F., Lange, M., Scholz, U. & Usadel, B. (2019). Computational aspects underlying genome to phenome analysis in plants. The Plant Journal, 97(1), 182-198.

Borevitz, J. O., & Nordborg, M. (2003). The impact of genomics on the study of natural variation in Arabidopsis. Plant Physiology, 132(2), 718-725.

Boyles, R. E., Cooper, E. A., Myers, M. T., Brenton, Z., Rauh, B. L., Morris, G. P., & Kresovich, S. (2016). Genome-wide association studies of grain yield components in diverse sorghum germplasm. The Plant Genome, 9. doi:10.3835/plantgenome2015.09.0091.

Browne, R. A. (2007). Components of resistance to *fusarium* head blight (FHB) in wheat detected in a seed-germination assay with *Microdochium majus* and the relationship to FHB disease development and mycotoxin accumulation from *Fusarium graminearum* infection. Plant Pathology, 56(1), 65-72.

Brown-Guedira, G., Griffey, C., Kolb, F., McKendry, A., Murphy, J., & Sanford, D. (2008). Breeding FHB-resistant soft winter wheat: Progress and prospects. Cereal Research Communications, 36 (Supplement 6), 31–35.

Buerstmayr, H., Ban, T., & Anderson, J. A. (2009). QTL mapping and marker-assisted selection for *Fusarium* head blight resistance in wheat: a review. Plant Breeding, 128(1), 1-26.

Bush, W. S., & Moore, J. H. (2012). Genome-wide association studies. PLoS Computational Biology, 8(12), e1002822.

Cabrera, A., Souza, E., Guttieri, M., Sturbaum, A., Hoffstetter, A., & Sneller, C. (2014). Genetic diversity, linkage disequilibrium, and genome evolution in soft winter wheat. Crop Science, 54(6), 2433-2448.

Cai, J. (2016). Meta-analysis of QTL for *Fusarium* head blight resistance in Chinese wheat landraces using genotyping by sequencing. Doctoral dissertation, Kansas State University, Mahattan, KS. https://krex.k-state.edu/dspace/handle/2097/32166.

Cainong, J. C., Bockus, W. W., Feng, Y., Chen, P., Qi, L., Sehgal, S. K., Danilova, T.V., Koo, D.H., Friebe, B. & Gill, B. S. (2015). Chromosome engineering, mapping, and transferring of resistance to *Fusarium* head blight disease from *Elymus tsukushiensis* into wheat. Theoretical and Applied Genetics, 128(6), 1019-1027.

Caligari, P. D., & Forster, B. P. (2001). Plant breeding and crop improvement. eLS, 1-11.

Caporaso, N., Whitworth, M. B., & Fisk, I. D. (2018). Near-Infrared spectroscopy and hyperspectral imaging for non-destructive quality assessment of cereal grains. Applied Spectroscopy Reviews, 53(8), 667-687.

Chang, C. I. (2000). An information-theoretic approach to spectral variability, similarity, and discrimination for hyperspectral image analysis. IEEE Transactions on Information Theory, 46(5), 1927-1932.

Chiurugwi, T., Kemp, S., Powell, W., & Hickey, L. T. (2019). Speed breeding orphan crops. Theoretical and Applied Genetics, 132(3), 607-616.

Chrispeels, M. J., & Raikhel, N. V. (1991). Lectins, lectin genes, and their role in plant defense. The Plant Cell, 3(1), 1-9.

Chu, C., Niu, Z., Zhong, S., Chao, S., Friesen, T. L., Halley, S., Elias, E.M., Dong, Y., Faris, J.D. & Xu, S. S. (2011). Identification and molecular mapping of two QTLs with major effects for resistance to *Fusarium* head blight in wheat. Theoretical and Applied Genetics, 123(7), 1107-1119.

Clark, A. J., Sarti-Dvorjak, D., Brown-Guedira, G., Dong, Y., Baik, B. K., & Van Sanford, D. A. (2016). Identifying rare FHB-resistant segregants in intransigent backcross and F_2 winter wheat populations. Frontiers in Microbiology, 7, 277. https://doi.org/10.3389/fmicb.2016.00277.

Collard, B. C., & Mackill, D. J. (2007). Marker-assisted selection: an approach for precision plant breeding in the twenty-first century. Philosophical Transactions of the Royal Society B: Biological Sciences, 363(1491), 557-572.

Paterson, A. H., Lander, E. S., Hewitt, J. D., Peterson, S., Lincoln, S. E., & Tanksley, S. D. (1988). Resolution of quantitative traits into Mendelian factors by using a complete linkage map of restriction fragment length polymorphisms. Nature, 335(6192), 721-726.

Crossa, J., Pérez-Rodríguez, P., Cuevas, J., Montesinos-López, O., Jarquín, D., de los Campos, G., Burgueño, J., González-Camacho, J.M., Pérez-Elizalde, S., Beyene, Y. &

Dreisigacker, S. (2017). Genomic selection in plant breeding: methods, models, and perspectives. Trends in Plant Science, 22(11), 961-975.

Crowell, S., Korniliev, P., Falcao, A., Ismail, A., Gregorio, G., Mezey, J., & McCouch, S. (2016). Genome-wide association and high-resolution phenotyping link *Oryza sativa* panicle traits to numerous trait-specific QTL clusters. Nature Communications, 7, 10527. DOI: 10.1038/ncomms10527.

Cuthbert, P. A., Somers, D. J., & Brulé-Babel, A. (2007). Mapping of *Fhb2* on chromosome 6BS: a gene controlling *Fusarium* head blight field resistance in bread wheat (*Triticum aestivum* L.). Theoretical and Applied Genetics, 114(3), 429-437.

Cuthbert, P. A., Somers, D. J., Thomas, J., Cloutier, S., & Brulé-Babel, A. (2006). Fine mapping *Fhb1*, a major gene controlling *Fusarium* head blight resistance in bread wheat (*Triticum aestivum* L.). Theoretical and Applied Genetics, 112(8), 1465. https://doi.org/10.1007/s00122-006-0249-7.

Del Blanco, I., Frohberg, R., Stack, R., Berzonsky, W., & Kianian, S. (2003). Detection of QTL linked to *Fusarium* head blight resistance in Sumai 3-derived North Dakota bread wheat lines. Theoretical and Applied Genetics, 106(6), 1027-1031.

Del Fiore, A., Reverberi, M., Ricelli, A., Pinzari, F., Serranti, S., Fabbri, A. A., Bonifazi, G. & Fanelli, C. (2010). Early detection of toxigenic fungi on maize by hyperspectral imaging analysis. International Journal of Food Microbiology, 144(1), 64-71.

Delwiche, S. R., & Gaines, C. S. (2005). Wavelength selection for monochromatic and bichromatic sorting of *Fusarium*-damaged wheat. Applied Engineering in Agriculture, 21(4), 681-688.

Delwiche, S. R., & Hareland, G. A. (2004). Detection of scab-damaged hard red spring wheat kernels by near-infrared reflectance. Cereal Chemistry, 81(5), 643-649.

Delwiche, S. R., & Kim, M. S. (2000). Hyperspectral imaging for detection of scab in wheat. In Biological Quality and Precision Agriculture II. Pp. 13-20. International Society for Optics and Photonics.

Delwiche, S. R., Kim, M. S., & Dong, Y. (2011). *Fusarium* damage assessment in wheat kernels by Vis/NIR hyperspectral imaging. Sensing and Instrumentation for Food Quality and Safety, 5(2), 63-71.

Delwiche, S. R., Pearson, T. C., & Brabec, D. L. (2005). High-speed optical sorting of soft wheat for reduction of deoxynivalenol. Plant Disease, 89(11), 1214-1219.

Dhokane, D., Karre, S., Kushalappa, A. C., & McCartney, C. (2016). Integrated metabolo-transcriptomics reveals *fusarium* head blight candidate resistance genes in wheat QTL-*Fhb2*. PloS One, 11(5), e0155851.

Dowell, F. E., Pearson, T. C., Maghirang, E. B., Xie, F., & Wicklow, D. T. (2002). Reflectance and transmittance spectroscopy applied to detecting fumonisin in single corn kernels infected with *Fusarium verticillioides*. Cereal Chemistry, 79(2), 222-226.

Dubcovsky, J., & Dvorak, J. (2007). Genome plasticity a key factor in the success of polyploid wheat under domestication. Science, 316(5833), 1862-1866.

Dweba, C. C., Figlan, S., Shimelis, H. A., Motaung, T. E., Sydenham, S., Mwadzingeni, L., & Tsilo, T. J. (2017). *Fusarium* head blight of wheat: Pathogenesis and control strategies. Crop Protection, 91, 114-122.

Eckard, J. T., Glover, K. D., Mergoum, M., Anderson, J. A., & Gonzalez-Hernandez, J. L. (2015). Multiple *Fusarium* head blight resistance loci mapped and pyramided onto elite

spring wheat *Fhb1* backgrounds using an IBD-based linkage approach. Euphytica, 204(1), 63-79.

Elshire, R. J., Glaubitz, J. C., Sun, Q., Poland, J. A., Kawamoto, K., Buckler, E. S., & Mitchell, S. E. (2011). A robust, simple genotyping-by-sequencing (GBS) approach for high diversity species. PloS one, 6(5), e19379.

FAO STAT, (2019). http://www.fao.org/resources/infographics/infographics-details/en/c/240943/.

FAO, (2013). http://www.fao.org/faostat/en/#rankings/countries_by_commodity.

Figueroa, M., Hammond-Kosack, K. E., & Solomon, P. S. (2018). A review of wheat diseases—a field perspective. Molecular Plant Pathology, 19(6), 1523-1536.

Flint-Garcia, S. A., Thornsberry, J. M., & Buckler IV, E. S. (2003). Structure of linkage disequilibrium in plants. Annual Review of Plant Biology, 54(1), 357-374.

Galiano-Carneiro, A. L., Boeven, P. H., Maurer, H. P., Würschum, T., & Miedaner, T. (2019). Genome-wide association study for an efficient selection of *Fusarium* head blight resistance in winter triticale. Euphytica, 215(1), 4.

Giancaspro, A., Giove, S. L., Zito, D., Blanco, A., & Gadaleta, A. (2016). Mapping QTLs for *Fusarium* head blight resistance in an interspecific wheat population. Frontiers in Plant Science, 7, 1381. https://doi.org/10.3389/fpls.2016.01381.

Giménez, I., Blesa, J., Herrera, M., & Ariño, A. (2014). Effects of bread making and wheat germ addition on the natural deoxynivalenol content in bread. Toxins, 6(1), 394-401.

Godfray, H. C. J., Mason-D'Croz, D., & Robinson, S. (2016). Food system consequences of a fungal disease epidemic in a major crop. Philosophical Transactions of the Royal Society B: Biological Sciences, 371(1709), 20150467.

Gopalakrishnan, S., Sharma, R. K., Anand Rajkumar, K., Joseph, M., Singh, V. P., Singh, A. K., Bhat, K.V., Singh, N.K. & Mohapatra, T. (2008). Integrating marker assisted background analysis with foreground selection for identification of superior bacterial blight resistant recombinants in Basmati rice. Plant Breeding, 127(2), 131-139.

Gatti, M., Choulet, F., Macadré, C., Guérard, F., Seng, J. M., Langin, T., & Dufresne, M. (2018). Identification, molecular cloning and functional characterization of a wheat UDP-glucosyltransferase involved in resistance to *Fusarium* Head Blight and to mycotoxin accumulation. Frontiers in Plant Science, 9, 1853. https://doi.org/10.3389/fpls.2018.01853.

Gunnaiah, R., & Kushalappa, A. C. (2014). Metabolomics deciphers the host resistance mechanisms in wheat cultivar Sumai-3, against *trichothecene* producing and non-producing isolates of *Fusarium graminearum*. Plant Physiology and Biochemistry, 83, 40-50.

Guo, J., Zhang, X., Hou, Y., Cai, J., Shen, X., Zhou, T., Xu, H., Ohm, H.W., Wang, H., Li, A. & Han, F. (2015). High-density mapping of the major FHB resistance gene *Fhb7* derived from *Thinopyrum ponticum* and its pyramiding with *Fhb1* by marker-assisted selection. Theoretical and Applied Genetics, 128(11), 2301-2316.

Guo, Z., Liu, G., Röder, M. S., Reif, J. C., Ganal, M. W., & Schnurbusch, T. (2018). Genome-wide association analyses of plant growth traits during the stem elongation phase in wheat. Plant Biotechnology Journal, 16(12), 2042-2052.

Gustafson, P., Raskina, O., Ma, X., & Nevo, E. (2009). Wheat evolution, domestication, and improvement. Wheat: science and trade. pp 5-30, Wiley, Danvers, 5-30.

Gwirtz, J. A., Willyard, M. R., & McFall, K. L. (2007). Wheat quality in the United States of America. Future of Flour-A Compendium of Flour Improvement. Agrimedia, Ahrensburg, 17-42.

Han, S., Miedaner, T., Utz, H. F., Schipprack, W., Schrag, T. A., & Melchinger, A. E. (2018). Genomic prediction and GWAS of *Gibberella* ear rot resistance traits in dent and flint lines of a public maize breeding program. Euphytica, 214(1), 6. https://doi.org/10.1007/s10681-017-2090-2.

Hatcher, D. W., Anderson, M. J., Clear, R. M., Gaba, D. G., & Dexter, J. E. (2003). *Fusarium* head blight: effect on white salted and yellow alkaline noodle properties. Canadian Journal of Plant Science, 83(1), 11-21.

He, Y., Zhang, X., Zhang, Y., Ahmad, D., Wu, L., Jiang, P., & Ma, H. (2018). Molecular characterization and expression of *PFT*, an FHB resistance gene at the *Fhb1* QTL in wheat. Phytopathology, 108(6), 730-736.

Herter, C. P., Ebmeyer, E., Kollers, S., Korzun, V., Würschum, T., & Miedaner, T. (2019). Accuracy of within-and among-family genomic prediction for *Fusarium* head blight and Septoria tritici blotch in winter wheat. Theoretical and Applied Genetics, 132(4), 1121-1135.

Hirschhorn, J. N., & Daly, M. J. (2005). Genome-wide association studies for common diseases and complex traits. Nature Reviews Genetics, 6(2), 95-108.

Holder, A. (2018). A Genome wide association study for *Fusarium* head blight resistance in southern soft red winter wheat. Master dissertation, University of Arkansas, Fayetteville, AR. https://scholarworks.uark.edu/etd/2636/.

Holland, J. B. (2007). Genetic architecture of complex traits in plants. Current Opinion in Plant Biology, 10(2), 156-161.

Huang, X., & Han, B. (2014). Natural variations and genome-wide association studies in crop plants. Annual Review of Plant Biology, 65, 531-551.

IWGSC, International Wheat Genome Sequencing Consortium. (2014). A chromosome-based draft sequence of the hexaploid bread wheat (*Triticum aestivum*) genome. Science, 345(6194), 1251788.

Jayatilake, D. V., Bai, G. H., & Dong, Y. H. (2011). A novel quantitative trait locus for *Fusarium* head blight resistance in chromosome 7A of wheat. Theoretical and Applied Genetics, 122(6), 1189-1198.

Jia, H., Zhou, J., Xue, S., Li, G., Yan, H., Ran, C., Zhang, Y., Shi, J., Jia, L., Wang, X. & Luo, J. (2018). A journey to understand wheat *Fusarium* head blight resistance in the Chinese wheat landrace Wangshuibai. The Crop Journal, 6(1), 48-59.

Jin, F., Bai, G., Zhang, D., Dong, Y., Ma, L., Bockus, W., & Dowell, F. (2014). *Fusarium*-damaged kernels and deoxynivalenol in *Fusarium*-infected US winter wheat. Phytopathology, 104(5), 472-478.

Jirsa, O., & Polišenská, I. (2014). Identification of *Fusarium* damaged wheat kernels using image analysis. Acta Universitatis Agriculturae et Silviculturae Mendelianae Brunensis, 59(5), 125-130.

Johnson, R. (2003). Marker-assisted selection. Plant Breeding Reviews: Part 1: Long-Term Selection: Maize, 24, 293-309.

Jones, R. K., & Mirocha, C. J. (1999). Quality parameters in small grains from Minnesota affected by *Fusarium* head blight. Plant Disease, 83(6), 506-511.

Joshi, R. K., & Nayak, S. (2010). Gene pyramiding-a broad spectrum technique for developing durable stress resistance in crops. Biotechnology and Molecular Biology Reviews, 5(3), 51-60.

Khan, M. K., Pandey, A., Choudhary, S., Hakki, E. E., Akkaya, M. S., & Thomas, G. (2014). From RFLP to DArT: molecular tools for wheat (*Triticum* spp.) diversity analysis. Genetic Resources and Crop Evolution, 61(5), 1001-1032.

Kollers, S., Rodemann, B., Ling, J., Korzun, V., Ebmeyer, E., Argillier, O., Hinze, M., Plieske, J., Kulosa, D., Ganal, M.W. & Röder, M. S. (2013). Whole genome association mapping of *Fusarium* head blight resistance in European winter wheat (*Triticum aestivum* L.). PLoS One, 8(2), e57500.

Korte, A., & Farlow, A. (2013). The advantages and limitations of trait analysis with GWAS: a review. Plant Methods, 9: 29. doi:10.1186/1746-4811-9-29.

Joshi, R. K., & Nayak, S. (2010). Gene pyramiding-A broad spectrum technique for developing durable stress resistance in crops. Biotechnology and Molecular Biology Reviews, 5(3), 51-60.

Lagudah, E. S., & Krattinger, S. G. (2019). A new player contributing to durable *Fusarium* resistance. Nature Genetics, 51(7), 1070-1071.

Lemes Da Silva, C. (2018). Genomic approaches for mapping and predicting disease resistance in wheat (*Triticum aestivum* L.). Doctoral dissertation, Kansas State University, Manhattan, KS. https://krex.k-state.edu/dspace/handle/2097/38555.

Lemes Da Silva, C. L., Fritz, A., Clinesmith, M., Poland, J., Dowell, F., & Peiris, K. (2019). QTL mapping of *Fusarium* head blight resistance and deoxynivalenol accumulation in

the Kansas wheat variety 'Everest'. Molecular Breeding, 39(3), 35. https://doi.org/10.1007/s11032-019-0937-z.

Leonova, I. N. (2013). Molecular markers: Implementation in crop plant breeding for identification, introgression and gene pyramiding. Russian Journal of Genetics: Applied Research, 3(6), 464-473.

Li, G., Zhou, J., Jia, H., Gao, Z., Fan, M., Luo, Y., Zhao, P., Xue, S., Li, N., Yuan, Y. & Ma, S. (2019). Mutation of a histidine-rich calcium-binding-protein gene in wheat confers resistance to *Fusarium* head blight. Nature Genetics, 51, 1106-1112.

Li, T., Zhang, D., Zhou, X., Bai, G., Li, L., & Gu, S. (2016). *Fusarium* head blight resistance loci in a stratified population of wheat landraces and varieties. Euphytica, 207(3), 551-561.

Li, X., Xiang, Z. P., Chen, W. Q., Huang, Q. L., Liu, T. G., Li, Q., Zhong, S. F., Zhang, M., Guo, J.W., Lei, L. & Luo, P. G. (2016). Reevaluation of two quantitative trait loci for type ii resistance to *Fusarium* head blight in wheat germplasm pi 672538. Phytopathology, 107(1), 92-99.

Lin, M., Zhang, D., Liu, S., Zhang, G., Yu, J., Fritz, A. K., & Bai, G. (2016). Genome-wide association analysis on pre-harvest sprouting resistance and grain color in US winter wheat. BMC Genomics, 17(1), 794. http://dx.doi.org/10.1186/s12864-016-3148-6.

Liu, S., Zhang, X., Pumphrey, M. O., Stack, R. W., Gill, B. S., & Anderson, J. A. (2006). Complex microcolinearity among wheat, rice, and barley revealed by fine mapping of the genomic region harboring a major QTL for resistance to *Fusarium* head blight in wheat. Functional & Integrative Genomics, 6(2), 83-89.

Löffler, M., Schön, C. C., & Miedaner, T. (2009). Revealing the genetic architecture of FHB resistance in hexaploid wheat (*Triticum aestivum* L.) by QTL meta-analysis. Molecular Breeding, 23(3), 473-488.

Long, Y. M., Chao, W. S., Ma, G. J., Xu, S. S., & Qi, L. L. (2017). An innovative SNP genotyping method adapting to multiple platforms and throughputs. Theoretical and Applied Genetics, 130(3), 597-607.

Lu, Q., Szabo-Hever, A., Bjørnstad, Å., Lillemo, M., Semagn, K., Mesterházy, A., Ji, F., Shi, J. & Skinnes, H. (2011). Two major resistance quantitative trait loci are required to counteract the increased susceptibility to *Fusarium* head blight of the *Rht-D1b* dwarfing gene in wheat. Crop Science, 51(6), 2430-2438.

Lupton, F. G. H. (1987). History of wheat breeding. In wheat Breeding. Pp. 51-70. Springer, Dordrecht.

Lv, C., Song, Y., Gao, L., Yao, Q., Zhou, R., Xu, R., & Jia, J. (2014). Integration of QTL detection and marker assisted selection for improving resistance to *Fusarium* head blight and important agronomic traits in wheat. The Crop Journal, 2(1), 70-78.

Malihipour, A., Gilbert, J., Fedak, G., Brûlé-Babel, A., & Cao, W. (2017). Mapping the A genome for QTL conditioning resistance to *Fusarium* head blight in a wheat population with *Triticum timopheevii* background. Plant Disease, 101(1), 11-19.

Maloney, P. V., Petersen, S., Navarro, R. A., Marshall, D., McKendry, A. L., Costa, J. M., & Murphy, J. P. (2014). Digital image analysis method for estimation of *Fusarium*-damaged kernels in wheat. Crop Science, 54(5), 2077-2083.

Manthey, F. A., Wolf-Hall, C. E., Yalla, S., Vijayakumar, C., & Carlson, D. (2004). Microbial loads, mycotoxins, and quality of durum wheat from the 2001 harvest of the northern plains region of the United States. Journal of Food Protection, 67(4), 772-780.

Maresca, M. (2013). From the gut to the brain: Journey and pathophysiological effects of the food-associated *trichothecene* mycotoxin deoxynivalenol. Toxins, 5(4), 784-820.

Massman, J., Cooper, B., Horsley, R., Neate, S., Dill-Macky, R., Chao, S., Dong, Y., Schwarz, P., Muehlbauer, G.J. & Smith, K. P. (2011). Genome-wide association mapping of *Fusarium* head blight resistance in contemporary barley breeding germplasm. Molecular Breeding, 27(4), 439-454.

Matsuoka, Y. (2011). Evolution of polyploid *Triticum* wheats under cultivation: the role of domestication, natural hybridization and allopolyploid speciation in their diversification. Plant and Cell Physiology, 52(5), 750-764.

McCartney, C. A., Somers, D. J., Fedak, G., & Cao, W. (2004). Haplotype diversity at *fusarium* head blight resistance QTLs in wheat. Theoretical and Applied Genetics, 109(2), 261-271.

McCartney, C. A., Somers, D. J., Fedak, G., DePauw, R. M., Thomas, J., Fox, S. L., Humphreys DG, Lukow O, Savard ME, McCallum BD & Gilbert, J. (2007). The evaluation of FHB resistance QTLs introgressed into elite Canadian spring wheat germplasm. Molecular Breeding, 20(3), 209-221.

McMullen, M., Bergstrom, G., De Wolf, E., Dill-macky, R., Hershman, D., Shaner, G., & Van Sanford, D. (2012). *Fusarium* head blight disease cycle, symptoms, and impact on grain yield and quality frequency and magnitude of epidemics since 1997. Plant Disease, 96(12), 1712-1728.

Menesatti, P., Antonucci, F., Pallottino, F., Giorgi, S., Matere, A., Nocente, F., Pasquini, M., D'Egidio, M.G. & Costa, C. (2013). Laboratory vs. in-field spectral proximal sensing for early detection of *Fusarium* head blight infection in durum wheat. Biosystems Engineering, 114(3), 289-293.

Mergoum, M., Frohberg, R. C., & Stack, R. W. (2007). Breeding hard red spring wheat for *Fusarium* head blight resistance. In Wheat Production in Stressed Environments. Pp. 161-167. Springer, Dordrecht.

Mesterházy, Á. (1997). Methodology of resistance testing and breeding against *Fusarium* head blight in wheat and results of the selection. Cereal Research Communications, 631-637.

Mesterházy, Á. (2002). Role of deoxynivalenol in aggressiveness of *Fusarium graminearum* and *F. culmorum* and in resistance to *Fusarium* head blight. In Mycotoxins in Plant Disease. Pp. 675-684. Springer, Dordrecht.

Miedaner, T., Kalih, R., Großmann, M. S., & Maurer, H. P. (2016). Correlation between *Fusarium* head blight severity and DON content in triticale as revealed by phenotypic and molecular data. Plant Breeding, 135(1), 31-37.

Miedaner, T., Würschum, T., Maurer, H. P., Korzun, V., Ebmeyer, E., & Reif, J. C. (2011). Association mapping for *Fusarium* head blight resistance in European soft winter wheat. Molecular Breeding, 28(4), 647-655.

Mwadzingeni, L., Shimelis, H., Dube, E., Laing, M. D., & Tsilo, T. J. (2016). Breeding wheat for drought tolerance: Progress and technologies. Journal of Integrative Agriculture, 15(5), 935-943.

Nadeem, M. A., Nawaz, M. A., Shahid, M. Q., Doğan, Y., Comertpay, G., Yıldız, M., Hatipoğlu, R., Ahmad, F., Alsaleh, A., Labhane, N. & Özkan, H. (2018). DNA molecular markers in

plant breeding: current status and recent advancements in genomic selection and genome editing. Biotechnology & Biotechnological Equipment, 32(2), 261-285.

Naroei, K., & Salari, M. (2015). Impacts of *Fusarium* head blight (FHB). Journal of Novel Applied Sciences, 4(11), 1109-1122.

Nesbitt, M. (2001). Wheat evolution: integrating archaeological and biological evidence. Wheat Taxonomy: The Legacy of John Percival, 3, 37-59.

Nicolau, M., Pimentel, M. B. M., Tibola, C. S., Fernandes, J. M. C., & Pavan, W. (2018). *Fusarium* damaged kernels detection using transfer learning on Deep neural network architecture. arXiv preprint arXiv:1802.00030.

Nishio, Z., Onoe, C., Ito, M., Tabiki, T., Nagasawa, K., & Miura, H. (2016). Mapping a QTL conferring resistance to *Fusarium* head blight on chromosome 1B in winter wheat (*Triticum aestivum* L.). Breeding Science, 16097. https://doi.org/10.1270/jsbbs.16097.

Ozaki, K., Ohnishi, Y., Iida, A., Sekine, A., Yamada, R., Tsunoda, T., Sato, H., Sato, H., Hori, M., Nakamura, Y. & Tanaka, T. (2002). Functional SNPs in the lymphotoxin-α gene that are associated with susceptibility to myocardial infarction. Nature genetics, 32(4), 650.

Pascual, L., Albert, E., Sauvage, C., Duangjit, J., Bouchet, J. P., Bitton, F., Desplat, N., Brunel, D., Le Paslier, M.C., Ranc, N. & Bruguier, L. (2016). Dissecting quantitative trait variation in the resequencing era: complementarity of bi-parental, multi-parental and association panels. Plant Science, 242, 120-130.

Patrício, D. I., & Rieder, R. (2018). Computer vision and artificial intelligence in precision agriculture for grain crops: A systematic review. Computers and Electronics in Agriculture, 153, 69-81.

Paul, P. A., Lipps, P. E., & Madden, L. V. (2005). Relationship between visual estimates of *Fusarium* head blight intensity and deoxynivalenol accumulation in harvested wheat grain: A meta-analysis. Phytopathology, 95(10), 1225-1236.

Paulsen, G. M. (2001). A History of Wheat Improvement at Kansas State University. Kansas Agricultural Experiment Station Research Reports, 0(12). https://doi.org/10.4148/2378-5977.7239.

Peiris, K. H. S., Pumphrey, M. O., Dong, Y., Maghirang, E. B., Berzonsky, W., & Dowell, F. E. (2010). Near-infrared spectroscopic method for identification of *Fusarium* head blight damage and prediction of deoxynivalenol in single wheat kernels. Cereal Chemistry, 87(6), 511-517.

Piperno, D. R., Weiss, E., Holst, I., & Nadel, D. (2004). Processing of wild cereal grains in the Upper Palaeolithic revealed by starch grain analysis. Nature, 430(7000), 670.

Polder, G., Van Der Heijden, G. W. A. M., Waalwijk, C., & Young, I. T. (2005). Detection of *Fusarium* in single wheat kernels using spectral imaging. Seed Science and Technology, 33(3), 655-668.

Pumphrey, M. O., Bernardo, R., & Anderson, J. A. (2007). Validating the *Fhb1* QTL for *Fusarium* head blight resistance in near-isogenic wheat lines developed from breeding populations. Crop Science, 47(1), 200-206.

Qi, L. L., Pumphrey, M. O., Friebe, B., Chen, P. D., & Gill, B. S. (2008). Molecular cytogenetic characterization of alien introgressions with gene *Fhb3* for resistance to *Fusarium* head blight disease of wheat. Theoretical and Applied Genetics, 117(7), 1155-1166.

Rafalski, J. A. (2010). Association genetics in crop improvement. Current Opinion in Plant Biology, 13(2), 174-180.

Randhawa, H. S., Mutti, J. S., Kidwell, K., Morris, C. F., Chen, X., & Gill, K. S. (2009). Rapid and targeted introgression of genes into popular wheat cultivars using marker-assisted background selection. PloS One, 4(6), e5752.

Rasheed, A., Hao, Y., Xia, X., Khan, A., Xu, Y., Varshney, R. K., & He, Z. (2017). Crop breeding chips and genotyping platforms: progress, challenges, and perspectives. Molecular Plant, 10(8), 1047-1064.

Rawat, N., Pumphrey, M. O., Liu, S., Zhang, X., Tiwari, V. K., Ando, K., Trick, H.N., Bockus, W.W., Akhunov, E., Anderson, J.A. & Gill, B. S. (2016). Wheat *Fhb1* encodes a chimeric lectin with agglutinin domains and a pore-forming toxin-like domain conferring resistance to *Fusarium* head blight. Nature Genetics, 48(12), 1576-1580.

Ray, D. K., Mueller, N. D., West, P. C., & Foley, J. A. (2013). Yield trends are insufficient to double global crop production by 2050. PloS One, 8(6), e66428.

Ren, J., Wang, Z., Du, Z., Che, M., Zhang, Y., Quan, W., Wang, Y., Jiang, X. & Zhang, Z. (2019). Detection and validation of a novel major QTL for resistance to *Fusarium* head blight from *Triticum aestivum* in the terminal region of chromosome 7DL. Theoretical and Applied Genetics, 132(1), 241-255.

Ruan, R., Ning, S., Song, A., Ning, A., Jones, R., & Chen, P. (1998). Estimation of *Fusarium* scab in wheat using machine vision and a neural network. Cereal Chemistry, 75(4), 455-459.

Saccon, F. A., Parcey, D., Paliwal, J., & Sherif, S. S. (2017). Assessment of *Fusarium* and deoxynivalenol using optical methods. Food and Bioprocess Technology, 10(1), 34-50.

Saharan, M. S., Kumar, J., Sharma, A. K., & Nagarajan, S. (2004). *Fusarium* head blight (FHB) or head scab of wheat-a review. Proceedings of the National Academy of Sciences, India Section B, 3, 255-268.

Saini, M., Singh, J., & Prakash, N. (2014). Analysis of wheat grain varieties using image processing–a review. International Journal of Science and Research, 3(6), 490-495.

Sankaran, S., Mishra, A., Ehsani, R., & Davis, C. (2010). A review of advanced techniques for detecting plant diseases. Computers and Electronics in Agriculture, 72(1), 1-13.

Sari, E., Berraies, S., Knox, R. E., Singh, A. K., Ruan, Y., Cuthbert, R. D., Pozniak, C.J., Henriquez, M.A., Kumar, S., Burt, A.J. & N'Diaye, A. (2018). High density genetic mapping of *Fusarium* head blight resistance QTL in tetraploid wheat. PloS One, 13(10), e0204362.

Schaafsma, A. W., Savard, M. E., Clear, R., & Dexter, J. (2004). Methods and issues regarding detection of deoxynivalenol, *Fusarium*-damaged kernels, and *Fusarium* spp. in commercial grain in Canada. Canadian Journal of Plant Pathology, 26(4), 443-452.

Schaart, J. G., van de Wiel, C. C., Lotz, L. A., & Smulders, M. J. (2016). Opportunities for products of new plant breeding techniques. Trends in Plant Science, 21(5), 438-449.

Schrag, T. A., Westhues, M., Schipprack, W., Seifert, F., Thiemann, A., Scholten, S., & Melchinger, A. E. (2018). Beyond genomic prediction: combining different types of omics data can improve prediction of hybrid performance in maize. Genetics, 208(4), 1373-1385.

Semagn, K., Babu, R., Hearne, S., & Olsen, M. (2014). Single nucleotide polymorphism genotyping using Kompetitive Allele Specific PCR (KASP): overview of the technology and its application in crop improvement. Molecular Breeding, 33(1), 1-14.

Semagn, K., Bjørnstad, Å., & Ndjiondjop, M. N. (2006). Progress and prospects of marker assisted backcrossing as a tool in crop breeding programs. African Journal of Biotechnology, 5(25), 2588-2603.

Serranti, S., Cesare, D., & Bonifazi, G. (2013). The development of a hyperspectral imaging method for the detection of *Fusarium*-damaged, yellow berry and vitreous Italian durum wheat kernels. Biosystems Engineering, 115(1), 20-30.

Servin, B., Martin, O. C., & Mézard, M. (2004). Toward a theory of marker-assisted gene pyramiding. Genetics, 168(1), 513-523.

Shah, L., Ali, A., Zhu, Y., Wang, S., Si, H., & Ma, C. (2017). Wheat resistance to *Fusarium* head blight and possibilities of its improvement using molecular marker-assisted selection. Czech Journal of Genetics and Plant Breeding, 53(2), 47-54.

Shahin, M. A., & Symons, S. J. (2011). Detection of *Fusarium* damaged kernels in Canada Western Red Spring wheat using visible/near-infrared hyperspectral imaging and principal component analysis. Computers and Electronics in Agriculture, 75(1), 107-112.

Shewry, P. R. (2009). Wheat. Journal of Experimental Botany, 60(6), 1537-1553.

Shi, J. R., Xu, D. H., Yang, H. Y., Lu, Q. X., & Ban, T. (2008). DNA marker analysis for pyramided of *Fusarium* head blight (FHB) resistance QTLs from different germplasm. Genetica, 133(1), 77-84.

Simons, K. J., Fellers, J. P., Trick, H. N., Zhang, Z., Tai, Y. S., Gill, B. S., & Faris, J. D. (2006). Molecular characterization of the major wheat domestication gene Q. Genetics, 172(1), 547-555.

Singh, C. B., Jayas, D. S., Paliwal, J., & White, N. D. G. (2012). Fungal damage detection in wheat using short-wave near-infrared hyperspectral and digital colour imaging. International Journal of Food Properties, 15(1), 11-24.

Sobrova, P., Adam, V., Vasatkova, A., Beklova, M., Zeman, L., & Kizek, R. (2010). Deoxynivalenol and its toxicity. Interdisciplinary Toxicology, 3(3), 94-99.

Song, J., Carver, B. F., Powers, C., Yan, L., Klápště, J., El-Kassaby, Y. A., & Chen, C. (2017). Practical application of genomic selection in a doubled-haploid winter wheat breeding program. Molecular Breeding, 37(10), 117. DOI 10.1007/s11032-017-0715-8.

Šramková, Z., Gregová, E., & Šturdík, E. (2009). Chemical composition and nutritional quality of wheat grain. Acta Chimica Slovaca, 2(1), 115-138.

Steiner, B., Buerstmayr, M., Michel, S., Schweiger, W., Lemmens, M., & Buerstmayr, H. (2017). Breeding strategies and advances in line selection for *Fusarium* head blight resistance in wheat. Tropical Plant Pathology, 42(3), 165-174.

Su, Z., Bernardo, A., Tian, B., Chen, H., Wang, S., Ma, H., Cai, S., Liu, D., Zhang, D., Li, T. & Trick, H. (2019). A deletion mutation in *TaHRC* confers *Fhb1* resistance to *Fusarium* head blight in wheat. Nature Genetics, 51, 1099-1105.

Su, Z., Jin, S., Zhang, D., & Bai, G. (2018). Development and validation of diagnostic markers for *Fhb1* region, a major QTL for *Fusarium* head blight resistance in wheat. Theoretical and Applied Genetics, 131(11), 2371-2380.

Sytar, O., Brestic, M., Zivcak, M., Olsovska, K., Kovar, M., Shao, H., & He, X. (2017). Applying hyperspectral imaging to explore natural plant diversity towards improving salt stress tolerance. Science of the Total Environment, 578, 90-99.

Tabatabaeefar, A., Emamzadeh, H., Varnamkhasti, M. G., Rahimizadeh, R., & Karimi, M. (2009). Comparison of energy of tillage systems in wheat production. Energy, 34(1), 41-45.

Taheri, P. (2018). Cereal diseases caused by *Fusarium graminearum*: from biology of the pathogen to oxidative burst-related host defense responses. European Journal of Plant Pathology, 152(1), 1-20.

Talukder, S. K., & Saha, M. C. (2017). Toward genomics-based breeding in C3 cool-season perennial grasses. Frontiers in Plant Science, 8, 1317. https://doi.org/10.3389/fpls.2017.01317.

Tardieu, F., Cabrera-Bosquet, L., Pridmore, T., & Bennett, M. (2017). Plant phenomics, from sensors to knowledge. Current Biology, 27(15), R770-R783.

Tekauz, A., McCallum, B., & Gilbert, J. (2000). *Fusarium* head blight of barley in western Canada. Canadian Journal of Plant Pathology, 22(1), 9-16.

Thomson, M. J. (2014). High-throughput SNP genotyping to accelerate crop improvement. Plant Breeding and Biotechnology, 2(3), 195-212.

Tyagi, S., Mir, R. R., Kaur, H., Chhuneja, P., Ramesh, B., Balyan, H. S., & Gupta, P. K. (2014). Marker-assisted pyramiding of eight QTLs/genes for seven different traits in common wheat (*Triticum aestivum* L.). Molecular Breeding, 34(1), 167-175.

Varshney, R. K., Graner, A., & Sorrells, M. E. (2005). Genic microsatellite markers in plants: features and applications. Trends in Biotechnology, 23(1), 48-55.

Varshney, R. K., Singh, V. K., Hickey, J. M., Xun, X., Marshall, D. F., Wang, J., Edwards, D. & Ribaut, J. M. (2016). Analytical and decision support tools for genomics-assisted breeding. Trends in Plant Science, 21(4), 354-363.

Visscher, P. M., Brown, M. A., McCarthy, M. I., & Yang, J. (2012). Five years of GWAS discovery. The American Journal of Human Genetics, 90(1), 7-24.

Visscher, P. M., Wray, N. R., Zhang, Q., Sklar, P., McCarthy, M. I., Brown, M. A., & Yang, J. (2017). 10 years of GWAS discovery: biology, function, and translation. The American Journal of Human Genetics, 101(1), 5-22.

Vocke, G., & Ali, M. (2013). US wheat production practices, costs, and yields: Variations across regions. EIB-116. U.S. Department of Agriculture, Economic Research Service (No. 1476-2017-3890).

Waldron, B. L., Moreno-Sevilla, B., Anderson, J. A., Stack, R. W., & Frohberg, R. C. (1999). RFLP mapping of QTL for *Fusarium* head blight resistance in wheat. Crop Science, 39(3), 805-811.

Wang, D., Dowell, F. E., Ram, M. S., & Schapaugh, W. T. (2004). Classification of fungal-damaged soybean seeds using near-infrared spectroscopy. International Journal of Food Properties, 7(1), 75-82.

Wang, H., & Qin, F. (2017). Genome-wide association study reveals natural variations contributing to drought resistance in crops. Frontiers in Plant Science, 8, 1110. https://doi.org/10.3389/fpls.2017.01110.

Wang, R., Chen, J., Anderson, J. A., Zhang, J., Zhao, W., Wheeler, J., Klassen, N., See, D.R. & Dong, Y. (2017). Genome-wide association mapping of *Fusarium* head blight resistance in spring wheat lines developed in the Pacific Northwest and CIMMYT. Phytopathology, 107(12), 1486-1495.

Wegulo, S. N., Baenziger, P. S., Nopsa, J. H., Bockus, W. W., & Hallen-Adams, H. (2015). Management of *Fusarium* head blight of wheat and barley. Crop Protection, 73, 100-107.

Wen, L., Chang, H. X., Brown, P. J., Domier, L. L., & Hartman, G. L. (2019). Genome-wide association and genomic prediction identifies soybean cyst nematode resistance in common bean including a syntenic region to soybean *Rhg1* locus. Horticulture Research, 6(1), 9. DOI 10.1038/s41438-018-0085-3.

Wiwart, M., Koczowska, I., & Borusiewicz, A. (2001, September). Estimation of *Fusarium* head blight of triticale using digital image analysis of grain. In International Conference on Computer Analysis of Images and Patterns. Pp. 563-569. Springer, Berlin, Heidelberg.

Wu, L., Zhang, Y., He, Y., Jiang, P., Zhang, X., & Ma, H. M. (2019). Genome-wide association mapping of resistance to *Fusarium* head blight spread and DON accumulation in Chinese elite wheat germplasm. Phytopathology, 109(7), 1208-1216.

Xie, G. Q., Zhang, M. C., Chakraborty, S., & Liu, C. J. (2007). The effect of 3BS locus of Sumai 3 on *Fusarium* head blight resistance in Australian wheats. Australian Journal of Experimental Agriculture, 47(5), 603-607.

Xu, Y., Li, P., Yang, Z., & Xu, C. (2017). Genetic mapping of quantitative trait loci in crops. The Crop Journal, 5(2), 175-184.

Xu, Y., Li, P., Zou, C., Lu, Y., Xie, C., Zhang, X., Prasanna, B.M. & Olsen, M. S. (2017). Enhancing genetic gain in the era of molecular breeding. Journal of Experimental Botany, 68(11), 2641-2666.

Xue, S., Li, G., Jia, H., Xu, F., Lin, F., Tang, M., Wang, Y., An, X., Xu, H., Zhang, L. & Kong, Z. (2010). Fine mapping *Fhb4*, a major QTL conditioning resistance to *Fusarium* infection in bread wheat (*Triticum aestivum* L.). Theoretical and Applied Genetics, 121(1), 147-156.

Xue, S., Xu, F., Tang, M., Zhou, Y., Li, G., An, X., Lin, F., Xu, H., Jia, H., Zhang, L. & Kong, Z. (2011). Precise mapping *Fhb5*, a major QTL conditioning resistance to *Fusarium* infection in bread wheat (*Triticum aestivum* L.). Theoretical and Applied Genetics, 123(6), 1055-1063.

Yang, J., Bai, G., & Shaner, G. E. (2005). Novel quantitative trait loci (QTL) for *Fusarium* head blight resistance in wheat cultivar Chokwang. Theoretical and Applied Genetics, 111(8), 1571-1579.

Yang, Z. P., Gilbert, J., Somers, D. J., Fedak, G., Procunier, J. D., & McKenzie, I. H. (2003). Marker assisted selection of *Fusarium* head blight resistance genes in two doubled haploid populations of wheat. Molecular Breeding, 12(4), 309-317.

Yao, J., Zhou, M., Zhang, X., Ren, L., Yu, G., & Lu, W. (2008). Molecular breeding for wheat *Fusarium* head blight resistance in China. Cereal Research Communications, 36, 203-212.

Zargar, S. M., Raatz, B., Sonah, H., Bhat, J. A., Dar, Z. A., Agrawal, G. K., & Rakwal, R. (2015). Recent advances in molecular marker techniques: insight into QTL mapping, GWAS and genomic selection in plants. Journal of Crop Science and Biotechnology, 18(5), 293-308.

Zayas, I., Lai, F. S., & Pomeranz, Y. (1986). Discrimination between wheat classes and varieties by image analysis. Cereal Chemistry, 63(1), 52-56.

Zhang, Q., Feitosa, M., & Borecki, I. B. (2014). Estimating and testing pleiotropy of single genetic variant for two quantitative traits. Genetic Epidemiology, 38(6), 523-530.

Zhang, Q., Szabo-Hever, A., Friesen, T. L., Zhong, S., Elias, E. M., Cai, X., Jin, Y., Faris, J.D., Chao, S. & Xu, S. S. (2018). Genetic diversity and resistance to *Fusarium* head blight in

synthetic hexaploid wheat derived from *Aegilops tauschii* and diverse *Triticum turgidum* subspecies. Frontiers in Plant Science, 9, 1829. https://doi.org/10.3389/fpls.2018.01829.

Zhao, M., Leng, Y., Chao, S., Xu, S. S., & Zhong, S. (2018). Molecular mapping of QTL for *Fusarium* head blight resistance introgressed into durum wheat. Theoretical and Applied Genetics, 131(9), 1939-1951.

Zheng, M. Z., Richard, J. L., & Binder, J. (2006). A review of rapid methods for the analysis of mycotoxins. Mycopathologia, 161(5), 261-273.

Zhou, W., Kolb, F. L., Bai, G., Shaner, G., & Domier, L. L. (2002). Genetic analysis of scab resistance QTL in wheat with microsatellite and AFLP markers. Genome, 45(4), 719-727.

Zwart, S. J., & Bastiaanssen, W. G. (2004). Review of measured crop water productivity values for irrigated wheat, rice, cotton and maize. Agricultural Water Management, 69(2), 115-133.

Table 1.1 Quantitative trait locus (QTL)s and linked markers for *Fusarium* head blight (FHB) resistance related taits reported from different spources.

Source	Ch.*	PVE%**	Linked markers	FHB trait***	Marker type	Mapping population
Wangshuibai	4BL	11.9-50.9	Xhbg226 - Xgwm149	PSS, incidence		Nanda2419 × Wangshuibai 530RILs, *Qfhi.nau-4B* NIL × Mianyang 99-323 66BC_3F_2 lines (Xue et al., 2010)
Wangshuibai	5AS	8.9-49.3	Xbarc56-Xbarc100	incidence, PSS		Miantang99-323 x Wangshuibai 94BC_3F_2 lines, PH691 × Wangshuibai 71BC_4F_2 lines, Nanda2419 × Wangshuibai 530RILs (Xue et al., 2011)
CS-Sumai3-7ADSL	7A	22.0-24.0	Xwmc17	PSS, DON content, FDK		Chinese Spring × CS-Sumai3-7ADSL 191 RILs (Jayatilake et al., 2011)
Stettler	2BL	16.2	Excalibur_rep_c108662_132 - RAC875_c25277_324, near Xgwm388	PSS	90K Wheat Infinium iSelect SNP arrays	FL62R1 × Stettler 185 DH lines (Zhang et al., 2018)
Joppa (durum)	2A	9.0-14.0	IWB10237	PSS, DON content	90K wheat Infinium iSelect SNP arrays	Joppa × 10Ae564 205RILs (Zhao et al., 2018)
10Ae564 (durum)	5A	7.0-19.0	IWB26525	PSS, DON content	90K wheat Infinium iSelect SNP arrays	Joppa × 10Ae564 205RILs (Zhao et al., 2018)
10Ae564 (durum)	7A	9.0-11.0	IWB74024	PSS, DON content	90K wheat Infinium iSelect SNP arrays	Joppa × 10Ae564 205RILs (Zhao et al., 2018)
-	4A	14.7	S4A_574518163	incidence	GBS SNP	Association mapping panel of 360 SRWW (Holder, 2018)
-	7A	13.4	S7A_11152072	incidence	GBS SNP	Association mapping panel of 360 SRWW (Holder, 2018)
-	2D	13.3	S2D_526929200	incidence	GBS SNP	Association mapping panel of 360 SRWW (Holder, 2018)
-	3B	12.1-12.3	S3B_784540562, S3B_795306092, S3B_784573154	PSS	GBS SNP	Association mapping panel of 360 SRWW (Holder, 2018)
-	3B	10.8	S3B_526480094	FDK	GBS SNP	Association mapping panel of 360 SRWW (Holder, 2018)
-	1A	7.3-7.6	S1A_282055814	DON content	GBS SNP	Association mapping panel of 360 SRWW (Holder, 2018)

-	4B	7.3-7.6	S4B_21625964	DON content	GBS SNP	Association mapping panel of 360 SRWW (Holder, 2018)
-	7B	7.3-7.6	7B_595827248	DON content	GBS SNP	Association mapping panel of 360 SRWW (Holder, 2018)
Yumechikara	1BS	36.4	GluB3-barc32	PSS		Yumrchikara × Kitahonami 94DH lines (Nishio et al., 2016)
Kitahonami	3BS	11.2	gwm384-wmc754	PSS		Yumrchikara × Kitahonami 94DH lines (Nishio et al., 2016)
PI672538	2B	11.6	Xbarc55-2B - Xbarc1155-2B	PSS		PI672538 × L661 229 F_2 and $F_{2:3}$ lines (Li et al., 2016)
PI672538	3B	10.0	Xwmc54-3B - Xgwm566-3B	PSS		PI672538 × L661 229 F_2 and $F_{2:3}$ lines (Li et al., 2016)
Tunisian108 (durum)	3BL	11.0		PSS	DArt	Tunisian108 × Ben 171BC_1F_7 lines (Pirseyedi et al., 2018)
Tunisian108 (durum)	2B	6.0		PSS	DArt	Tunisian108 × Ben 171BC_1F_7 lines (Pirseyedi et al., 2018)
AQ24788-83	7DL	22.0-32.0	gwm428	PSS	DArt, 90K wheat Infinium iSelect SNP arrays	AQ24788-83 × Luke 1652RILs (Ren et al., 2019)
Everest	1BS	6.5-20.1	snp-1B-287267552	PSS, DON content, FDK	GBS SNP	Everest × WB-Cedar 176DH lines (Lemes Da Silva et al., 2019)
Everest	3DS	5.5-7.8	snp-3D-27244923	DON content	GBS SNP	Everest × WB-Cedar 176DH lines (Lemes Da Silva et al., 2019)
Everest	4BL	7.8	snp-4B-44943599	PSS	GBS SNP	Everest × WB-Cedar 176DH lines (Lemes Da Silva et al., 2019)
Everest	5AS	12.6-13.9	snp-5A-436264964	DON content	GBS SNP	Everest × WB-Cedar 176DH lines (Lemes Da Silva et al., 2019)
WB-Cedar	1AS	5.2-9.3	snp-1A-367438030,snp-1A-15978869,snp-1A-511609396	PSS, DON content, FDK	GBS SNP	Everest × WB-Cedar 176DH lines (Lemes Da Silva et al., 2019)

PI277012	5AS	20.0	Xbarc40	PSS, DON content, FDK		PI277017 × WB-Grandin 130DH lines (Chu et al., 2011)
PI277012	5AL	32.0	Xcfd39	PSS, DON content, FDK		PI277017 × WB-Grandin 130DH lines (Chu et al., 2011)
DT696 (durum)	5A	3.8-25.7	Ex_c6161_335, wsnp_Ex_c54193_57155632	PSS	90K wheat Infinium iSelect SNP arrays	DT707 × DT969 432DH lines (Sari et al., 2018)
Blackbird (durum)	1A	11.3-26.8	Tdurum_contig11679_319	PSS	90K wheat Infinium iSelect SNP arrays	Strongfield × Blackbird 102DH lines (Sari et al., 2018)
02-5B-318	2AS	11.0-12.0	IWB63138	incidence, PSS	90K wheat Infinium iSelect SNP arrays	02-5B-318 × Saragolla 135RILs (Giancaspro et al., 2016)
02-5B-318	3AL	9.0-11.0	IWB37509	incidence	90K wheat Infinium iSelect SNP arrays	02-5B-318 × Saragolla 135RILs (Giancaspro et al., 2016)
Saragolla	7AL	8.0-9.0	IWB43304	incidence	90K wheat Infinium iSelect SNP arrays	02-5B-318 × Saragolla 135RILs (Giancaspro et al., 2016)
Saragolla	2BS	8.0-12.0	IWB55365	PSS	90K wheat Infinium iSelect SNP arrays	02-5B-318 × Saragolla 135RILs (Giancaspro et al., 2016)
02-5B-318	5BS	7.0-8.0	IWB816	PSS	90K wheat Infinium iSelect SNP arrays	02-5B-318 × Saragolla 135RILs (Giancaspro et al., 2016)
Yanzhan1	2D	4.7	Xwmc111–Xwmc112	incidence, PSS		Neixiang188 × Yanzhan1 199RILs (Lv et al., 2014)
Yanzhan1	4B	5.7	Xgwm0925–Xgwm0898	incidence, PSS		Neixiang188 × Yanzhan1 199RILs (Lv et al., 2014)
Neixiang188	4D	9.3	Xpsp3007–DFMR2	incidence, PSS		Neixiang188 × Yanzhan1 199RILs (Lv et al., 2014)
Neixiang188	5B	1.0	Xwmc235–Xwmc28	incidence, PSS		Neixiang188 × Yanzhan1 199RILs (Lv et al., 2014)
Neixiang188	5D	12.9	Xgwm292–Vrn-D1	incidence, PSS		Neixiang188 × Yanzhan1 199RILs (Lv et al., 2014)

TC67	5AL	5.2-10.9	cfd6.1-barc48	PSS, incidence, FDK		ACBrio × TC67 100RILs (Malihipour et al., 2016)
TC67	5AL	19.4-20.6	cfd39-cfa2185	PSS, incidence, FDK		ACBrio × TC67 100RILs (Malihipour et al., 2016)
TC67	6A	6.8-11.8	gwm132.1-wmc621	PSS, incidence, FDK		ACBrio × TC67 100RILs (Malihipour et al., 2016)
-	1A	3.2-4.8	IWB24089	PSS	90K wheat Infinium iSelect SNP arrays	Association mapping panel of 213 elite Chinese wheat germplasms (Wu et al., 2019)
-	2BL	3.3-3.8	IWB6480	PSS	90K wheat Infinium iSelect SNP arrays	Association mapping panel of 213 elite Chinese wheat germplasms (Wu et al., 2019)
-	3A	4.0-5.7	IWB50548	PSS	90K wheat Infinium iSelect SNP arrays	Association mapping panel of 213 elite Chinese wheat germplasms (Wu et al., 2019)
-	3B	3.6-6.9	IWB12053	PSS	90K wheat Infinium iSelect SNP arrays	Association mapping panel of 213 elite Chinese wheat germplasms (Wu et al., 2019)
-	3B	3.1-5.8	IWB10842	PSS	90K wheat Infinium iSelect SNP arrays	Association mapping panel of 213 elite Chinese wheat germplasms (Wu et al., 2019)
-	2BL	3.1-7.5	IWB52433	PSS, DON content	90K wheat Infinium iSelect SNP arrays	Association mapping panel of 213 elite Chinese wheat germplasms (Wu et al., 2019)
-	3A	3.4-4.1	IWB50548	DON content	90K wheat Infinium iSelect SNP arrays	Association mapping panel of 213 elite Chinese wheat germplasms (Wu et al., 2019)
-	7A	3.6-5.2	IWA3423	DON content	90K wheat Infinium iSelect SNP arrays	Association mapping panel of 213 elite Chinese wheat germplasms (Wu et al., 2019)

*Ch.: chromosome
**PVE: percentage of variance explained by the QTL
***PSS: percentage of symptomatic spikelets; FDK: *Fusarium* damaged kernels.

Table 1.2 Types of selectable markers used in the breeding programs.

Marker type	Description	Advantages	Disadvantages
Morphological Markers (Classical markers)	The qualities can be visually distinguished. e.g., color or structures.	Easy to use.	Not too many; may be affected by the environment and growth stages.
Cytological Markers (Classical markers)	The markers related to the characters of the chromosomes. e.g., Giemsa stain for G bands.	Easy to find the chromosome level mutations, useful for physical mapping.	Not suitable to find DNA level mutations.
Isozymes/Biochemical Markers (Classical markers)	The different molecular enzymes that have the same catalytic function.	Co-dominant markers. Easy to use. Cost effective.	Low in number. Affected by many factors
RFLP (Restriction Fragment Length Polymorphism)	DNA cut by restriction enzymes. Based on hybridization.	Specific to a single enzyme, co-dominant markers.	Laborious, need large amount of DNA
RAPD (Random Amplified Polymorphic DNA)	The fragment of DNA randomly amplified. Different genotype has various bands patterns.	No need to know the target DNA sequence.	Dominant marker; hard to interpret heterozygotes
AFLP (Amplified Fragment Length Polymorphism)	Digest DNA by using two restriction enzymes, then do PCR to amplify the fragments with both sticky ends.	Cost effective, no need for prior sequence information, reliable	Dominant marker; high-quality DNA required
SSR (Simple Sequence Repeats)	With the information of an SSR library for a species, flanking SSR markers can be designed for a target region. PCR with the SSR primers then can be used for genotyping	Co-dominant markers, high reproducibility, friendly for large genome.	Costly for development, many null alleles, medium genome abundance.
STS (Sequence-Tagged Sites)	a short sequence of DNA can be uniquely amplified by PCR (in a broad sense, contain microsatellites and, ISSRs, SCAPs and CAPs.)	Low cost, co-dominant marker, easy to convert to other marker systems.	The specific unique sequences needed for marker development
ISSR (Inter-Simple Sequence Repeats)	PCR amplify the sequences flanking by simple sequence repeats. One kind of STS.	Low cost, high reliability	Dominant markers

SRAP (Sequence-Related Amplified Polymorphism)	Amplify coding regions only, based on the targeting open reading frames. One kind of STS.	Robust, highly variable, high repeatability	Require known sequence of the coding region, dominant markers
CAPS (Cleaved Amplified Polymorphic Sequences)	Based on the various length caused by SNP or indels for the same restriction enzyme in different individuals, CAPS can be used to genotype. One kind of STS.	Co-dominant markers, easy to score, easy to share between labs	Relatively laborious and costly to use
VNTR (Variable Number Tandem Repeats)	The variation of tandem repeats in individuates causes the length of the repeated sequences, which can be detected after PCR.	Easy to use, cheap	Numbers are limited
SSLP (Simple Sequence Length Polymorphism)	The repeated DNA sequence with different length. By the polymorphisms of the sequence length, they can use for genotyping.	Easy to use, inexpensive	Numbers are limited
SNP (Single Nucleotide Polymorphism)	A marker system that genotype DNA based on single nucleotide polymorphisms. According to this character, diverse testing systems were created.	High throughput, vast application areas	Cost and complexicity depends on platforms used
KASP (Kompetitive Allele Specific PCR)	Based on an SNP sequence, two forward primers and one reverse primer are designed. Then PCR applied to amplify signals for detecting.	High efficiency, can be multiplied together for high throughput testing	Singleplex throughput, relatively low cost per datapoint
RAD (Restriction site-associated DNA)	By using the RAD tag, the DNA sequences adjacently flanking the restriction enzyme, the marker can be used to detect the SNP in different individuals	The vast application can be used for high throughput projects	Costly for assays
DArT (Diversity Arrays Technology)	Diverse DNA primers are stable on a chip, combined with detecting SSR and SNP variations	Vast application suit high throughput projects. Cheap to run.	Dominant markers, need to be done only in one company

STARP (Semi-thermal Asymmetric Reverse PCR)	Use two AMAS-primers (asymmetrically modified allele-specific primers) and one same reverse primer for PCR.	Flexible SNP detection, amplify DNA in repetitive regions, cheaper than KASP	Relatively new, primer design is not strait forward, gel based assays
EST (Expressed sequence tag)	Based on the expressed sequence tag differences to design markers	Detect gene region variance, co-dominant markers	Relatively expensive to find the expressed tags
Retrotransposons	Different types, including IRAP (inter-retrotransposon amplified polymorphism), REMAP (Retrotransposon microsatellite amplification polymorphisms), RBIP (Retrotransposon-based insertion polymorphism)	Easy to use, no need to know the prior sequences. Cheap to run.	Dominant marker, not too many breeding programs use now

Chapter 2 - Pyramiding Wheat *Fusarium* Head Blight Resistance Genes from Different Sources by Marker-Assisted Backcrossing

Introduction

Fusarium head blight (FHB), also called scab, is a devastating disease of wheat, barley and some other cereal crops all over the world. FHB, mainly caused by the pathogen *Fusarium graminearum* in the U.S., can result in severe losses in grain yield and quality, especially when the weather condition is suitable for FHB epidemics (Bai and Shaner, 2004; Dahl and Wilson, 2018). Mycotoxins, particularly deoxynivalenol (DON) also known as vomitoxin, produced by the pathogen can cause human sicknesses, such as vomiting, loss of appetite, stomachache and intestinal disorders, and headache etc. Besides, animals that consumed DON-contaminated feed can suffer feed refusal, vomiting and weight losses (Mayer et al., 2017; Sobrova et al., 2010; Pestka, 2010). Although the application of fungicides and other cultural practices can reduce FHB damage, growing wheat FHB resistant cultivars is still the most effective approach to reduce the losses. Unfortunately, no immune wheat germplasm has been found yet to date (Bai et al., 2018). Most cultivars currently used in production in the U.S. Great Plains are highly susceptible to FHB, and only a few cultivars have partial resistance. Many accessions with different degrees of resistance have been reported worldwide, only a few are highly resistant and most of them are landraces from China and Japan. Those landraces have poor agronomic traits that are not suitable for direct use as parents in U.S. breeding programs (Cai, 2016; Jia et al., 2018; Petersen et al., 2017).

Marker-assisted backcrossing (MABC) is an effective method for transferring desirable trait-associated gene(s) from different sources into a new cultivar. MABC can significantly shorten the time and cost required for background recovery of the recurrent parents during

backcrossing (Gupta et al., 2010, Arunakumari et al., 2016; Somers et al., 2005). Besides, MABC also have the advantages for screening the target recessive genes without generating homozygous lines for phenotypic evaluation (Frisch and Melchinger, 2005; Hasan et al., 2015; Neeraja et al., 2007; Semagn et al., 2014). Since the genotyping cost has been quickly reduced in recent years, MABC has many applications in different breeding programs, such as pyramiding multiple genes for both disease resistance and high yield in a single background (Devi et al., 2017; Gupta et al., 2010; Mundt, 2018).

MABC can also be an effective method for breeding FHB resistant wheat lines. To date more than 150 FHB resistance QTLs have been reported from different sources (Bai et al., 2018; Buerstmayr et al., 2009; Cai, 2016), and only several QTLs show major effects on FHB resistance (Bai et al., 2018). Among them, *Fhb1* is a major gene identified initially from a well-known Chinese spring wheat cultivar 'Sumai 3'. This gene shows a stable effect on FHB resistance in many wheat backgrounds (Gunupuru et al., 2017; Salameh et al., 2011; Steiner et al., 2017). Recently, two groups reported the cloning of *Fhb1* gene which codes a histidine-rich calcium-binding-protein and found that a large deletion in the gene caused phenotypic changes from FHB susceptibility to resistance (Li et al., 2019; Su et al., 2019). Although further evidence is needed to clarify the *Fhb1* gene functions, the diagnostic markers are available for selecting the gene in breeding programs (Lagudah and Krattinger, 2019; Su et al., 2018).

Aside from *Fhb1*, two other QTLs on wheat chromosome 5A have been recently identified from wheat germplasm ‘PI 277012’ that was also reported to show a large effect on FHB resistance (Chu et al., 2011). The QTL on the 5AS chromosome was the same as the *Qfhs.ifa-5A*, while the one on the 5AL chromosome arm was newly reported (Chu et al., 2011). The two QTLs together contribute to a high level of FHB resistance. However, the germplasm

line that carries the two 5A QTLs is not suitable for direct use as a resistant parent for hard winter wheat breeding because it has poor agronomic traits such as tall plant, hard glumes and spring type. Thus, it can be hypothesized that transferring these two 5A QTLs into hard winter wheat backgrounds and pyramiding them with *Fhb1* may provide useful bridge parents for improvement of FHB resistance in hard winter wheat.

Marker-assisted background selection may facilitate quick removal of the donor's genome and recover the recurrent genome to speed up the MABC process. Multiplex restriction amplicon sequencing (MRASeq) is a newly developed, low-cost, PCR based, next-generation-sequencing method that is suitable for background selection (Bernardo et al., 2019). Compared with the traditional GBS methods, the MRAseq has advantages such as having a low cost per sample and using simple assay, which makes it more suitable for most breeding programs. This newly developed genome-wide marker technology can be an alternative to the GBS for breeding applications. Using MRASeq, genome-wide comparisons can be conducted for the genetic similarities between the backcrossed progenies and the recurrent parents to select the lines with target genes and maximum recurrent parental genome.

The objectives of this study are to 1) use MABC to pyramid *Fhb1* with the two QTLs on chromosome 5A, *Qfhs.ifa-5A* on the 5AS chromosome arm and *Qfhb.rwg-5A.2* on the 5AL chromosome arm, into two Kansas hard red winter wheat cultivars, 'Everest' and 'Overland'; 2) evaluate genome composition of backcrossing progenies using MRASeq to select lines with maximum recurrent parent backgrounds to develop locally adapted FHB-resistant hard red winter wheat germplasms. This work will provide useful sources of germplasm for improving FHB resistance in the U.S. hard red winter wheat.

Materials and methods

Plant materials and workflow

'NE106Fhb1' is a resistant hard red winter wheat line carrying the *Fhb1* with a pedigree (ND2928/Wesley*3) developed by USDA Central Small Grain Genotyping Laboratory at Manhattan KS and used as the *Fhb1* donor parent in this study. 'ND2928' is a North Dakota line that was developed by using 'Sumai 3' as the source of *Fhb1* (Bakhsh, 2012). The donor parent of two 5A QTLs is a resistant hard red spring wheat line 'GP-80', which is a double haploid (DH) line from the cross 'Grandin × PI 277012' (Chu et al., 2011). Two recurrent parents were 'Everest' (HBK1064-3/Jaggerw//X960103) and 'Overland' (Millennium sib//Seward/Archer), both are hard red winter wheat cultivars with moderate resistance and moderate susceptibility, respectively to FHB (Eckard et al., 2015; Lemes Da Silva et al., 2019).

Backcross and marker screening

Figure 2.1 is the workflow of the crosses and backcrosses. Briefly, a cross was made between 'NE106Fhb1' and 'GP-80' in the greenhouse at Kansas State University in spring 2015 to combine *Fhb1* with the two QTLs from 5A chromosome. Then the F_1 plants were crossed to 'Everest' and 'Overland', respectively. The derived BC_1F_1 plants from the two crosses were screened using DNA markers that linked to the three QTLs. The marker selected BC_1F_1 plants with all three QTLs were transplanted after vernalization at 6 °C for 50 d and then backcrossed to both recurrent parents, respectively. All BC_1F_1 plants were screened with the same set of markers to identify plants with different numbers of QTLs and the selected plants were selfed to generate homozygous lines for primary phenotyping in the 2017 spring greenhouse experiments. Meanwhile, the selected BC_1F_1 plants with all three QTLs were backcrossed to the recurrent parents again and all the BC_2F_1 plants were screened with markers for all the QTLs. Only the

plants with markers for all three QTLs were selected for selfing. Both BC_2F_2 and BC_1F_2 plants were screened with the same markers for the three QTLs, which resulted in eight types of the homozygous lines with all possible combinations of the three QTLs. These selected lines were transplanted in the greenhouse for seed increasing and FHB phenotyping later in both greenhouse and field experiments.

DNA extraction and marker analysis

A modified cetyl trimethyl ammonium bromide method was used to extract DNA with the aid of the Beckman Biomek NXp Robot (https://hwwgenotyping.ksu.edu/protocols/). For the *Fhb1*, two types of diagnostic markers, one KASP and one STS marker, were used for screening (Su et al., 2018). For the 5AS QTL, two SSR markers, GWM186 and BARC165, were applied as flanking markers for selection. Eight SSR markers linked with the 5AL QTL (WMC479, CFA2163, CFA2185, WMC96, CFD39, GWM179, GWM595, BARC48) were screened for polymorphisms among parents (Chu et al., 2011). Only one marker, BARC48, linked to the QTL was polymorphic between the donor and recurrent parents, and thus was used as selection marker for 5AL QTL in this study. For KASP markers, a 5 µl KASP reaction mix contains 2.5 µl 2X KASP master mix, 0.07 µl KASP primer mix (two forward primers and one reverse primer) and 2.5 µl DNA (~ 20 ng/µl). Polymerase chain reaction (PCR) was done following the manufacturer's instruction (LGC Genomics, www.lgc genomics.com). The KASP marker was scored using the FLUO star® Omega filter based multi-mode microplate reader (BMG Labtech Inc. Cary, NC) and the KlusterCaller™ software (LGC, Middlesex, UK). The STS marker for *Fhb1* was analyzed following Su et al. (2018). For the three SSR markers, the PCR was done in a C1000 Touch™ Thermal Cycler (BioRad Laboratory Inc. Hercules, CA) using the same profile described by Cai (2016). For each sample, a 13 ul of PCR mix contained 30.0 nM tailed forward

primer, 80.0 nM reverse primer, 30 nM M13 Dye labeled primer, 60 ng sample DNA, 0.6 U *Taq* polymerase, 1X ASB buffer, 200.0 μM dNTP and 2.5 mM $MgCl_2$. The PCR products labeled with four different dyes for different markers (FAM, VIC, NED, PET) were pooled and mixed with the size standard that was labeled with the ROX dye and formamide to denature the DNA before loading to the ABI PRISM 3730 DNA Analyzer (Applied Biosystems, Foster City, CA). GeneMarker software v1.75 (SoftGenetics LLC, State College, PA) was used to analyze the marker data.

FHB evaluation in greenhouses

FHB resistance of the BC_2F_3 lines in both backgrounds was evaluated in spring 2018 greenhouse experiment and BC_2F_4 lines were evaluated in fall 2018 and spring 2019 greenhouse experiments at Kansas State University, Manhattan, KS. In these experiments, seeds were planted in 128-cell plastic seedling trays (T.O. Plastics, Clearwater, MN) filled with the Berger BM1 all-purpose soil mix (Hummert International, Topeka, KS). Young seedling leaf tissues at the 3-leaf stage were collected from each plant for DNA extraction. Seedlings were then vernalized in a 6 °C cold room for 50 d before transplanting. Only the selected plants based on marker data were transplanted to 4" X 4" Dura pots with Berger BM1 all-purpose soil mix in the Kansas State University greenhouse. The pots were arranged in a randomized complete block design (RCBD). The plants were watered with the Miracle-Gro water soluble all-purpose plant food (The Scotts Company LLC, Marysville, OH) once a week for the first three weeks. Also, all the pots with wheat plants were fertilized with the Osmocote classic 19-6-12 slow-release fertilizer (The Scotts Company LLC, Marysville, OH). The supplemental greenhouse lights were set for 12 hours from 7:00 to 19:00 during the day, and the temperatures were set at 22 ± 5 °C for daytime and 17 ± 5 °C for nighttime.

Point inoculation was applied for all the plants after flowering to evaluate Type II resistance. The inoculum was prepared using a Kansas *F. graminearum* strain GZ3639 followed Bai et al. (1999). For inoculation, a central spikelet of a wheat spike was injected with a 10 µl spore suspension at ~1000 spores/spike at the flowering stage (around Fakes 10.5) using a Hamilton PB600-1 syringe (Hamilton Company, Reno, NV). After inoculation, plants were moved to a sealed plastic moist chamber to keep 100% humidity for 48-72 h at 22 ± 5 °C. When the necrosis (the symptoms of infection) appeared on the inoculated spikelets, all the plants were moved to the original greenhouse benches for FHB symptom development. Percentage of the symptomatic spikelets (PSS) were recorded for each inoculated plant at 16 d after inoculation according to Equation 2.1.

$$\text{PSS (\%)} = \frac{\textit{Number of symptomatic spikelets in a spike}}{\textit{Total number of spikelets in a spike}} (\times 100) \quad \text{(Equation 2.1)}$$

BC_2F_4 plants were also evaluated for FHB resistance in one field experiments in 2018 - 2019 field growing seasons. The field experiments used the randomized complete block design with two replications at the Rocky Ford FHB Nursery in Kansas State University, Manhattan, KS. About 40 seeds per line were planted in a single row of 1.3 m long in October of the first year. The FHB nursery was inoculated by spreading the *F. graminearum*-infected corn (*Zea mays* L.) kernels on the soil surface twice with one at booting stage (Fakes 8) and another before heading (about Fakes 10.1). After the first inoculation, plots were misted with sprinklers for 3 min per hour daily from 19:00 to 6:00 until early dough stage to create favorable conditions for pathogen spore growing and initiating infection. About 19 to 25 d after heading, depending on temperatures during this period, PSS notes were taken for each line based on their overall performance and checked for the second time three days after the first note.

MRASeq genotyping

MRASeq was used for background selection. An MRASeq library was constructed for all the selected BC_2F_4 lines with all different combinations of the three QTLs and four parents following the methods described by Bernardo et al. (2019). In brief, this method only needs two PCR steps for library construction (Figure 2.2). First PCR amplified wheat genomic DNA using the forward fusion primers which consisted of, from the 5'end, an M13-tail, wheat sequences (sequences with 6-10 nucleotides from the *in silico* amplicon target) and a sequence of *PstI* restriction site. The reverse primers consisted of 6-12 nucleotides of wheat sequences with *MspI* restriction site sequence, and the Ion trP1B adapter sequence. In the second PCR, the forward primer consists of, from 5'to 3' end, the Ion A sequence, barcode sequences, and the M13-tail sequence. The reverse primer is Ion trP1B sequence. The PCR products were size-selected for sequencing in an Ion Torrent Proton sequencer (Thermo Fisher Scientific, Waltham, MA). The SNPs were analyzed from MRASeq data using the TASSEL5 reference pipeline and the wheat Chinese Spring reference genome v1.0 (IWGSC et al., 2018) followed Bernardo et al. (2019). In brief, before using the TASSEL5 reference pipeline, the M13 tail and the specific wheat sequences were removed from all sequences since the TASSEL5 reference pipeline expects each read to include barcode, *PstI* restriction site and genomic sequence from the sample. The read depth of MRAseq was about 5× per marker. The SNPs with less than 20% missing data and more than 5% minor allele frequency were kept for further analysis. All the SNPs were separated into four subgroups based on the combinations of four parental lines, 'Everest/GP-80', 'Everest/NE106Fhb1', 'Overland/GP-80', and 'Overland/NE106Fhb1'. SNP markers in each subgroup were analyzed using the Flapjack software (Milne et al., 2010) to calculate the

similarity between the progeny lines and the corresponding recurrent parents using the default parameters.

Statistical analysis

The two-way ANOVA were conducted using the PROC GLM procedure in the SAS 9.4 (SAS Institute Inc., Cary, NC) using the general linear model that PSS ~ μ + Environment + Genotype + Environment×Genotype + Error, where the μ is the common mean. To analyze the QTL effects, PROC GLM procedure was applied using the general linear model in both backgrounds. Duncan's multiple range test was applied for the multiple comparison among the different genotypes and the recurrent parents. and F-test used 0.05 as a threshold for significance. The independent variables were three QTLs. The independent variable was the PSS value. The model was: PSS ~ μ + A + B + C + A×B+ A×C + B×C + A×B×C + Error, where the A represents the *Fhb1* on chromosomes 3BS, B represents *Qfhb.rwg-5A.2* on 5AL, and C represents *Qfhs.ifa-5A* on 5AS.

The mixed linear model analysis was conducted using the R package "lme4" (R team, 2011). To estimate the variances for broad sense heritability calculation, the model PSS ~ μ + Environment + Line + Environment×Line + Replication (Environment) + Error, were applied. In the model genotype, environment, genotype by environment interaction, replication (environment) were set as random factors. The PSS values of the BC_2F_4 lines from 2018 fall greenhouse experiments and 2019 spring greenhouse experiments were used to calculate heritability. The broad sense heritability was calculated using Equation 2.2 with *e* and *r* representing the numbers of environments and replications within an environment, respectively, σ_G^2 representing the genetic variance, σ_{GE}^2 representing the variance caused by G×E, and σ_e^2 representing the variance caused by random error.

$$H^2 = \frac{\sigma_G^2}{\sigma_G^2 + (\sigma_{GE}^2/e) + (\sigma_e^2/re)}$$ (Equation 2.2)

Results

Selection of lines with different combinations of the three QTLs using MABC

Since fall 2016, 5127 plants (598 plants in fall 2016, 1472 plants in spring 2017, 2576 plants in fall 2017, 302 plants in spring 2018; 179 plants in fall 2018) have been screened with the same set DNA markers for the three QTLs in different generations of backcrossing and selfing. In the spring 2018, 94 BC_2F_3 lines in 'Everest' background and 84 BC_2F_3 lines in 'Overland' backgrounds with different allele combinations at the three QTLs were selected for phenotyping (Table 2.1). The broad sense heritability for all the 'Overland' background lines was 0.75 using the PSS data from the three greenhouse experiments, while the 'Everest' background was 0.61.

All the selected BC_2F_3 lines have different numbers of QTLs they carried in each recurrent parental background. In total, 71 lines carried the desired allele at only one of the three QTLs (AAbbcc, aaBBcc, aabbCC) has 41 lines in 'Everest' background and 30 lines in 'Overland' background. Seventy-four lines carried desirable alleles at two of the three QTLs (AABBcc, AAbbCC, and aaBBCC) in each line, which has 40 lines in the 'Everest' background and 34 lines in the 'Overland' background. Seventeen lines contained three desirable alleles at all the three QTLs (AABBCC), which has seven lines with the 'Everest' background and eight lines with the 'Overland' background. Eighteen lines did not carry any desirable allele at the three QTLs (aabbcc) and had six lines in the 'Everest' background and 12 lines in the 'Overland' background.

FHB performance of the selected lines in the greenhouse

In general, plants in 'Overland' background showed better resistance than the lines in 'Everest' background when the PSS from the three greenhouse experiments were averaged (Figure 2.3 and 2.4), which is consistent with the mean PSS of the two corresponding parents. In 'Everest' background, the lines with resistance QTLs showed significant lower PSS than the lines without any of the three QTLs. The lines with *Fhb1* had a significantly higher resistance than the lines without *Fhb1*. The lines with all three QTLs had the lowest PSS value but not significantly different from these lines with *Fhb1* only. The lines with *Fhb1*, the lines with both *Qfhb.rwg-5A.2* on 5AL and *Qfhs.ifa-5A on* 5AS showed better resistance than the 'Everest' parent lines. The lines with only *Qfhb.rwg-5A.2* on 5AL or *Qfhs.ifa-5A on* 5AS did not have significant less PSS than the 'Everest' parent.

In 'Overland' background, the lines with *Fhb1* and 5AL QTL together had the lowest PSS value. All the lines with the *Fhb1* gene and the lines with only the *Qfhb.rwg-5A.2* on 5AL performed better than 'Overland' the other genotype lines.

The recovered genome of the recurrent parents in the selected lines

Using the MRAseq, 670 SNPs in total were polymorphic in at least one subgroup based on the combination of four parental lines: 'Everest/GP-80', 'Everest/NE106Fhb1', 'Overland/GP-80', 'Overland/NE106Fhb1', all distributed across 21 wheat chromosomes. 347 SNPs between 'Everest' and 'GP-80', 202 SNPs between 'Everest' and 'NE106Fhb1', 288 SNPs between 'Overland' and 'GP-80' and 206 SNPs between 'Overland' and 'NE106Fhb1' (Figure 2.7). The similarities of each line to the recurrent parents were calculated using the SNPs from each subgroup (Figure 2.8).

The mean similarity of progenies to 'Everest' was 0.82, ranging from 0.64 to 0.98, which was slightly lower than the expected 0.875 for two backcrosses. In the 'Overland' background, the similarity of progeny to the recurrent parent was slightly higher (0.87), ranging from 0.71 to 0.97. For 'Everest' background lines, no significant ($P > 0.05$) correlations were detected between the similarity and the test trait values (including PSS and some agronomic traits). The same was true for the PSS in the lines with 'Overland' backgrounds. However, spikelet length (r = 0.35, $P = 0.002$) and heading date (r = 0.37, $P = 0.002$) were positively correlated with the similarity of the lines in Overland background, and number of spikelets per spike is negatively correlated with the similarity (r = -0.29, $P = 0.01$).

Discussion

The effects of the three QTLs in two HWW backgrounds

FHB resistance is a quantitative trait and conditioned by a few major resistance genes and many minor resistance genes (Bai et al., 2018). In this study, we pyramided three QTLs into two different hard winter wheat genetic backgrounds and investigated their effects on Type II resistance when they were alone or in combinations. All three QTLs significantly ($P < 0.05$) lowered the PSS in three greenhouse experiments, but with unequal effects (Table 2.2 and Table 2.3).

In both backgrounds, the lines containing *Fhb1* had lower PSS compared to these lines without *Fhb1*, indicating that *Fhb1* showed the major effect on Type II resistance in both genetic backgrounds. In the 'Everest' background, the lines with all three QTLs give the smallest PSS value, while in the 'Overland' background the lines with *Fhb1* and *Qfhb.rwg-5A.2* showed the lowest PSS. These results agree with the previous reports that *Fhb1* showed a large effect on Type II resistance in many different backgrounds (Kang et al., 2011; Cai, 2016; Fatima, 2016).

The QTL on 5AS chromosome arm has been considered to be the same as *Qfhs.ifa-5A* (*Fhb5*) region (Bai et al., 2018; Chu et al., 2011; Somers et al., 2003). This QTL was demonstrated to show Type II resistance in some reports (Chu et al., 2011; Xue et al., 2011; Zhang et al., 2018), and Type I resistance in the others (Brar et al., 2019; Xue et al., 2011). In this study, *Qfhs.ifa-5A* had a significant effect on Type II resistance in the 'Everest' background, which reduced 31.1% of PSS compared to these lines without the QTL (Figure 2.3). QTL mapping did not detect any QTL for low PSS on the chromosome arm 5AS in 'Everest' (Lemes Da Silva et al., 2019). Only one QTL for low DON was reported, but was in a different location (Lemes Da Silva et al., 2019). In the 'Overland' background, however, the effect of *Qfhs.ifa-5A* was not significant for type II resistance. The lines carrying only *Qfhs.ifa-5A* appeared to have similar PSS to. If not higher than, the PSS of 'Overland' parent, which suggests that 'Overland' may carry a resistance allele at the *Qfhs.ifa-5A* locus as reported by Eckard et al. (2015). However, further mapping study is needed to confirm the assumption.

Attempt has been made to pyramid *Qfhs.ifa-5A* with *Fhb1* in two spring wheat cultivars. They found that the lines with both *Fhb1* and *Qfhs.ifa-5A* showed the lowest FHB severity and DON content (Miedaner et al., 2006), which not always agree with the results from the current study. The discrepancy may be due to the inoculation methods in the two studies. We used point injection in the greenhouse and spawn-infection in the field, whereas Miedaner et al. sprayed spores in field experiments. The result from this study showed that the addition of *Qfhs.ifa-5A* to *Fhb1* in 'Overland' background did not always increase the resistance of the plants. Similar results were also observed in a MAS project by combining the 5AS QTL with QTLs on 2D, 4B and 3BS into three elite Canadian spring wheat germplasms (McCartney et al., 2007). The

combination of 3BS and 5AS QTLs were not always gave the best performance for FHB resistance and it depends on background where these two genes are moved to.

QTLs on the 5AL was reported from 'Renan', 'Arina', 'TC67' and 'PI277012' in several previous studies (Liu et al., 2009; Schnurbusch et al., 2003; Chu et al., 2011). The QTL on the 5AL chromosome used in this study was formerly reported as *Qfhb.rwg-5A.2* from 'PI277012' (Chu et al., 2011), and was reported to show a large effect on Type II resistance in both spring wheat and durum wheat (Buerstmayr et al., 2009; Chu et al., 2011; Zhao et al., 2018). In the current study, *Qfhb.rwg-5A.2* performed differently in the two backgrounds: it reduced 20.5% of PSS in 'Everest' background and 50.5% of PSS in 'Overland' background compared to the corresponding lines without any of the three QTLs (Figure 2.3 and 2.4). In the 'Overland' background, the effects of *Qfhb.rwg-5A.2* was significantly higher than *Qfhs.ifa-5A*, while the difference in PSS was not significant between the two QTLs in the 'Everest' background. These results suggested that in the hard winter wheat genetic backgrounds, *Qfhb.rwg-5A.2* may perform differently in different backgrounds for the Type II resistance. There might be epistasis effects among the resistant genes and the recurrent parents backgrounds.

Responses of two genetic backgrounds to environmental variations

In this study, we mainly focused on the Type II resistances of FHB, the resistance to FHB spread within the spike. The phenotyping environments significantly affected FHB resistance in both field and greenhouse conditions (Tables 2.2 and 2.3). It was observed that the environmental effects on PSS were different between the two backgrounds, as the G by E effects were statistically significant for the lines with 'Everest' background while not significant for the lines with 'Overland' background (Tables 2.2 and 2.3). For the lines with 'Everest' background, all the lines with different combinations of the three resistance QTLs were performed differently

in the three greenhouse experiments (Figure 2.5), whereas the progenies without *Fhb1* (except for the lines with only *Qfhb.rwg-5A.2*) in 'Overland' were always more susceptible than other genotypes. At the same time, the line had only *Fhb1* and the lines with *Fhb1* plus the *Qfhb.rwg-5A.2* always had better Type II resistance than others in all the greenhouse experiments (Figure 2.6). Two recurrent parents may be responsible for this discrepancy because several studies also reported that the genetic background differences could result in different performances in different experiments (Bai et al., 2001; Buerstmayr et al., 2003).

Performance of selected resistant lines

Based on the marker data, similarity analysis, and the phenotypic data from the three greenhouse and one field experiments, 11 lines in the 'Overland' background and 9 lines in the 'Everest' background were selected as the best lines for further agronomic performance tests (Table 2.4). All the selected lines have the similar agronomic traits with the corresponding recurrent parents (plant height differences within 15 cm, spike length differences within 2 cm differences, heading time differences within 2 weeks, and number of spikelet per spike within 6 differences)

The selected lines all had relatively lower PSS than their corresponding parents in all three phenotyping experiments. Since markers used in this project were not all diagnostic markers for the resistance genes, not all the lines with the resistant QTLs were selected. All the lines were selected based on performance in the greenhouse and field and the genetic marker results.

The marker for *Fhb1* used in this study is a diagnostic marker that was designed based on the causal mutation in the gene (Su et al., 2018) and have been successfully used in many breeding programs for transferring *Fhb1* to locally adapted new cultivars. However, for the two

QTLs on the 5A chromosome, diagnostic markers are not available since the genes have not cloned yet. In particular, for *Qfhb.rwg-5A.2*, the QTL region covered 40.6 cM in the original report (Chu et al., 2011). Further fine mapping result is not available. The marker Xcfd39 at the QTL peak was not polymorphic between parents in the current study. The genetic markers we applied for selection may be still far from the causal genes, thus the low effect of the QTL could be due to recombination between markers and the function gene of the QTL. Thus, to improve selection efficiency, better functional markers are needed for selecting the QTL in breeding.

Besides MABC, a phenotypic selection of the agronomic traits and PSS was also applied for all the lines to find the ones that carried target QTLs and had the most similar background genome to the recurrent parents. The background similarity testing in this study was done using a newly developed next-generation sequencing method (Bernardo et al., 2019). The detected polymorphic (at least in one in at least one of four subgroups: 'Everest' and 'GP-80', 'Everest' and 'NE106Fhb1', 'Overland' and 'GP-80' and 'Overland' and 'NE106Fhb1') markers were mainly distributed on all the wheat chromosomes (Figure 2.7). However, on some chromosomes, the markers were not evenly distributed. This may because the lines were generated from the backcross and the most recombination tends to occur in the non-centromere euchromatin regions of chromosomes (Jordan et al., 2018; Wijnker et al., 2013).

In this study, we used MABC to transfer three major FHB resistance QTLs: *Fhb1* on chromosome arm 3BS, *Qfhs.ifa-5A* on chromosome arm 5AS, and *Qfhb.rwg-5A.2* on chromosome arm 5AL into two Kansas hard winter wheat cultivars, 'Everest' and 'Overland'. At the same time, we also applied MRASeq for background selection to develop locally adapted FHB-resistant hard winter wheat germplasm lines. After two backcrosses, near 100 lines with eight possible combinations of the three genes were selected by gene-linked markers. The

marker-selected lines were analyzed using MRASeq to further select the lines with the least backgrounds from the donor parents. The PSS data from the phenotyping experiments revealed that the lines with all the three QTLs have the better resistance in both backgrounds compared with the corresponding recurrent parents, indicated that adding multiple resistant QTLs into the same background can increase the Type II resistance. However, the Type II resistance from the different QTL combinations varied with backgrounds. Ten lines with 'Overland' background and nine lines with 'Everest' background were selected germplasms with an improved FHB resistance and agronomic traits that can be used as FHB resistant germplasms for genetic improvement of the FHB resistance in hard winter wheat breeding programs.

References

Arunakumari, K., Durgarani, C. V., Satturu, V., Sarikonda, K. R., Chittoor, P. D. R., Vutukuri, B., Laha, G.S., Nelli, A.P.K., Gattu, S., Jamal, M. & Prasadbabu, A. (2016). Marker-assisted pyramiding of genes conferring resistance against bacterial blight and blast diseases into Indian rice variety MTU1010. Rice Science, 23(6), 306-316.

Bai, G., & Shaner, G. (2004). Management and resistance in wheat and barley to *Fusarium* head blight. Annual Review of Phytopathology, 42, 135-161.

Bai, G., Kolb, F. L., Shaner, G., & Domier, L. L. (1999). Amplified fragment length polymorphism markers linked to a major quantitative trait locus controlling scab resistance in wheat. Phytopathology, 89(4), 343-348.

Bai, G., Su, Z., & Cai, J. (2018). Wheat resistance to *Fusarium* head blight. Canadian Journal of Plant Pathology, 40(3), 336-346.

Bakhsh, A. (2012). Breeding hard red winter wheat (*Triticum aestivum* L.) for *Fusarium* head blight (FHB) resistance with the *Fhb1* gene. Doctoral dissertation, The University of Nebraska-Lincoln, Lincoln, Nebraska. https://digitalcommons.unl.edu/dissertations/AAI3504927/.

Brar, G. S., Pozniak, C. J., Kutcher, H. R., & Hucl, P. J. (2019). Evaluation of Fusarium head blight resistance genes *Fhb1*, *Fhb2*, and *Fhb5* introgressed into elite Canadian hard red spring wheats: effect on agronomic and end-use quality traits and implications for breeding. Molecular Breeding, 39(3), 44.

Bernardo, A., Amand, P. S., Le, H. Q., Su, Z., & Bai, G. (2019). Multiplex Restriction Amplicon Sequencing (MRAS eq), a novel next generation sequencing based marker platform for

high-throughput genotyping. Plant Biotechnology Journal, Pp.1-14. https://doi.org/10.1111/pbi.13192.

Buerstmayr, H., Stierschneider, M., Steiner, B., Lemmens, M., Griesser, M., Nevo, E., & Fahima, T. (2003). Variation for resistance to head blight caused by *Fusarium graminearum* in wild emmer (*Triticum dicoccoides*) originating from Israel. Euphytica, 130(1), 17-23.

Cai, J. (2016). Meta-analysis of QTL for *Fusarium* head blight resistance in Chinese wheat landraces using genotyping by sequencing. Doctoral dissertation, Kansas State University, Manhattan, KS. https://krex.k-state.edu/dspace/handle/2097/32166.

Chu, C., Niu, Z., Zhong, S., Chao, S., Friesen, T. L., Halley, S., Elias, E.M., Dong, Y., Faris, J.D. & Xu, S. S. (2011). Identification and molecular mapping of two QTLs with major effects for resistance to *Fusarium* head blight in wheat. Theoretical and Applied Genetics, 123(7), 1107-1119.

Dahl, B., & Wilson, W. W. (2018). Risk premiums due to *Fusarium* Head Blight (FHB) in wheat and barley. Agricultural Systems, 162, 145-153.

Devi, E. L., Devi, C. P., Kumar, S., Sharma, S. K., Beemrote, A., Chongtham, S. K., Singh, C.H., Tania, C., Singh, T.B., Ningombam, A. & Akoijam, R. (2017). Marker assisted selection (MAS) towards generating stress tolerant crop plants. Plant Gene, 11, 205-218.

Eckard, J. T., Gonzalez-Hernandez, J. L., Caffe, M., Berzonsky, W., Bockus, W. W., Marais, G. F., & Baenziger, P. S. (2015). Native *Fusarium* head blight resistance from winter wheat cultivars 'Lyman,''Overland,''Ernie,'and 'Freedom'mapped and pyramided onto 'Wesley'-Fhb1 backgrounds. Molecular Breeding, 35(1), 6. https://doi.org/10.1007/s11032-015-0200-1.

Fatima, N. (2016). Identification and deployment of QTL for *Fusarium* head blight resistance in US hard winter wheat. Master dissertation, Kansas State University, Manhattan, KS. https://krex.k-state.edu/dspace/handle/2097/32679.

Frisch, M., & Melchinger, A. E. (2005). Selection theory for marker-assisted backcrossing. Genetics, 170(2), 909-917.

Gunupuru, L. R., Perochon, A., & Doohan, F. M. (2017). Deoxynivalenol resistance as a component of FHB resistance. Tropical Plant Pathology, 42(3), 175-183.

Gupta, P. K., Langridge, P., & Mir, R. R. (2010). Marker-assisted wheat breeding: present status and future possibilities. Molecular Breeding, 26(2), 145-161.

Hasan, M. M., Rafii, M. Y., Ismail, M. R., Mahmood, M., Rahim, H. A., Alam, M. A., Ashkani, S., Malek, M.A. & Latif, M. A. (2015). Marker-assisted backcrossing: a useful method for rice improvement. Biotechnology & Biotechnological Equipment, 29(2), 237-254.

IWGSC, International Wheat Genome Sequencing Consortium, Appels, R., Eversole, K., Feuillet, C., Keller, B., Rogers, J., Stein, N., Pozniak, C.J., Choulet, F., Distelfeld, A., Poland, J. & Ronen, G. (2018). Shifting the limits in wheat research and breeding using a fully annotated reference genome. Science, 361(6403), eaar7191.

Jia, H., Zhou, J., Xue, S., Li, G., Yan, H., Ran, C., Zhang, Y., Shi, J., Jia, L., Wang, X. & Luo, J. (2018). A journey to understand wheat *Fusarium* head blight resistance in the Chinese wheat landrace Wangshuibai. The Crop Journal, 6(1), 48-59.

Jordan, K. W., Wang, S., He, F., Chao, S., Lun, Y., Paux, E., Sourdille, P., Sherman, J., Akhunova, A., Blake, N.K. & Pumphrey, M. O. (2018). The genetic architecture of genome-wide recombination rate variation in allopolyploid wheat revealed by nested association mapping. The Plant Journal, 95(6), 1039-1054.

Kang, J., Clark, A., Sanford, D. V., Griffey, C., Brown-Guedira, G., Dong, Y., Murphy, J.P. & Costa, J. (2011). Exotic scab resistance quantitative trait loci effects on soft red winter wheat. Crop Science, 51(3), 924-933.

Lagudah, E. S., & Krattinger, S. G. (2019). A new player contributing to durable *Fusarium* resistance. Nature Genetics, 51(7), 1070-1071.

Lemes Da Silva, C. L., Fritz, A., Clinesmith, M., Poland, J., Dowell, F., & Peiris, K. (2019). QTL mapping of *Fusarium* head blight resistance and deoxynivalenol accumulation in the Kansas wheat variety 'Everest'. Molecular Breeding, 39(3), 35. https://doi.org/10.1007/s11032-019-0937-z.

Li, G., Zhou, J., Jia, H., Gao, Z., Fan, M., Luo, Y., Zhao, P., Xue, S., Li, N., Yuan, Y. & Ma, S. (2019). Mutation of a histidine-rich calcium-binding-protein gene in wheat confers resistance to *Fusarium* head blight. Nature Genetics, 51, 1106-1112.

Liu, S., Hall, M. D., Griffey, C. A., & McKendry, A. L. (2009). Meta-analysis of QTL associated with Fusarium head blight resistance in wheat. Crop Science, 49(6), 1955-1968.

Mayer, E., Novak, B., Springler, A., Schwartz-Zimmermann, H. E., Nagl, V., Reisinger, N., Hessenberger, S. & Schatzmayr, G. (2017). Effects of deoxynivalenol (DON) and its microbial biotransformation product deepoxy-deoxynivalenol (DOM-1) on a trout, pig, mouse, and human cell line. Mycotoxin Research, 33(4), 297-308.

McCartney, C. A., Somers, D. J., Fedak, G., DePauw, R. M., Thomas, J., Fox, S. L., Humphreys, D.G., Lukow, O., Savard, M.E., McCallum, B.D. & Gilbert, J. (2007). The evaluation of FHB resistance QTLs introgressed into elite Canadian spring wheat germplasm. Molecular Breeding, 20(3), 209-221.

Miedaner, T., Wilde, F., Steiner, B., Buerstmayr, H., Korzun, V., & Ebmeyer, E. (2006). Stacking quantitative trait loci (QTL) for *Fusarium* head blight resistance from non-adapted sources in a European elite spring wheat background and assessing their effects on deoxynivalenol (DON) content and disease severity. Theoretical and Applied Genetics, 112(3), 562-569.

Milne, I., Shaw, P., Stephen, G., Bayer, M., Cardle, L., Thomas, W. T., Flavell, A.J. & Marshall, D. (2010). Flapjack-graphical genotype visualization. Bioinformatics, 26(24), 3133-3134.

Mundt, C. C. (2018). Pyramiding for resistance durability: theory and practice. Phytopathology, 108(7), 792-802.

Neeraja, C. N., Maghirang-Rodriguez, R., Pamplona, A., Heuer, S., Collard, B. C., Septiningsih, E. M., Vergara, G., Sanchez, D., Xu, K., Ismail, A.M. & Mackill, D. J. (2007). A marker-assisted backcross approach for developing submergence-tolerant rice cultivars. Theoretical and Applied Genetics, 115(6), 767-776.

Perochon, A., Kahla, A., Vranić, M., Jia, J., Malla, K. B., Craze, M., Wallington, E. & Doohan, F. M. (2019). A wheat NAC interacts with an orphan protein and enhances resistance to *Fusarium* Head Blight disease. Plant Biotechnology Journal. https://doi.org/10.1111/pbi.13105.

Pestka, J. (2010). Toxicological mechanisms and potential health effects of deoxynivalenol and nivalenol. World Mycotoxin Journal, 3(4), 323-347.

Petersen, S., Lyerly, J. H., McKendry, A. L., Islam, M. S., Brown-Guedira, G., Cowger, C., Dong, Y. & Murphy, J. P. (2017). Validation of *Fusarium* head blight resistance QTL in US winter wheat. Crop Science, 57(1), 1-12.

Salameh, A., Buerstmayr, M., Steiner, B., Neumayer, A., Lemmens, M., & Buerstmayr, H. (2011). Effects of introgression of two QTL for *fusarium* head blight resistance from Asian spring wheat by marker-assisted backcrossing into European winter wheat on *fusarium* head blight resistance, yield and quality traits. Molecular Breeding, 28(4), 485-494.

Schnurbusch, T., Paillard, S., Fossati, D., Messmer, M., Schachermayr, G., Winzeler, M., & Keller, B. (2003). Detection of QTLs for Stagonospora glume blotch resistance in Swiss winter wheat. Theoretical and Applied Genetics, 107(7), 1226-1234.

Semagn, K., Babu, R., Hearne, S., & Olsen, M. (2014). Single nucleotide polymorphism genotyping using Kompetitive Allele Specific PCR (KASP): overview of the technology and its application in crop improvement. Molecular Breeding, 33(1), 1-14.

Sobrova, P., Adam, V., Vasatkova, A., Beklova, M., Zeman, L., & Kizek, R. (2010). Deoxynivalenol and its toxicity. Interdisciplinary Toxicology, 3(3), 94-99.

Somers, D. J., Thomas, J., DePauw, R., Fox, S., Humphreys, G., & Fedak, G. (2005). Assembling complex genotypes to resist *Fusarium* in wheat (*Triticum aestivum* L.). Theoretical and Applied Genetics, 111(8), 1623-1631.

Steiner, B., Buerstmayr, M., Michel, S., Schweiger, W., Lemmens, M., & Buerstmayr, H. (2017). Breeding strategies and advances in line selection for *Fusarium* head blight resistance in wheat. Tropical Plant Pathology, 42(3), 165-174.

Su, Z., Bernardo, A., Tian, B., Chen, H., Wang, S., Ma, H., Cai, S., Liu, D., Zhang, D., Li, T. & Trick, H. (2019). A deletion mutation in *TaHRC* confers *Fhb1* resistance to *Fusarium* head blight in wheat. Nature Genetics, 51, 1099-1105.

Su, Z., Jin, S., Zhang, D., & Bai, G. (2018). Development and validation of diagnostic markers for *Fhb1* region, a major QTL for *Fusarium* head blight resistance in wheat. Theoretical and Applied Genetics, 131(11), 2371-2380.

Wijnker, E., James, G. V., Ding, J., Becker, F., Klasen, J. R., Rawat, V., Rowan, B.A., de Jong, D.F., de Snoo, C.B., Zapata, L. & Huettel, B. (2013). The genomic landscape of meiotic crossovers and gene conversions in *Arabidopsis thaliana*. Elife, 2, e01426.

Xue, S., Xu, F., Tang, M., Zhou, Y., Li, G., An, X., Lin, F., Xu, H., Jia, H., Zhang, L. & Kong, Z. (2011). Precise mapping *Fhb5*, a major QTL conditioning resistance to *Fusarium* infection in bread wheat (*Triticum aestivum* L.). Theoretical and Applied Genetics, 123(6), 1055-1063.

Zhang, W., Francis, T., Gao, P., Boyle, K., Jiang, F., Eudes, F., Cuthbert, R., Sharpe, A. & Fobert, P. R. (2018). Genetic characterization of type II *Fusarium* head blight resistance derived from transgressive segregation in a cross between Eastern and Western Canadian spring wheat. Molecular Breeding, 38(1), 13. https://doi.org/10.1007/s11032-017-0761-2.

Zhao, M., Leng, Y., Chao, S., Xu, S. S., & Zhong, S. (2018). Molecular mapping of QTL for *Fusarium* head blight resistance introgressed into durum wheat. Theoretical and Applied Genetics, 131(9), 1939-1951.

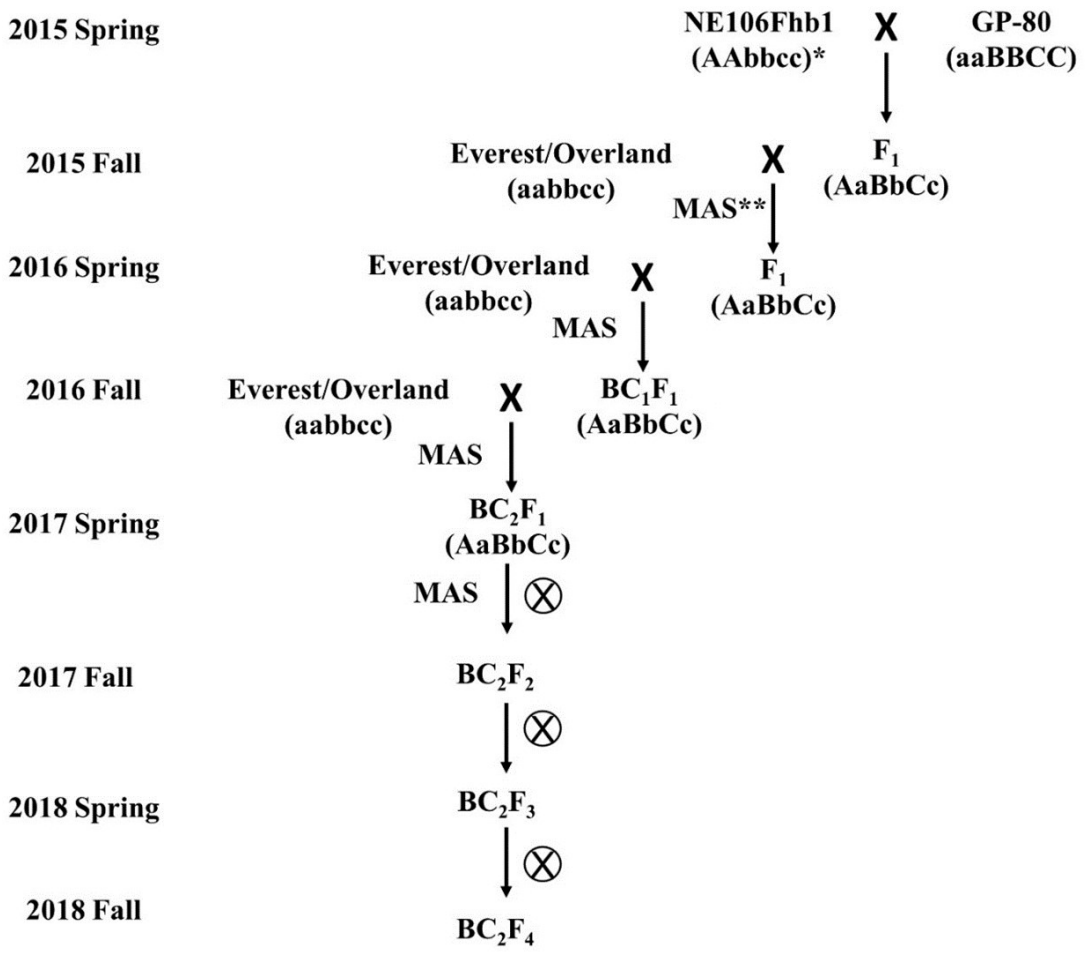

Figure 2.1 The workflow for marker-assisted backcrossing (MABC).

Left column is the experimental years and seasons when the work (right) was done.

* AA, BB and CC represent quantitative trait locus (QTL)s *Fhb1* on chromosomes 3BS, *Qfhb.rwg-5A.2* on 5AL and *Qfhs.ifa-5A on* 5AS respectively; while aa, bb and cc represent susceptibility alleles at the three QTLs. 'AaBbCc' refers to the heterozygotes at all the three QTLs.

**MAS stands for marker-assisted selection.

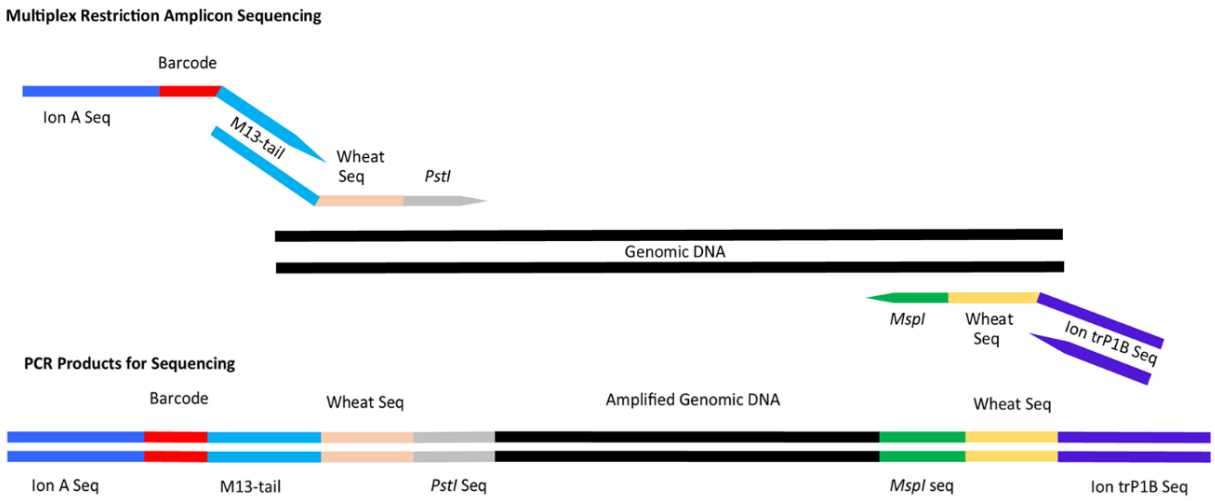

Figure 2.2 A diagram for MRASeq showing primer sequences used for two PCR steps (up) and final PCR products for sequencing.

The primers for the first PCR include a forward primer consisting of, from the 3'-end, wheat sequence (restriction site and its adjacent sequences) and an M13-tail sequence, and a reverse primer consisting of wheat sequence (restriction site and its adjacent sequences) and the Ion trP1B sequence; the primers for the second PCR include a forward fusion primer consisting of, from 5'-end, the Ion A sequence, barcode, and an M13-tail sequence, and the reverse primer is Ion trP1B primer.

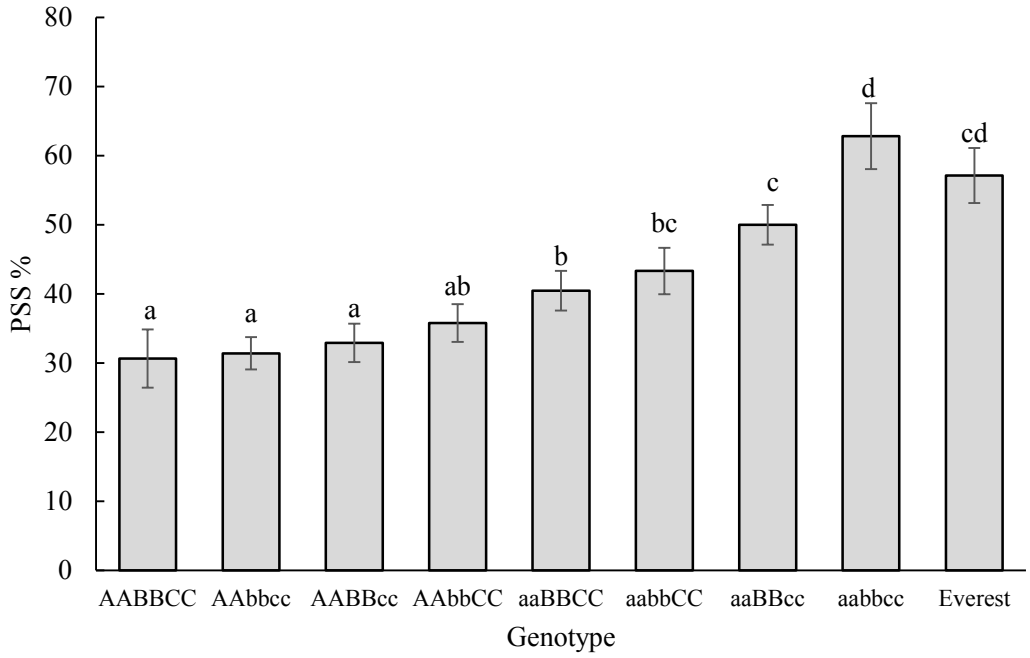

Figure 2.3 The mean percentage of symptomatic spikelets in a spike (PSS) of selected lines in 'Everest' background evaluated in the spring and fall 2018, and spring 2019 greenhouse experiments.

The error bars represent the standard error of each genotype. AA, BB and CC represent resistance alleles at *Fhb1* on chromosomes 3BS, *Qfhb.rwg-5A.2* on 5AL and *Qfhs.ifa-5A on* 5AS, respectively. while aa, bb and cc represent susceptibility alleles at the three QTLs.

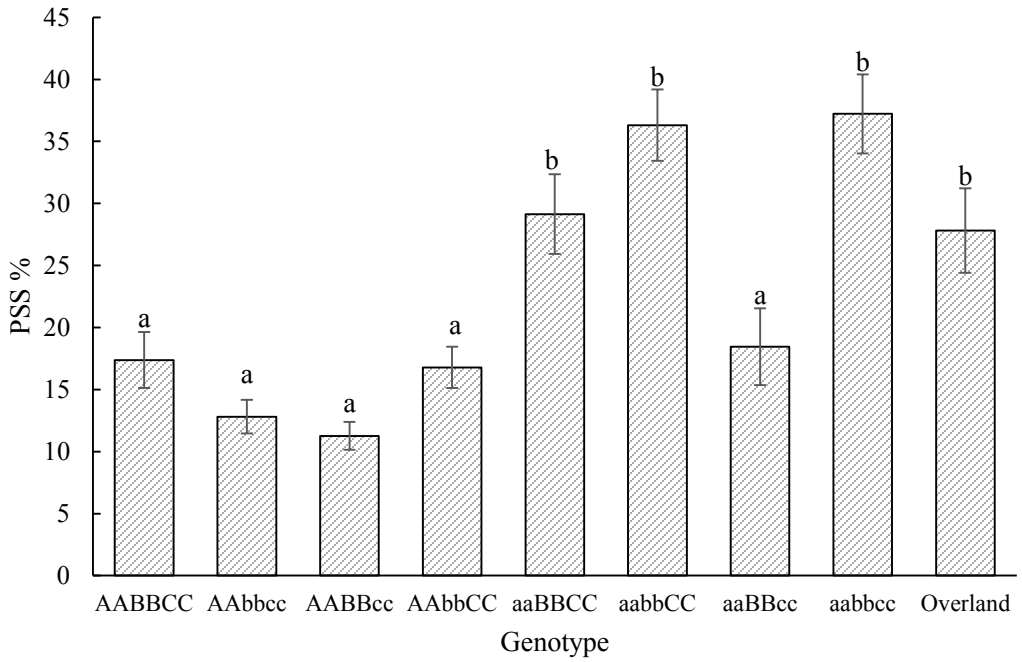

Figure 2.4 The mean percentage of symptomatic spikelets in a spike (PSS) of selected BC_2F_4 lines in 'Overland' background evaluated in the spring and fall 2018, and spring 2019 greenhouse experiments.

The error bars represent the standard error of each genotype. AA, BB and CC represent resistance alleles at *Fhb1* on chromosomes 3BS, *Qfhb.rwg-5A.2* on 5AL and *Qfhs.ifa-5A on* 5AS, respectively. while aa, bb and cc represent susceptibility alleles at the three QTLs.

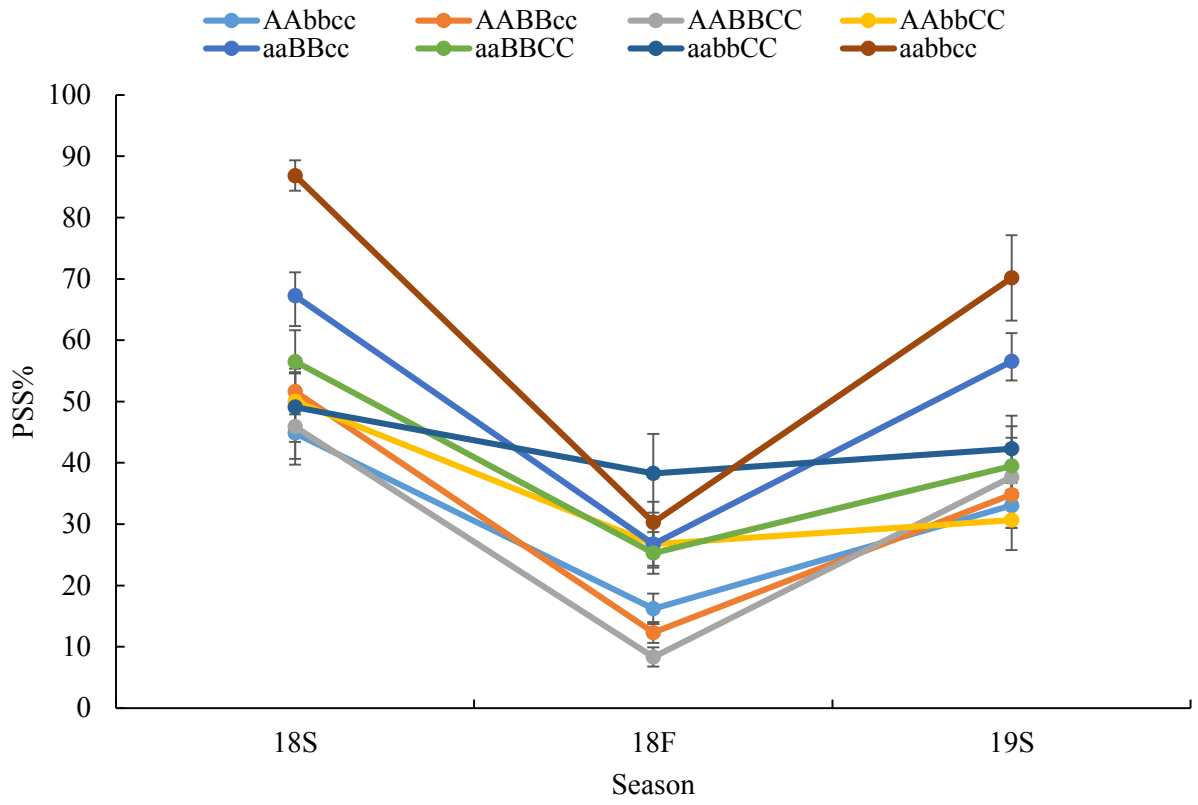

Figure 2.5 Mean percentage of symptomatic spikelets in a spike (PSS) of selected lines with 'Everest' background evaluated in greenhouse experiments of spring 2018 (18S), fall 2018 (18F) and spring 2019 (19S).

AA, BB and CC represent resistance alleles at *Fhb1* on chromosomes 3BS, *Qfhb.rwg-5A.2* on 5AL and *Qfhs.ifa-5A on* 5AS, respectively. while aa, bb and cc represent susceptibility alleles at the three QTLs. Error bars represent the standard errors.

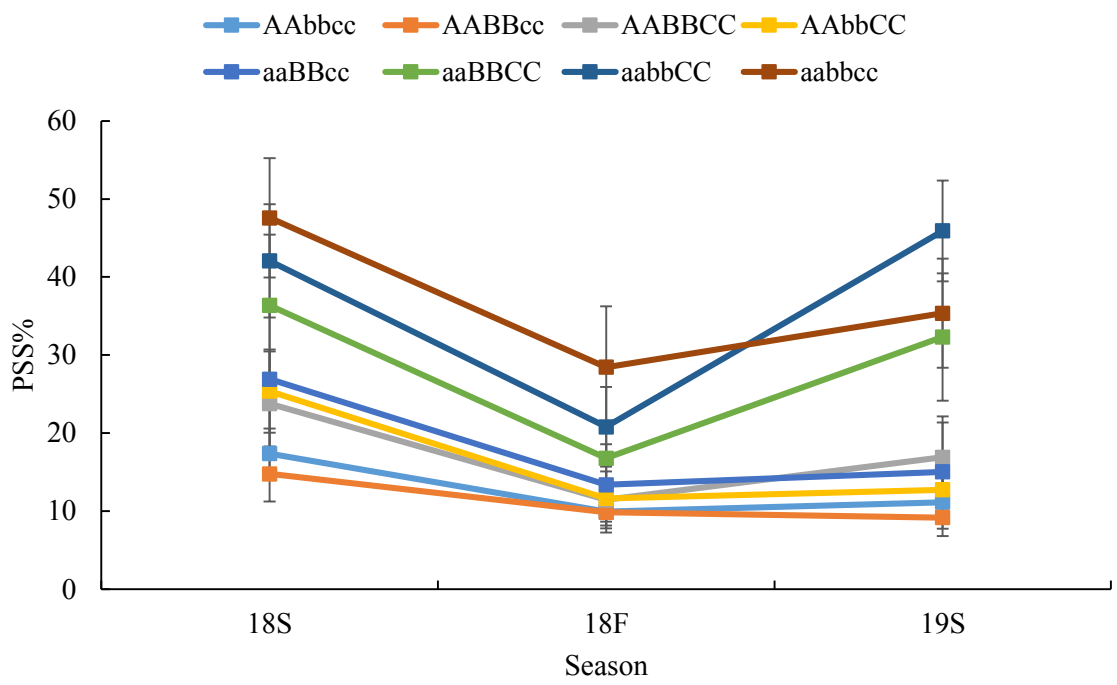

Figure 2.6 Mean percentage of symptomatic spikelets in a spike (PSS) of selected lines with 'Overland' background evaluated in greenhouse experiments of spring 2018 (18S), fall 2018 (18F) and spring 2019 (19S).

AA, BB and CC represent resistance alleles at *Fhb1* on chromosomes 3BS, *Qfhb.rwg-5A.2* on 5AL and *Qfhs.ifa-5A on* 5AS, respectively. while aa, bb and cc represent susceptibility alleles at the three QTLs. Error bars represent the standard errors.

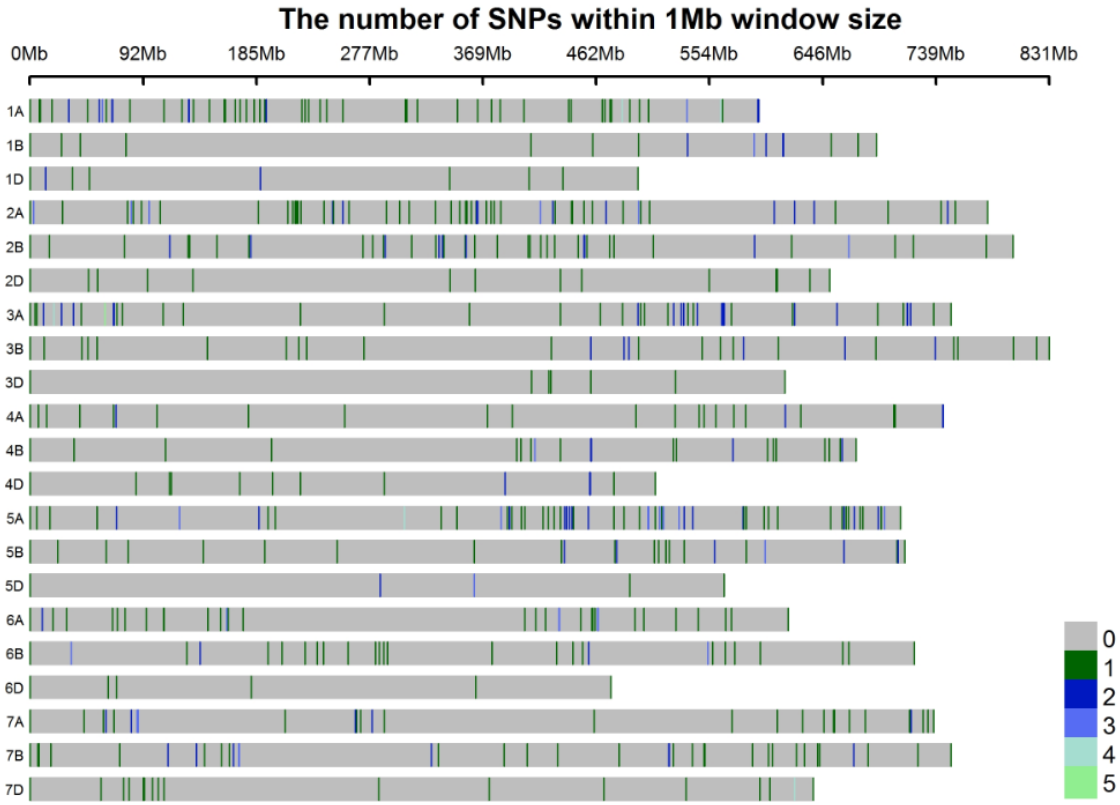

Figure 2.7 Distribution of single nucleotide polymorphisms (SNPs) generated by the multiplex restriction amplicon sequencing (MRASeq) on 21 wheat chromosomes. The legend illustrates the number of SNPs within 1Mb window size. The figure was constructed using the SNPs that have < 20% missing or low-quality data, minor allele frequency (MAF) > 0.05 polymorphic in at least one subgroup based on the combination of four parental lines: 'Everest/GP-80', 'Everest/NE106Fhb1', 'Overland/GP-80', 'Overland/NE106Fhb1'.

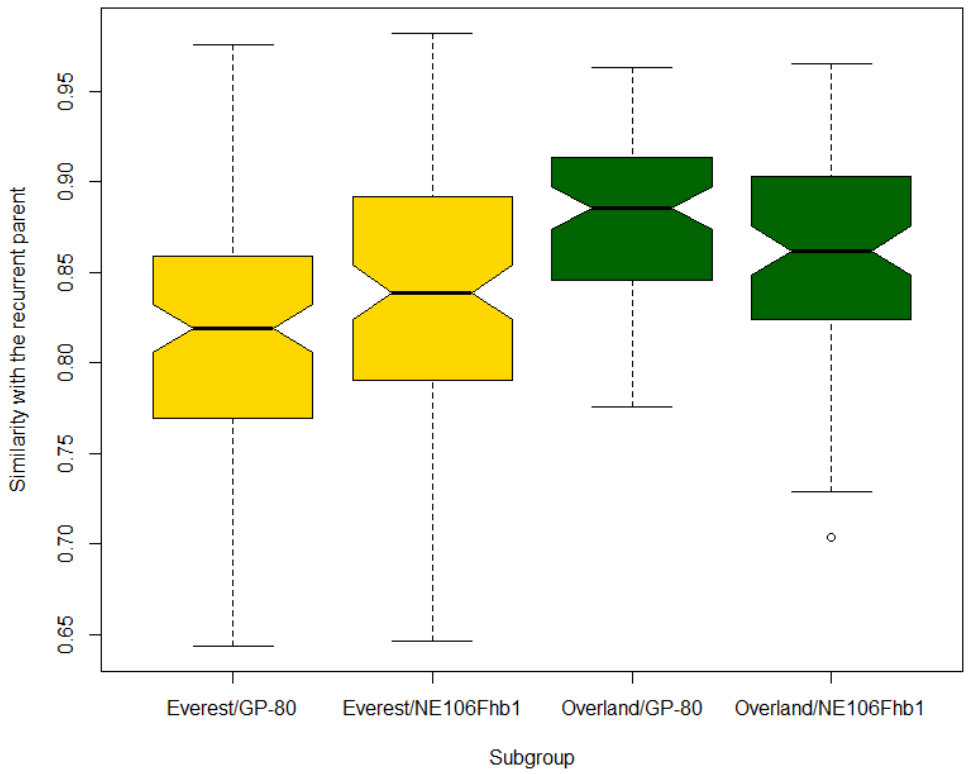

Figure 2.8 The mean similarities between the selected progeny lines and the corresponding recurrent parents relative to subgroups with *Fhb1* and 5A QTL donor parents, respectively, based on single nucleotide polymorphism (SNP) data.

Table 2.1 Number of selected BC_2F_3 lines with different allele combinations at the quantitative trait loci (QTLs) *Fhb1* (AA), *Qfhb.rwg-5A.2* (BB) and *Qfhs.ifa-5A* (CC) in Everest and Overland backgrounds.

Genotype*	Everest background	Overland background
AABBCC	7	8
AABBcc	10	10
AAbbCC	15	11
aaBBCC	15	13
AAbbcc	17	10
aaBBcc	15	5
aabbCC	9	15
aabbcc	6	12

*AA, BB and CC represent resistance alleles at *Fhb1* on chromosomes 3BS, *Qfhb.rwg-5A.2* on 5AL and *Qfhs.ifa-5A on* 5AS, respectively; while aa, bb and cc represent susceptibility alleles at the three QTLs.

Table 2.2 Analysis of variance of the percentage of symptomatic spikelets in a spike (PSS) data for the three quantitative trait locus (QTL)s in the 'Everest' background lines based on the greenhouse experiments.

Source*	DF	Type III SS	Mean Square	*F*-value	*P*-value
A	1	3.44	3.44	51.55	<.0001
B	1	0.30	0.30	4.44	0.036
A*B	1	0.12	0.12	1.75	0.187
C	1	0.58	0.58	8.65	0.003
A*C	1	0.77	0.77	11.57	0.001
B*C	1	0.01	0.01	0.14	0.712
A*B*C	1	0.22	0.22	3.29	0.070
Error	565	37.66	0.07		
Total	572	42.23			

*A, B and C represent QTLs *Fhb1* on chromosomes 3BS, *Qfhb.rwg-5A.2* on 5AL and *Qfhs.ifa-5A* on 5AS respectively. DF: degree of freedom; SS: sum of squares.

Table 2.3 Analysis of variance of the percentage of symptomatic spikelets in a spike (PSS) data for the three quantitative trait locus (QTL)s in the 'Overland' background lines based on the greenhouse experiments.

Source*	DF	Type III SS	Mean Square	*F*-value	*P*-value
A	1	2.78	2.78	62.45	<.0001
B	1	0.52	0.52	11.68	0.001
A*B	1	0.47	0.47	10.61	0.001
C	1	0.26	0.26	5.73	0.017
A*C	1	0.00	0.00	0.01	0.943
B*C	1	0.13	0.13	2.94	0.087
A*B*C	1	0.05	0.05	1.19	0.276
Error	496	22.11	0.04		
Total	503	27.40			

*A, B and C represent QTLs *Fhb1*, *Qfhb.rwg-5A.2* and *Qfhs.ifa-5A,* respectively. DF: degree of freedom; SS: sum of squares.

Table 2.4 Selected lines with *Fusarium* height blight (FHB) resistance and similar agronomic traits to recurrent parents as evaluated in spring 2018 greenhouse (18SGH), fall 2018 greenhouse (18FGH), spring 2019 greenhouse (19SGH) experiments and 2018-19 field (19FD) experiments.

Recurrent parent	QTL allele combination *	Line number	Mean similarity to recurrent parent (%)	Plant height (cm)	Spike length (cm)	Heading date (day)	Number of spikelets per spike	18SGH PSS** (%)	18FGH PSS (%)	19SGH PSS (%)	19FD PSS (%)
Overland				77.4	8.6	149	24.1	38	22	19	55
Overland	AAbbcc	7	0.90	63.3	7.5	141	20.0	26	13	9	46
Overland	AAbbcc	8	0.89	63.8	6.4	137	20.8	13	8	5	39
Overland	AABBcc	7	0.91	71.4	8.2	135	28.5	9	7	7	44
Overland	AABBcc	13	0.90	71.9	9.1	150	25.5	11	8	6	43
Overland	AABBCC	3	0.82	77.6	7.5	142	22.3	25	21	15	43
Overland	AABBCC	4	0.81	68.1	7.9	138	23.7	16	13	5	41
Overland	AABBCC	6	0.89	72.2	6.2	142	22.3	12	8	12	41
Overland	AAbbCC	5	0.92	75.6	6.9	137	25.0	15	14	7	44
Overland	aaBBcc	4	0.84	70.5	7.5	150	22.3	15	8	14	43
Overland	aaBBCC	16	0.85	80.3	7.2	149	19.0	8	11	15	41
Everest				72.2	6.6	103	26.7	77	35	61	65
Everest	AAbbcc	1	0.88	75.1	6.78	101	25.0	23	10	26	31
Everest	AAbbcc	9	0.90	87.6	8.2	104	26.0	48	6	27	44
Everest	AAbbcc	19	0.82	84.8	6.9	103	26.7	30	10	12	41
Everest	AABBcc	1	0.89	73.5	6.5	101	27.8	54	14	35	31
Everest	AABBcc	6	0.92	82.8	6.4	102	25.6	44	18	30	49
Everest	AABBCC	7	0.82	70.8	6.6	102	26.9	40	8	24	45
Everest	AAbbCC	2	0.83	73.4	6.6	102	24.8	61	30	32	31
Everest	AAbbCC	5	0.91	79.5	6.1	102	25.9	28	23	26	40
Everest	AAbbCC	9	0.85	79.1	8.4	102	27.2	58	15	7	41

*AA, BB and CC represent resistance alleles of quantitative trait loci (QTLs) *Fhb1*, *Qfhb.rwg-5A.2* and *Qfhs.ifa-5A,* respectively; while aa, bb and cc represent susceptibility alleles at the three QTLs. **PSS: percentage of symptomatic spikelets in a spike.

Chapter 3 - Association Mapping of Native QTLs for FHB Resistance in the U.S. Wheat Breeding Lines

Introduction

As described in Chapter 1, U.S. wheat can be classified into six classes according to their grain hardness, color, and growing environments (Vocke and Ali, 2013). Unfortunately, FHB can infect all classes of wheat and result in severe losses in grain yield and quality (McMullen et al., 2012; Appel et al., 2015). Although fungicide application can reduce the yield losses, it is costly and only effective with a short application time window during the wheat anthesis. Thus, the most effective and environment-friendly way to minimize FHB damage is to grow FHB resistant cultivars (Bai et al., 2018).

Previous studies demonstrated that wheat accessions showed a significant difference in FHB resistance, and these resistant germplasm lines can be used as resistant sources to improve the level of FHB resistance in new cultivars (Bai and Shaner, 2004; Gilbert and Tekauz, 2000; Kolb et al., 2001). Most of the highly resistant wheat accessions reported so far are from China and Japan, including well-known ‘Sumai 3’ and Chinese landrace ‘Wangshuibai’ (Bai et al., 2018; Jia et al., 2018). However, direct use of these materials as parents in the U.S. wheat breeding programs have not been successful due to linkage drag with undesired traits in these exotic accessions (Dong et al., 2018). Therefore, breeders in the U.S. have worked hard to transfer these resistance QTLs from exotic sources into U.S. germplasm to create germplasms with target QTLs in more locally adapted genetic backgrounds by gradual removal of these unadapted traits.

Meantime, breeders have started to search their native germplasm and breeding lines for FHB resistant sources that adapt to local wheat growing environments. As a result, many

accessions have been identified to have some levels of resistance, including ‘Heyne’, ‘Ernie’, ‘Hondo’, ‘Lyman’ and ‘Everest’(Bai et al., 2018; Zhang et al., 2012; Liu et al., 2007; Lemes Da Silva et al., 2019; Jin et al., 2013). These accessions most likely do not carry the major resistance genes identified from Chinese sources. Although they may not have an high level of FHB resistance as in ‘Sumai 3’, they are locally adapted cultivars with desirable agronomic and adaptation traits for the U.S. environments, thus can be quickly incorporated into new cultivars without concern of poor linkage drag (Steiner et al., 2017). Also, these QTLs in locally adapted backgrounds can be pyramided with resistance genes from exotic sources to improve the level of FHB resistance for developing new cultivars in the U.S. However, many QTLs from these locally adapted lines usually show minor effects and have not been mapped, thus the chromosome locations and markers linked to these QTLs are not available for marker-assisted selection, which hampers progress in the use of those QTLs in breeding. Therefore, identification of these native FHB resistance QTLs from locally adapted wheat accessions is important for breeders to use these QTL more effectively in developing new FHB resistant cultivars (Clark et al., 2016; Eckard et al., 2015).

Constructing bi-parental populations for mapping different native FHB resistance QTLs from locally adapted wheat accessions can be both time and labor extensive (Arruda et al., 2016; Steiner et al., 2017). As the development of sequencing technologies and statistical analysis tools, genome-wide association mapping (GWAS) becomes an efficient alternative for identification of trait-associated loci in a natural population that can take advantage of historical recombination (Hamblin et al., 2011). GWAS uses linkage disequilibrium (LD) in the genome to find trait related loci (Korte et al., 2013), and was first used in human genetics to find the disease-related loci using large human populations. It was then applied in plant genetics for

identifying genomic regions associated with many important traits in many economically important crops including wheat, barley, corn, rice and sorghum (Huang et al., 2014; Wang et al., 2017, Guo et al., 2018; Kidane et al., 2017; Lin et al., 2016; Visscher et al., 2017; F. Zhang et al., 2017). Recently, several GWAS have been conducted to find FHB-related QTLs in different germplasm collections (Arruda et al., 2016; Massman et al., 2011; Schulthess et al., 2018; Shah et al., 2017). Based on the introduction, we hypothesize that genetic architecture for the FHB resistance is complicated, which may be controlled by a few large effect genes along with many small effect genes. In the present study, we conduct GWAS on a panel of 201 elite wheat breeding lines collected across the U.S. major winter wheat growing areas to identify QTL for FHB resistance and associated markers to the QTLs.

Materials and methods

Plant materials

A panel of 201 wheat accessions was collected from two major U.S. winter wheat regions, hard winter wheat and soft winter wheat regions as described in Zhang et al. (2010). In brief, it includes 108 hard red winter wheat (HRW), 28 hard white winter wheat (HWW), and 65 soft red winter wheat (SRW).

Phenotyping the wheat panel for FHB resistance

Three FHB related traits were evaluated for the panel in three greenhouse experiments (fall 2009, spring and fall 2010) and two field experiments (2009-2010 and 2010-2011) using randomized complete block design (RCBD) with two replications. Percentage of symptomatic spikelets (PSS) per spike was evaluated in both the greenhouse and field experiments as described in Chapter 2. In the field experiments, all the seeds were harvested and the percentage of *Fusarium* damaged kernels (FDK), and deoxynivalenol (DON) content were evaluated. FDK

was evaluated using visual estimation by comparing FDK between testing samples and standards with a known percentage of FDK. Different standards (for red wheat kernels, white wheat kernels) with different proportions of FDK were prepared by mixing FDK and healthy kernels in different ratios calculated using Equation 3.1 (Figure 3.1, only showed the checks of red wheat kernels).

$$\text{FDK}(\%) = \frac{No.\ of\ FDK}{Total\ No.\ of\ tested\ kernels} \times 100\% \quad \text{(Equation 3.1)}$$

The mean FDK value from two replications was used as final FDK value for each line in GWAS. DON content of each line was measured in part per million (ppm) using a gas chromatography-mass spectrometry (GC-MS) (Mirocha et al., 1998) with two replications per line in the University of Minnesota, St. Paul, MN. Mean over the two replications was used for each line in the analysis.

For each trait, the best linear unbiased prediction (BLUP) analysis was applied using the R package "lme4" (R team, 2011), with the model: Trait ~ μ + Environment + Genotype + Environment×Genotype + Replication (Environment) + Error. In the model genotype, environment, genotype by environment interaction, replication (environment) were set as random factors. The broad sense heritability (H^2) for each trait was calculated using equation 2.2 described in Chapter 2.

Genotyping methods and genome-wide association analysis

DNA was extracted as described in Chapter 2. The panel was genotyped using the Illumina wheat 90K Infinium iSelect SNP assay (Wang et al., 2014) genotyped at USDA-ARS Cereal Crops Research Unit (Fargo, ND). Protocols for SNP calling, and data quality control was described by Lin et al. (2016). The population structure (Q matrix) was calculated using all the filtered 21,600 SNPs and the ADMIXTURE software (Alexander et al., 2009). Twenty k levels

(k = 1 to 20) were tested, and k=4 was selected as the most proper k number for the number of subpopulations based on the cross validation (CV) error from ADMIXTURE software.

For the best linear unbiased predictions (BLUP) of PSS in the greenhouse experiments, PSS in the field experiments, FDK, DON content two GWAS models were applied, using the same 216,000 SNPs. One is the general linear model (GLM), without control of the population structure and the kinship. One is the mixed linear model (MLM) in the genome association and prediction integrated tool (GAPIT) with the kinship matrix (K) (Zhang et al., 2016). Mean values of PSS in the greenhouse and field experiments, FDK in the field experiments and DON content in the field experiments were calculated from two replications for each accession. These mean values were used as the phenotypic data for marker-trait association analysis of each trait in each environment in only MLM for GWAS. Two threshholds were used to determine the significant marker trait association (MTA), the Bonferroni correction with the α=0.05 and p-value < 0.001 as reported in a previous GWAS on wheat FHB resistance (Wang et al., 2017). Only the MTAs appeared in at least two environments or at least for two traits were considered as significant in this study. Regional linkage disequilibrium was calculated using the R package "LDheatmap" (Shin et al., 2006).

Results

PSS, FDK and DON content in the association mapping panel

Descriptive statistics and broad sense heritability (H^2) were calculated using the best linear unbiased predictions (BLUPs) for all three FHB related traits (Table 3.1). The highest broad sense heritability was observed for PSS from the field experiment (0.78), while the lowest for DON content (0.68). All the traits showed a large variation in the BLUP values. The range for BLUPs values of PSS from greenhouse experiments (72.19%, with a mean of 62.26%) was

larger than that from the field experiments (66.66%, with a mean of 58.29%), indicating a large variation in Type II resistance among accessions in this association panel.

For each trait in each environment, the frequency of distribution in the population was calculated (Figure 3.2). Since PSS were quite different between the greenhouse and the field experiments, the frequency distributions of PSS were plotted separately for greenhouse and field experiments (Figure 3.2). PSS from three greenhouse experiments were similar with most lines in the highly susceptible category (PSS > 80%). In the fall 2009 greenhouse experiment, 83 lines had PSS greater than 90%. In all three greenhouse experiments, about 10% of the lines showed high resistance (PSS < 20 %) (12.94 % for 2009 fall, 5.97 % for 2010 spring, and 11.94 % for 2010 fall), and only one line 'INW0411' had less than 10% PSS in all three experiments.

In the field experiments, the two years' data were not the same. In the 2010-2011 experiments, 42 lines had a PSS value < 40%, while only 24 lines had a PSS value < 40% in 2009-2010 experiments. About 5% lines had a PSS < 20% in the field experiments, and only one accession 'P02444A1-23-9' had less than 20% PSS in both field experiments. However, 55 more accessions (21 HRW, 5 HWW and 29 SRW) had low (< 20%) FDK in the 2010-2011 field experiment than the 2009-2010 experiment. Nine lines had < 20% FDK in both experiments including six SRW and three HRW. A similar result was obtained for the DON content, and 44 more accessions (8 HRW, 3 HWW and 23 SRW) had low DON content (< 5ppm) in the 2010-2011 field experiment than the 2009-2010 experiment. Thirty-two lines had lower than 5ppm DON in both field experiments, including 21 SRW and 11 HRW (Table 3.2 and Figure 3.2).

Correlations among three FHB traits

Positive correlations were observed among the three FHB related traits that were evaluated in each of the three experiments (Figure 3.3). In general, the correlations of the same

traits (e.g. the correlation of 11F-PSS and 10F-PSS) among the experiments were higher than the correlations among different traits under the same or different environments. The highest correlation (0.69, $P < 0.01$) was observed between PSS from the two field experiments, while the lowest (0.08, $P > 0.05$) was between PSS from the fall 2019 greenhouse experiment and DON content from the 2009-2010 field experiment.

Distribution of SNPs in the wheat genome

A total of 21,600 high-quality SNPs was identified from the wheat 90K SNP arrays after filtering (Lin et al, 2016). Among them, 21,553 SNPs were mapped on the 21 wheat chromosomes based on the previous information (Wang et al., 2014), and 47 SNPs could not be mapped on any of the chromosomes. The B genome contained the most SNPs (41.86%), and the D genome had fewest SNPs (24.98%). Among the chromosomes, 2B has the most SNPs (2,548), and 7D has the fewest with only 321 SNPs (Figure 3.4).

Population structure

The panel can be separated into four subpopulations (Figure 3.5). Subpopulation 1 included 28 HRW lines all with a Kansas wheat 'Jagger' in their pedigrees; subpopulation 2 had 50 SRW wheat lines; subpopulation 3 had 14 SRW lines; and subpopulation 4 consisted of 108 lines with majority of hard winter (red or white) wheat and only one soft wheat line ("Atlas 66"). The proportion of the four subgroups were different in each state' accessions collected in this study (Figure 3.5). Most of the lines that were collected from the Great Plains belonged to subpopulations 1 and 4.

GWAS on the FHB related traits

Using the BLUPs for each trait, different numbers of the MTA were detected using different models (Table 3.1, Manhattan plot in Figure 3.10). Using the GLM methods, a

numerous number of associations were detected, indicating that the elite lines used in this project might have a close relationship or clear population structure, which were not considered in the model. When using the MLM methods, the number of MTA were reduced. Only the MLM methods were applied for the separate FHB related trait in each environment. In total, 38 MTAs were significant for at least two environments or traits (Table 3.3, Manhattan plot for each experiment can be found in Figure 3.9). Among these MTAs, five were only significantly associated with low PSS in the greenhouse, and 28 were significantly associated with both low FDK and DON content. Nine MTAs on chromosomes 1A, 1D, 2B, 3A, 3B, and 5Bwere significant for PSS in at least one experiment, with the significant MTAs on chromosomes 2B, 3A, 3B, 5B detected only in greenhouse experiments, the MTA on chromosome 1D detected in field experiments and the MTA on chromosome 1A detected in one greenhouse and one field experiments. Three genetic regions (4A, 5B and 5D) with more than one MTA were significant for low FDK and low DON. For the significant MTAs on chromosome 5D, 25 significant SNPs were in the same LD (Figure 3.6) but did not have LD ($r^2 > 0.6$) with other markers in this chromosome. This 5DL QTL had the largest effect (9.35%) on low FDK and low DON content (8.41%).

Discussion

Significant QTLs for PSS

Wheat 90K infinium array was reported in 2014 (Wang et al., 2014) which used a wide range of materials from including tetraploid and hexaploid wheat, landraces, U.S. wheat cultivars, Canadian wheat cultivars, European wheat cultivars, Asian wheat cultivars and Australian wheat cultivars. In this project our plant materials were elite U.S. wheat breeding lines and cultivars which should not have the ascertainment bias using the 90K infinium array.

More than 150 QTLs have been previously reported for the FHB resistance (Buerstmayr et al., 2009; Bai et al., 2018). To determine if the QTLs identified in this study is new or previously reported QTLs, we compared the physical positions of significant MTAs detected in this study (Table 3.3) with those previously reported (Table 1.1) using Basic Local Alignment Search Tool (BLAST) by aligning the reported marker sequences to IWGSC reference genome (IWGSC et al., 2018).

The MTAs associated with low PSS on 1A and 2B chromosomes share the same chromosome regions with some previously reported QTLs (Buerstmayr et al., 2009; Liu et al., 2009). Because of the limited marker position information available for QTLs on 2B, 3B, 1D, 3A and 5B (due to either limited information of genetic markers or no BLAST results), if the MTAs on these chromosomes are previous reported QTLs remains undetermined.

The MTA on chromosome 2B was significant in three greenhouse experiments, which may be a constant QTL for low PSS. Previous studies reported several QTLs on the 2B chromosome for FHB resistance in bread and durum wheat (Li et al., 2016; Pirseyedi et al., 2018; Zhang et al., 2018; Wu et al., 2019; Giancaspro et al., 2016; Buerstmayr et al., 2009). Some of these studies also used the Illumina wheat 90K Infinium iSelect SNP chips for genotyping. Those SNPs were not the same as detected in this study, however, further research is needed to determine if they are the same or different QTLs.

QTLs for low FDK and low DON

The same QTL that associates with both low FDK and low DON have been reported in many previous studies (Chu et al., 2011; Draeger et al., 2007; McCartney et al., 2007). This may be due to that they are highly correlated traits, indicating they might have similar genetic architectures. In this study, multiple MTAs on chromosome 4A, 5B and 5D were significant for

both low FDK and low DON. The MTAs on the 4A chromosome came from two closely linked genes (Excalibur_c687 and Kukri_c1073, within 3Kb), and SNPs in both genes showed the same effect on low FDK and DON.

Similarly, the MTAs on the 5B also came from two closely linked genes (within 1Mb). However, due to the lack of the marker information from previously reported QTLs, we cannot determine if these QTLs on 4A and 5B were previously reported QTLs or novel ones (Buerstmayr et al., 2009; Liu et al., 2009).

A few previous studies reported the QTL for FHB resistance on the 5D chromosome (Lv et al., 2014, Yang et al., 2005; Yu et al., 2008), with one of the reports for low DON content (Yu et al., 2008). In the current study, 25 significant SNPs were detected in the same linkage block of this region (Figure 3.6) and did not show LD ($r^2 > 0.6$) with other markers in this chromosome. Compared with previously reported QTLs, the 5DL QTL appears to be a new QTL identified in this study, which showed the largest effect (9.35%) on low FDK and on low DON content (8.41%). The low DON QTL was only significant in one year maybe due to the environmental effects that the 2010 -2011 field FHB was more severe than the 2009 -2010 wheat year.

Number of the resistance alleles and phenotypic data

The genetic architecture for the FHB resistance is complicated (Löffler et al., 2009; Mirdita et al., 2015). To discover the possible native resistant QTLs in this project, we conducted GWAS using GLM and MLM methods for the BLUPs data first since the models can vary the results for different traits (Gurung et al., 2014). The results indicated the MLM model was suitable for the FHB related traits (Table 3.1, Figure 3.10). For *Fusarium* head blight related traits evaluated in three greenhouse experiments and two field experiments, MLM method was applied for each analysis and determined 38 MTAs in at least two experiments or at least for two

traits (Table 3.3). Like in the previous reports (Arruda et al., 2016), the number of resistance alleles from the MTA significantly ($P < 0.05$) correlated with the corresponding phenotypic data in this study. However, correlations between PSS and DON were relatively low, and independent MTAs were detected for PSS, FDK and DON.

For PSS, MTAs from 1A, 1D, 2B, 3A, 3B, and 5B chromosomes were detected. A significant ($P < 0.05$) negative correlation was observed between the PSS and number of the resistance alleles from the MTAs (r = -0.40 for the field PSS data, r = -0.56 for the greenhouse PSS data). With more MTAs, PSS from both greenhouse and field were lower than these without any of the resistance alleles at those MTAs (Figure 3.7, Table 3.4). With six resistance alleles from the MTAs, the average PSS of field experiments was reduced by 66.2% (all susceptible alleles group mean PSS: 0.82, for all resistant alleles group: 0.28), and the average greenhouse experiments PSS was reduced by 71.3% (all susceptible alleles group mean PSS: 0.87, all resistant alleles group: 0.25). The lines contain all the six resistance alleles are 'T153', 'T154', 'OK05128' (Table 3.4), which could be used as the Type II resistant parents for breeding.

For low FDK and DON, the MTAs with the smallest *p*-value on 4A, 5B and 5D were selected for counting the number of resistance alleles. About 88.5% of accessions carry three resistance alleles for low FDK (FDK < 20%), and 86.2% of lines contain three resistance alleles for low DON content (DON < 4 ppm). However, unlike the PSS, the lines with all three resistance alleles did not always have lower DON content nor low FDK (Figure 3.8, Table 3.4), therefore some MTAs with minor effect remain to be not detected in this study. Besides, the environmental effects can be another factor since the mean values of FDK and DON were used for the calculation.

In this study, by conducting genome-wide association studies, we identified 38 significantly SNPs on chromosomes 1A, 1D, 2B, 3A, 3B, 4A, 5B and 5D, which were associated with the FHB resistance-related traits in the U.S. wheat germplasms. One QTL on the 5DL were firstly reported for the FDK and DON, which can be considered as the native QTL from the U.S. elite breeding lines or cultivars. These QTLs can be used in the future breeding programs for providing more local adapted FHB resistant lines more efficiently.

References

Alexander, D. H., Novembre, J., & Lange, K. (2009). Fast model-based estimation of ancestry in unrelated individuals. Genome Research, 19(9), 1655-1664.

Appel, J. A., De Wolf, E., Todd, T., & Bockus, W. W. (2015). Preliminary 2015 Kansas Wheat Disease Loss Estimates. Kansas Coop. Plant Dis. Survey Rep. http://agriculture. ks. gov/docs/default-source/pp-disease-reports-2012/2015-ks-wheat-disease-loss-estimates35b3d4002e6262e1aa5bff0000620720. pdf.

Arruda, M. P., Brown, P., Brown-Guedira, G., Krill, A. M., Thurber, C., Merrill, K. R., Foresman, B.J. & Kolb, F. L. (2016). Genome-wide association mapping of *Fusarium* head blight resistance in wheat using genotyping-by-sequencing. The Plant Genome, 9(1). doi:10.3835/plantgenome2015.04.0028.

Bai, G., & Shaner, G. (2004). Management and resistance in wheat and barley to *Fusarium* head blight. Annual Review of Phytopathology, 42, 135-161.

Bai, G., Su, Z., & Cai, J. (2018). Wheat resistance to *Fusarium* head blight. Canadian Journal of Plant Pathology, 40(3), 336-346.

Buerstmayr, H., Ban, T., & Anderson, J. A. (2009). QTL mapping and marker-assisted selection for *Fusarium* head blight resistance in wheat: a review. Plant Breeding, 128(1), 1-26.

Chu, C., Niu, Z., Zhong, S., Chao, S., Friesen, T. L., Halley, S., Elias, E.M., Dong, Y., Faris, J.D. & Xu, S. S. (2011). Identification and molecular mapping of two QTLs with major effects for resistance to *Fusarium* head blight in wheat. Theoretical and Applied Genetics, 123(7), 1107-1119.

Clark, A. J., Sarti-Dvorjak, D., Brown-Guedira, G., Dong, Y., Baik, B. K., & Van Sanford, D. A. (2016). Identifying rare FHB-resistant segregants in intransigent backcross and F2 winter

wheat populations. Frontiers in Microbiology, 7, 277. https://doi.org/10.3389/fmicb.2016.00277.

Dong, H., Wang, R., Yuan, Y., Anderson, J., Pumphrey, M. O., Zhang, Z., & Chen, J. (2018). Evaluation of the potential for genomic selection to improve spring wheat resistance to *Fusarium* head blight in the Pacific Northwest. Frontiers in Plant Science, 9, 911. https://doi.org/10.3389/fpls.2018.00911.

Draeger, R., Gosman, N., Steed, A., Chandler, E., Thomsett, M., Schondelmaier, J., Buerstmayr, H., Lemmens, M., Schmolke, M., Mesterházy, A. & Nicholson, P. (2007). Identification of QTLs for resistance to *Fusarium* head blight, DON accumulation and associated traits in the winter wheat variety Arina. Theoretical and Applied Genetics, 115(5), 617-625.

Eckard, J. T., Gonzalez-Hernandez, J. L., Caffe, M., Berzonsky, W., Bockus, W. W., Marais, G. F., & Baenziger, P. S. (2015). Native Fusarium head blight resistance from winter wheat cultivars 'Lyman', 'Overland', 'Ernie'and 'Freedom' mapped and pyramided onto 'Wesley'-*Fhb1* backgrounds. Molecular Breeding, 35(1), 6. https://doi.org/10.1007/s11032-015-0200-1.

Giancaspro, A., Giove, S. L., Zito, D., Blanco, A., & Gadaleta, A. (2016). Mapping QTLs for *Fusarium* head blight resistance in an interspecific wheat population. Frontiers in Plant Science, 7, 1381. https://doi.org/10.3389/fpls.2016.01381.

Gilbert, J., & Tekauz, A. (2000). Recent developments in research on *Fusarium* head blight of wheat in Canada. Canadian Journal of Plant Pathology, 22(1), 1-8.

Giménez, I., Blesa, J., Herrera, M., & Ariño, A. (2014). Effects of bread making and wheat germ addition on the natural deoxynivalenol content in bread. Toxins, 6(1), 394-401.

Guo, Z., Chen, D., Röder, M. S., Ganal, M. W., & Schnurbusch, T. (2018). Genetic dissection of pre-anthesis sub-phase durations during the reproductive spike development of wheat. The Plant Journal, 95(5), 909-918.

Gurung, S., S. Mamidi, J.M. Bonman, M. Xiong, G. Brown-Guedira, and T.B. Adhikari. (2014). Genome-wide association study reveals novel quantitative trait loci associated with resistance to multiple leaf spot diseases of spring wheat. PLoS One 9(9), e108179.

Hamblin, M. T., Buckler, E. S., & Jannink, J. L. (2011). Population genetics of genomics-based crop improvement methods. Trends in Genetics, 27(3), 98-106.

Huang, X., & Han, B. (2014). Natural variations and genome-wide association studies in crop plants. Annual Review of Plant Biology, 65, 531-551.

IWGSC, International Wheat Genome Sequencing Consortium, Appels, R., Eversole, K., Feuillet, C., Keller, B., Rogers, J., Stein, N., Pozniak, C.J., Choulet, F., Distelfeld, A., Poland, J. & Ronen, G. (2018). Shifting the limits in wheat research and breeding using a fully annotated reference genome. Science, 361(6403), eaar7191.

Jia, H., Zhou, J., Xue, S., Li, G., Yan, H., Ran, C., Zhang, Y., Shi, J., Jia, L., Wang, X. & Luo, J. (2018). A journey to understand wheat *Fusarium* head blight resistance in the Chinese wheat landrace Wangshuibai. The Crop Journal, 6(1), 48-59.

Kidane, Y. G., Mancini, C., Mengistu, D. K., Frascaroli, E., Fadda, C., Pè, M. E., & Dell'Acqua, M. (2017). Genome wide association study to identify the genetic base of smallholder farmer preferences of durum wheat traits. Frontiers in Plant Science, 8, 1230. https://doi.org/10.3389/fpls.2017.01230.

Kolb, F. L., Bai, G. H., Muehlbauer, G. J., Anderson, J. A., Smith, K. P., & Fedak, G. (2001). Host plant resistance genes for *Fusarium* head blight. Crop Science, 41(3), 611-619.

Korte, A., & Farlow, A. (2013). The advantages and limitations of trait analysis with GWAS: a review. Plant Methods, 9: 29. doi:10.1186/1746-4811-9-29.

Lemes Da Silva, C. L., Fritz, A., Clinesmith, M., Poland, J., Dowell, F., & Peiris, K. (2019). QTL mapping of *Fusarium* head blight resistance and deoxynivalenol accumulation in the Kansas wheat variety 'Everest'. Molecular Breeding, 39(3), 35. https://doi.org/10.1007/s11032-019-0937-z.

Li, T., Zhang, D., Zhou, X., Bai, G., Li, L., & Gu, S. (2016). *Fusarium* head blight resistance loci in a stratified population of wheat landraces and varieties. Euphytica, 207(3), 551-561.

Lin, M., Zhang, D., Liu, S., Zhang, G., Yu, J., Fritz, A. K., & Bai, G. (2016). Genome-wide association analysis on pre-harvest sprouting resistance and grain color in US winter wheat. BMC Genomics, 17(1), 794. http://dx.doi.org/10.1186/s12864-016-3148-6.

Liu, S., Abate, Z. A., Lu, H., Musket, T., Davis, G. L., & McKendry, A. L. (2007). QTL associated with *Fusarium* head blight resistance in the soft red winter wheat Ernie. Theoretical and Applied Genetics, 115(3), 417-427.

Liu, S., Hall, M. D., Griffey, C. A., & McKendry, A. L. (2009). Meta-analysis of QTL associated with *Fusarium* head blight resistance in wheat. Crop Science, 49(6), 1955-1968.

Löffler, M., Schön, C. C., & Miedaner, T. (2009). Revealing the genetic architecture of FHB resistance in hexaploid wheat (Triticum aestivum L.) by QTL meta-analysis. Molecular Breeding, 23(3), 473-488.

Lv, C., Song, Y., Gao, L., Yao, Q., Zhou, R., Xu, R., & Jia, J. (2014). Integration of QTL detection and marker assisted selection for improving resistance to *Fusarium* head blight and important agronomic traits in wheat. The Crop Journal, 2(1), 70-78.

Massman, J., Cooper, B., Horsley, R., Neate, S., Dill-Macky, R., Chao, S., Dong, Y., Schwarz, P., Muehlbauer, G.J. & Smith, K. P. (2011). Genome-wide association mapping of *Fusarium* head blight resistance in contemporary barley breeding germplasm. Molecular Breeding, 27(4), 439-454.

McCartney, C. A., Somers, D. J., Fedak, G., DePauw, R. M., Thomas, J., Fox, S. L., Humphreys, D.G., Lukow, O., Savard, M.E., McCallum, B.D. & Gilbert, J. (2007). The evaluation of FHB resistance QTLs introgressed into elite Canadian spring wheat germplasm. Molecular Breeding, 20(3), 209-221.

McMullen, M., Bergstrom, G., De Wolf, E., Dill-macky, R., Hershman, D., Shaner, G., & Van Sanford, D. (2012). *Fusarium* head blight disease cycle, symptoms, and impact on grain yield and quality frequency and magnitude of epidemics since 1997. Plant Disease, 96(12), 1712-1728.

Mirocha, C. J., Kolaczkowski, E., Xie, W., Yu, H., & Jelen, H. (1998). Analysis of deoxynivalenol and its derivatives (batch and single kernel) using gas chromatography/mass spectrometry. Journal of Agricultural and Food Chemistry, 46(4), 1414-1418.

Mirdita, V., Liu, G., Zhao, Y., Miedaner, T., Longin, C. F. H., Gowda, M., Mette, M.F. & Reif, J. C. (2015). Genetic architecture is more complex for resistance to Septoria tritici blotch than to Fusarium head blight in Central European winter wheat. BMC genomics, 16(1), 430.

Pirseyedi, S. M., Kumar, A., Ghavami, F., Hegstad, J. B., Mergoum, M., Mazaheri, M., Kianian, S.F. & Elias, E. M. (2019). Mapping QTL for *Fusarium* head blight resistance in a

tunisian-derived durum wheat population. Cereal Research Communications, 47(1), 78-87.

Schulthess, A. W., Zhao, Y., Longin, C. F. H., & Reif, J. C. (2018). Advantages and limitations of multiple-trait genomic prediction for *Fusarium* head blight severity in hybrid wheat (*Triticum aestivum* L.). Theoretical and Applied Genetics, 131(3), 685-701.

Shah, L., Ali, A., Zhu, Y., Wang, S., Si, H., & Ma, C. (2017). Wheat resistance to *Fusarium* head blight and possibilities of its improvement using molecular marker-assisted selection. Czech Journal of Genetics and Plant Breeding, 53(2), 47-54.

Shin, J. H., Blay, S., McNeney, B., & Graham, J. (2006). LDheatmap: an R function for graphical display of pairwise linkage disequilibria between single nucleotide polymorphisms. Journal of Statistical Software, 16(3), 1-10.

Steiner, B., Buerstmayr, M., Michel, S., Schweiger, W., Lemmens, M., & Buerstmayr, H. (2017). Breeding strategies and advances in line selection for *Fusarium* head blight resistance in wheat. Tropical Plant Pathology, 42(3), 165-174.

Su, Z., Jin, S., Zhang, D., & Bai, G. (2018). Development and validation of diagnostic markers for *Fhb1* region, a major QTL for *Fusarium* head blight resistance in wheat. Theoretical and Applied Genetics, 131(11), 2371-2380.

Visscher, P. M., Wray, N. R., Zhang, Q., Sklar, P., McCarthy, M. I., Brown, M. A., & Yang, J. (2017). 10 years of GWAS discovery: biology, function, and translation. The American Journal of Human Genetics, 101(1), 5-22.

Vocke, G., & Ali, M. (2013). US wheat production practices, costs, and yields: Variations across regions. EIB-116. U.S. Department of Agriculture, Economic Research Service (No. 1476-2017-3890).

Wang, H., & Qin, F. (2017). Genome-wide association study reveals natural variations contributing to drought resistance in crops. Frontiers in Plant Science, 8, 1110. https://doi.org/10.3389/fpls.2017.01110.

Wang, S., Wong, D., Forrest, K., Allen, A., Chao, S., Huang, B. E., Maccaferri, M., Salvi, S., Milner, S.G., Cattivelli, L. & Mastrangelo, A. M. (2014). Characterization of polyploid wheat genomic diversity using a high-density 90 000 single nucleotide polymorphism array. Plant Biotechnology Journal, 12(6), 787-796.

Wu, L., Zhang, Y., He, Y., Jiang, P., Zhang, X., & Ma, H. M. (2019). Genome-wide association mapping of resistance to *Fusarium* head blight spread and DON accumulation in Chinese elite wheat germplasm. Phytopathology, 109(7), 1208-1216.

Yang, J., Bai, G., & Shaner, G. E. (2005). Novel quantitative trait loci (QTL) for *Fusarium* head blight resistance in wheat cultivar Chokwang. Theoretical and Applied Genetics, 111(8), 1571-1579.

Yu, J. B., Bai, G. H., Zhou, W. C., Dong, Y. H., & Kolb, F. L. (2008). Quantitative trait loci for *Fusarium* head blight resistance in a recombinant inbred population of Wangshuibai/Wheaton. Phytopathology, 98(1), 87-94.

Zhang, D., Bai, G., Zhu, C., Yu, J., & Carver, B. F. (2010). Genetic diversity, population structure, and linkage disequilibrium in US elite winter wheat. The Plant Genome, 3(2), 117-127.

Sun, C., Zhang, F., Yan, X., Zhang, X., Dong, Z., Cui, D., & Chen, F. (2017). Genome-wide association study for 13 agronomic traits reveals distribution of superior alleles in bread wheat from the Yellow and Huai Valley of China. Plant Biotechnology Journal, 15(8), 953-969.

Zhang, Q., Szabo-Hever, A., Friesen, T. L., Zhong, S., Elias, E. M., Cai, X., Jin, Y., Faris, J.D., Chao, S. & Xu, S. S. (2018). Genetic diversity and resistance to *Fusarium* head blight in synthetic hexaploid wheat derived from *Aegilops tauschii* and diverse *Triticum turgidum* subspecies. Frontiers in Plant Science, 9, 1829. https://doi.org/10.3389/fpls.2018.01829.

Zhang, X., Bai, G., Bockus, W., Ji, X., & Pan, H. (2012). Quantitative trait loci for *Fusarium* head blight resistance in US hard winter wheat cultivar Heyne. Crop science, 52(3), 1187-1194.

Tang, Y., Liu, X., Wang, J., Li, M., Wang, Q., Tian, F., Su Z, Pan Y, Liu D, Lipka AE & Buckler, E. S. (2016). GAPIT version 2: an enhanced integrated tool for genomic association and prediction. The Plant Genome, 9(2). doi:10.3835/plantgenome2015.11.0120.

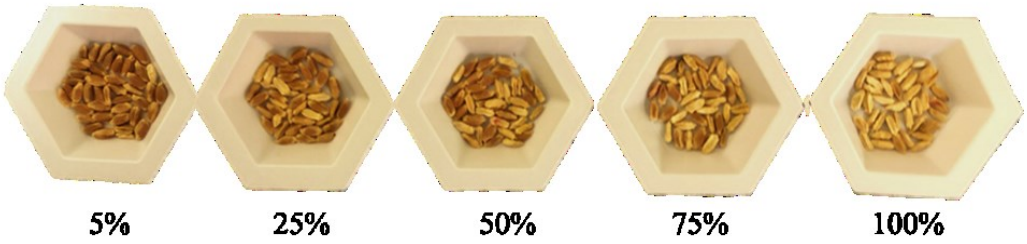

Figure 3.1 Checks used for visual evaluation of *Fusarium* damaged kernels (FDK) using red wheat kernels.

The ratios for each check were calculated based on the actual counts of the FDK and total kernel numbers in each check.

a)

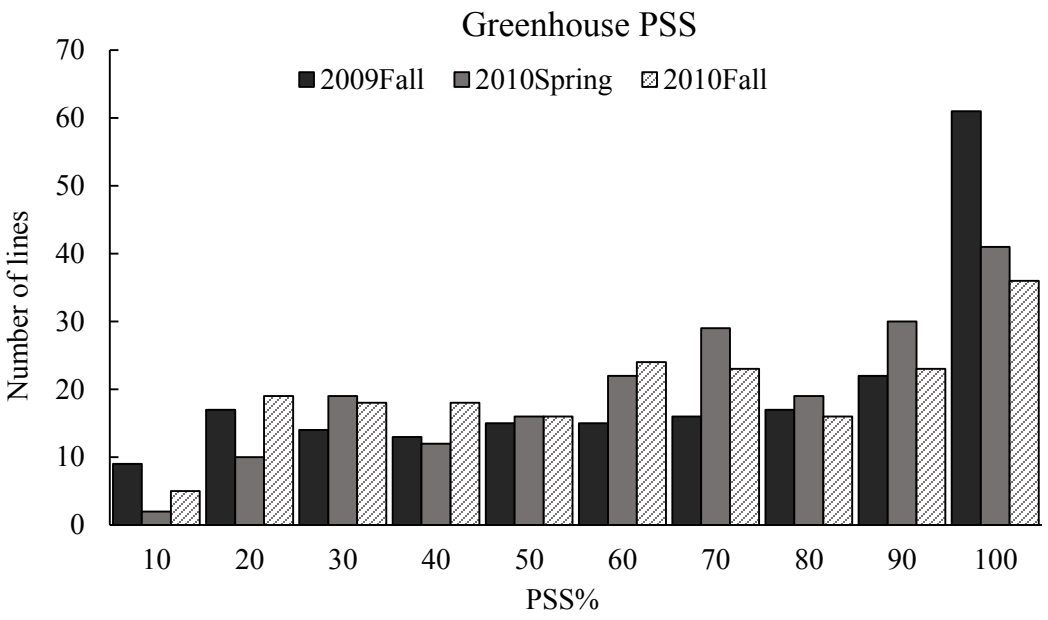
Greenhouse PSS
2009Fall
2010Spring
2010Fall
Number of lines
PSS%
0
10
20
30
40
50
60
70
10
20
30
40
50
60
70
80
90
100

b)

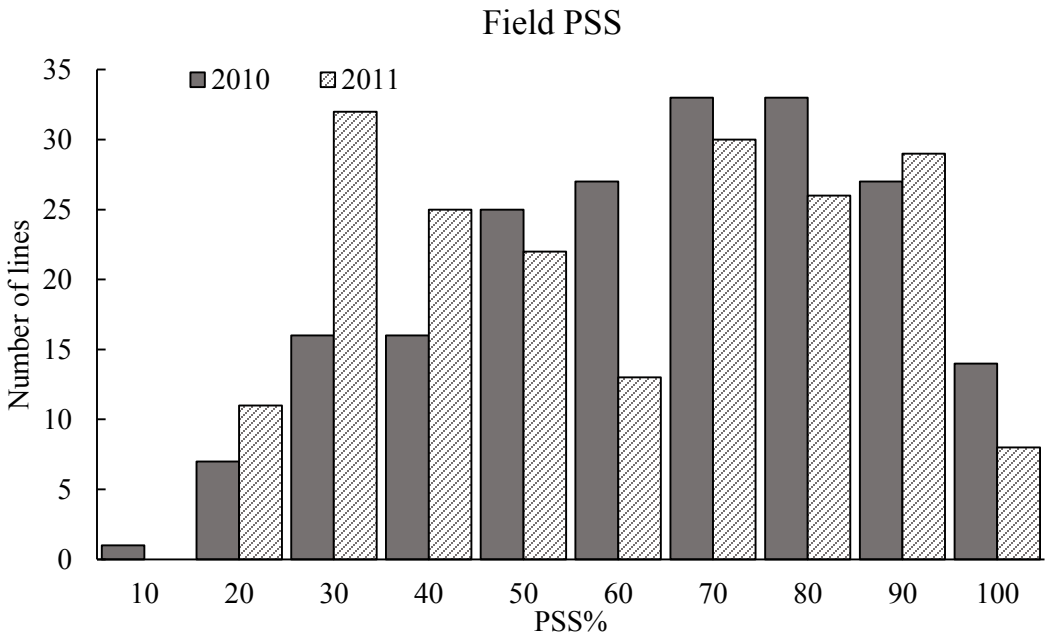
Field PSS
2010
2011
Number of lines
PSS%
0
5
10
15
20
25
30
35
10
20
30
40
50
60
70
80
90
100

c)

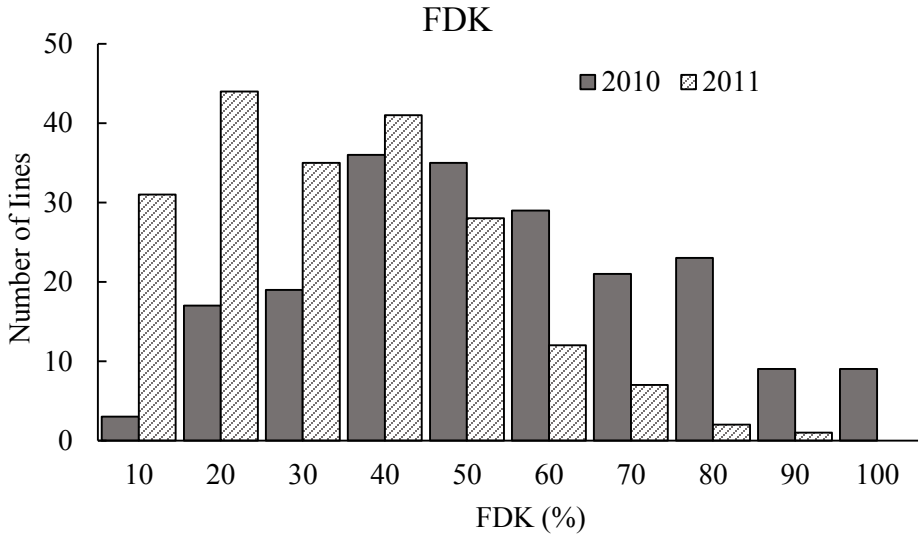

d)

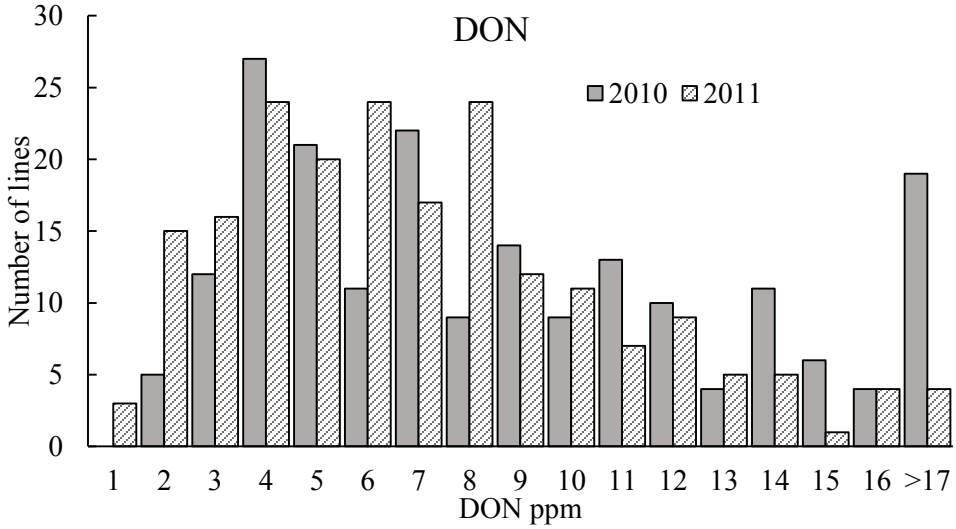

Figure 3.2 The frequency distribution of the percentage of symptomatic spikelets in a spike (PSS) evaluated in both greenhouse and field experiments, and the frequency distribution of *Fusarium* damaged kernels (FDK) and deoxynivalenol (DON) content in field experiments.

(a) PSS frequency distribution for three greenhouse experiments: 2009 fall, 2010 spring and 2010 fall; (b) PSS frequency distribution for two field experiments; (c) Frequency distribution of FDK; and (d) Frequency distribution of DON content. Both FDK and DON contents were from the two field experiments conducted in 2009-2010 growing season (2010) and 2010-2011 growing season (2011).

Figure 3.3 Pearson correlations among all the percentage of symptomatic spikelets in a spike (PSS), *Fusarium* damaged kernels (FDK) and deoxynivalenol (DON) content, evaluated in fall 2009 greenhouse (GH09), spring 2010 greenhouse (GH10), fall 2010 greenhouse (GH11) experiments, and 2009-2010 field (FD10), 2010-2011 field (FD11) experiments.

*Except for the correlation between FD10DON and GH09PSS, all the correlations are significant from zero ($P < 0.05$).

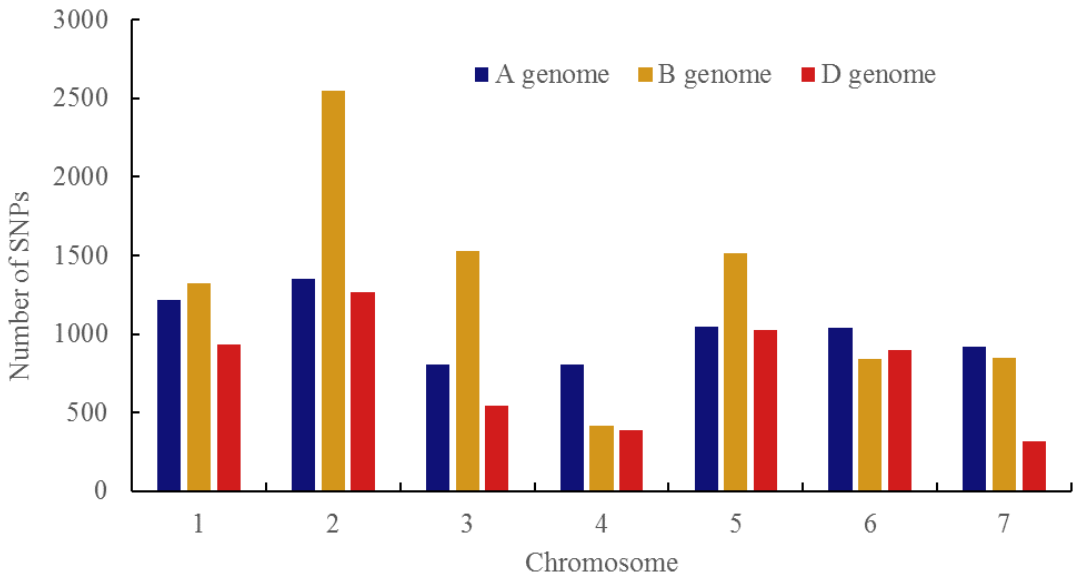

Figure 3.4 The distribution of all the filtered single nucleotide polymorphisms (SNPs) on the wheat genome.

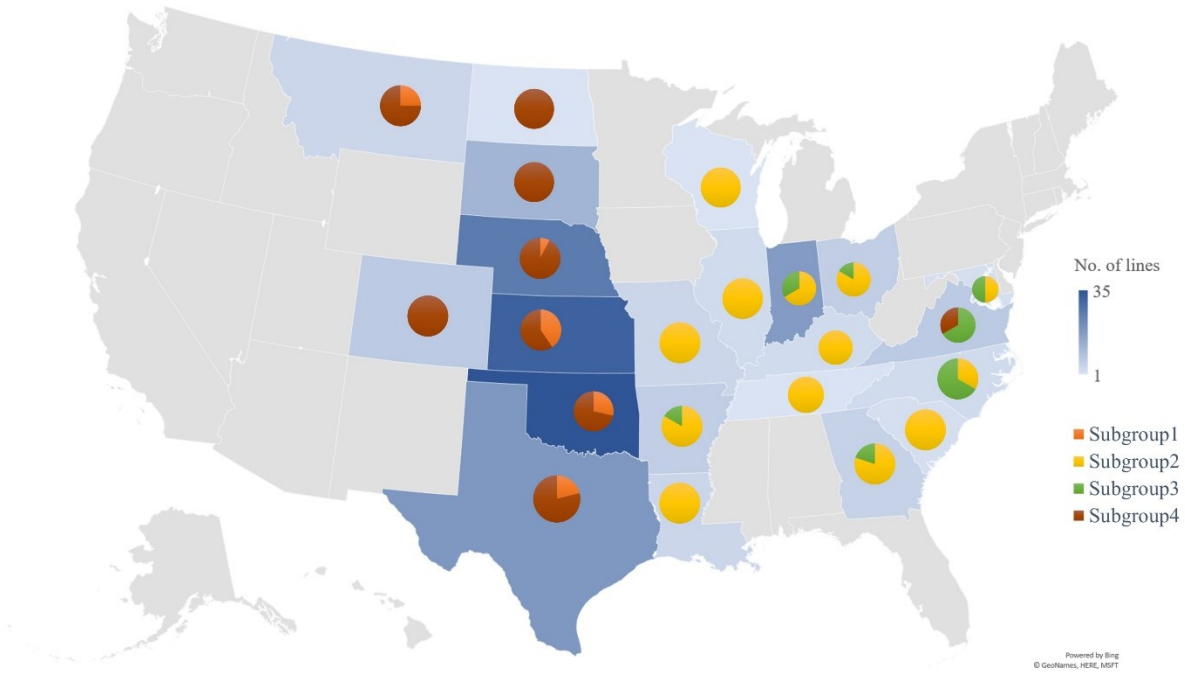

Figure 3.5 The distribution of all the lines across the U.S.

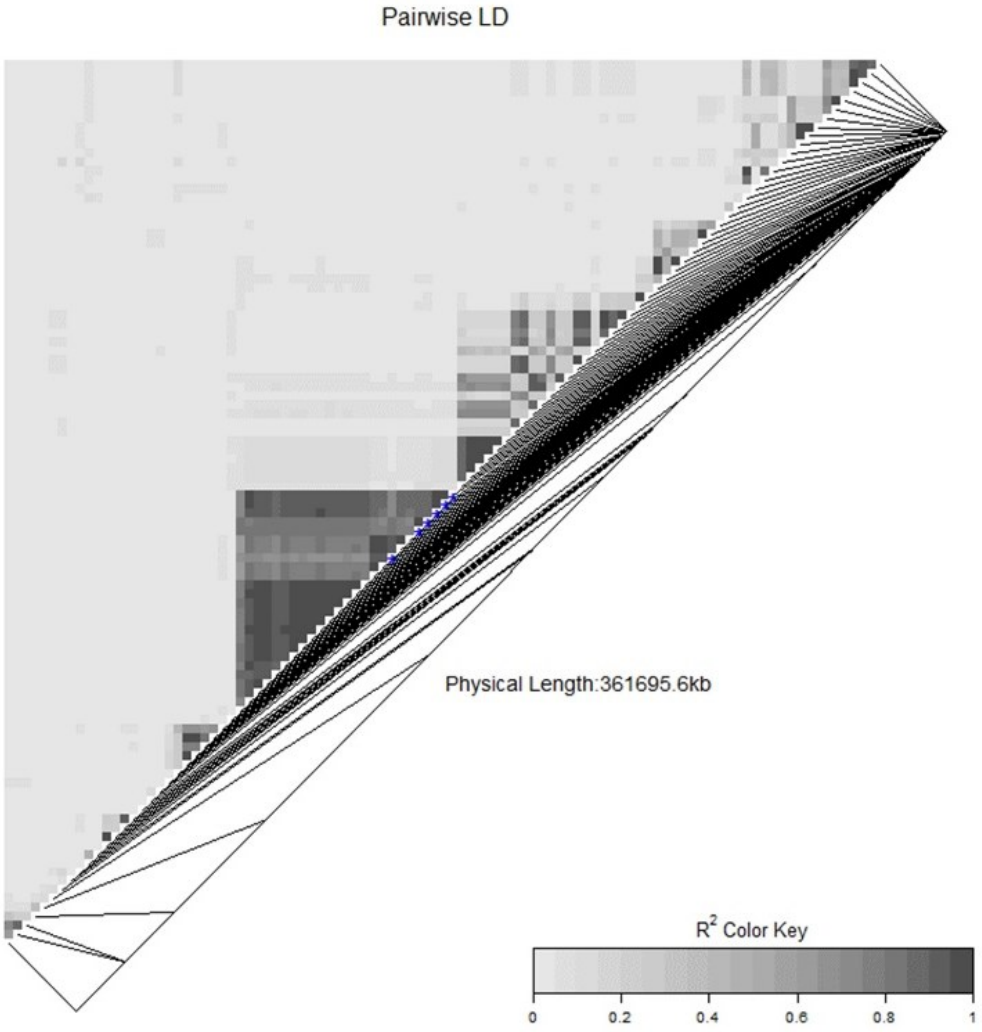

Figure 3.6 The pairwise linkage disequilibrium of markers on the chromosome arm 5DL. The blue dots represent the six single nucleotide polymorphisms (SNPs) with the smallest *P-value*.

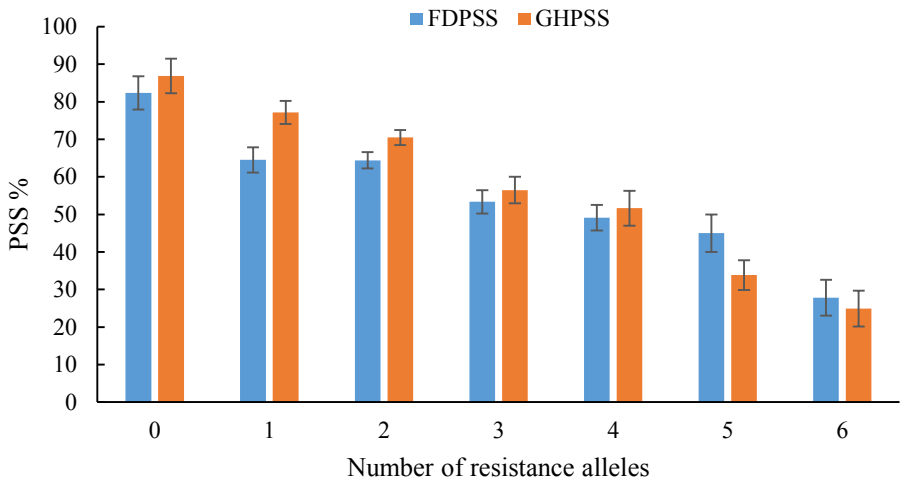

Figure 3.7 The mean percentage of symptomatic spikelets (PSS) within a spike for the lines with different numbers of detected quantitative trait loci (QTLs).

The error bars represent the standard error. FDPSS: percentage of symptomatic spikelets (PSS) within a spike from the field experiments; GHPSS: percentage of symptomatic spikelets (PSS) within a spike from the greenhouse experiments. The six QTLs were on chromosomes 1A, 1D, 2B, 3A, 3B and 5D.

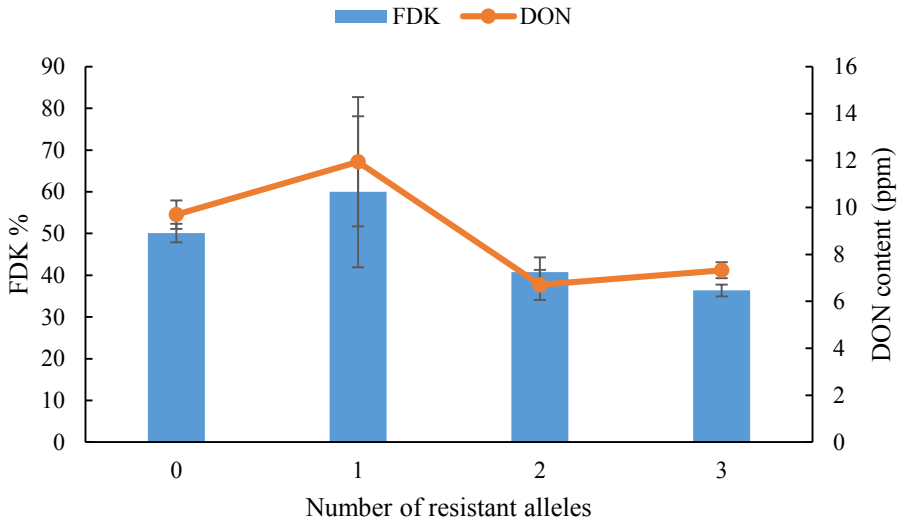

Figure 3.8 *Fusarium* damaged kernels (FDK) and deoxynivalenol (DON) content of the lines with different numbers of detected quantitative trait loci (QTLs).

The error bars represent the standard error. The three QTLs were on chromosomes 4A, 5B and 5D.

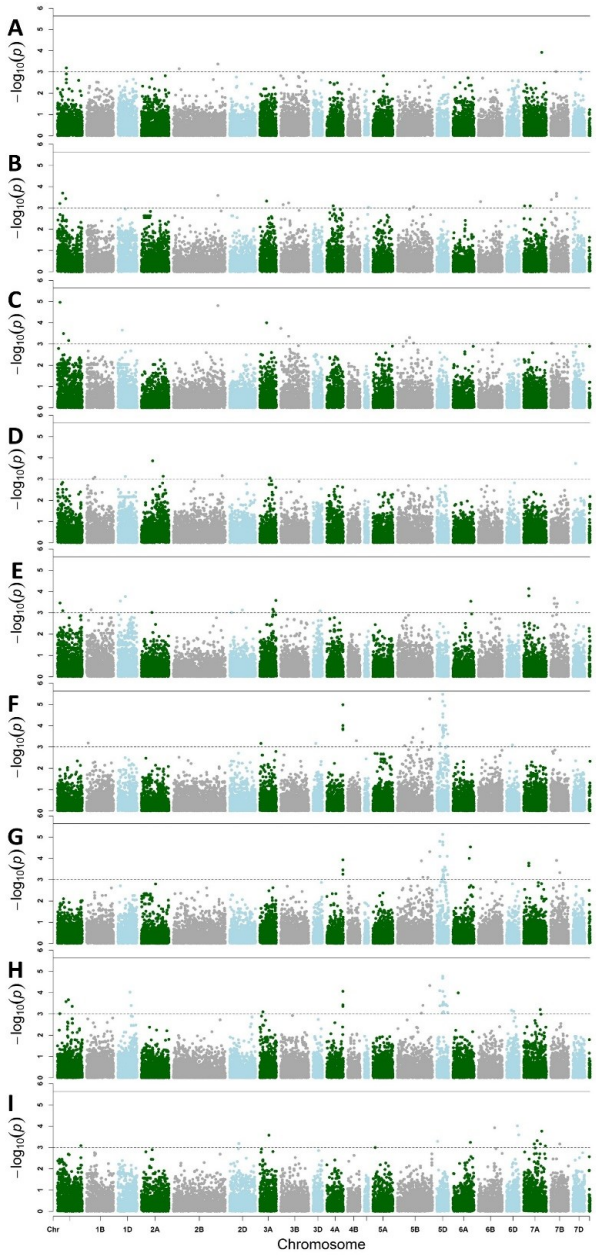

Figure 3.9 Manhattan plot for *Fusarium* head blight related traits evaluated in three greenhouse experiments and two field experiments using mixed linear model (MLM). Manhattan plot for (A) fall 2009 greenhouse percentage of symptomatic spikelets (PSS), (B) spring 2010 greenhouse PSS, (C) fall 2010 greenhouse PSS, (D) 2009-2010 field PSS, (E) 2010-2011 field PSS, (F) 2009-2010 field *Fusarium* damaged kernels (FDK), (G) 2010-2011 field FDK, (H) 2009-2010 field deoxynivalenol (DON) content, (I) 2010-2011 field DON content.

The solid line represents for the Bonferroni correction threshold with $\alpha = 0.05$. The dash line represents the threshold of $P = 0.001$.

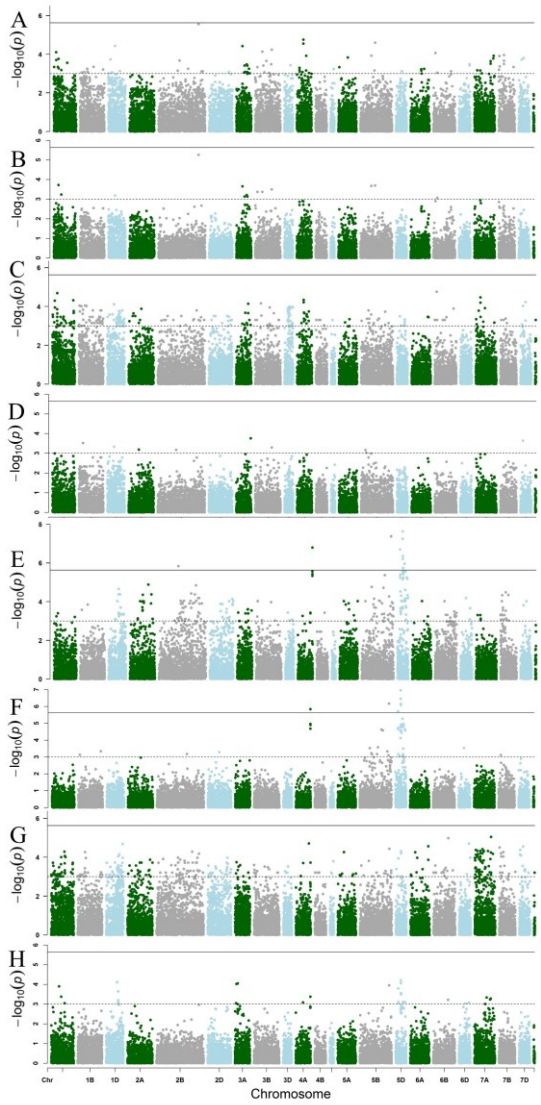

Figure 3.10 Manhattan plots for best linear unbiased predictions (BLUPs) of *Fusarium* head blight-related traits using general linear model (GLM) and mixed linear model (MLM). Manhattan plots generated using BLUP values of (A) percentage of symptomatic spikelets in a spike (PSS) from the greenhouse experiments by GLM, (B) PSS from the greenhouse experiments by MLM, (C) PSS from the field experiments by GLM, (D) PSS from the field experiments BLUP by MLM, (E) *Fusarium* damaged kernels (FDK) from the field experiments by GLM, (F) FDK from the field experiments by MLM, (G) deoxynivalenol (DON) content from the field experiments by GLM, (H) DON content from the field experiments by MLM.

The solid lines represent the Bonferroni correction thresholds for significance at $\alpha = 0.05$, and the dash lines represent the thresholds for significance at $P = 0.001$.

Table 3.1 Descriptive statistics, broad sense heritability (H^2) and number of single nucleotide polymorphism (SNP) associated with *Fusarium*-head-blight-related traits best linear unbiased predictions (BLUPs).

Trait*	H^2	Descriptive statistics**					Models***	
		Mean	Min	Max	Range	SD	GLM	MLM
FDPSS (%)	0.78	58.29	24.29	90.95	66.66	16.40	280	10
GHPSS (%)	0.77	62.26	19.02	91.21	72.19	17.96	93	14
FDK (%)	0.77	40.97	14.42	80.38	65.96	13.55	272	54
DON (ppm)	0.68	8.06	3.81	17.31	13.50	2.85	369	34

*GHPSS: percentage of symptomatic spikelets in greenhouse experiments; FDPSS: percentage of symptomatic spikelets in field experiments; FDK: *Fusarium* damaged kernels; DON: deoxynivalenol content.

**Min: the minimum value of the sample; Max: the maximum value of the sample; SD: standard deviation of the sample.

***GLM: general linear model; MLM: mixed linear model

Table 3.2 Sources, classes, origins and three *Fusarium* head blight traits, percentage of symptomatic spikelets in a spike (PSS), *Fusarium* damaged kernels (FDK) and deoxynivalenol (DON) content, evaluated in fall 2009 greenhouse (GH09), spring 2010 greenhouse (GH10), fall 2010 greenhouse (GH11) experiments, and 2009-2010 (FD10) and 2010-2011 (FD11) field experiments.

Accessions	Source*	Origin	Class**	FD10 PSS%	FD11 PSS%	GH09 PSS%	GH10 PSS%	GH11 PSS%	FD10 FDK%	FD11 FDK%	FD10 DON ppm	FD11 DON ppm
Atlas66	Citr12561	NC	SRW	56.7	40.0	18.5	34.8	10.8	40.0	45.0	27.85	15.57
OK04505	SRPN	OK	HRW	62.3	80.0	100.0	80.3	72.7	45.0	40.0	5.50	11.14
KS05HW136-3	SRPN	KS	HWW	73.9	77.5	75.8	79.6	73.9	25.0	50.0	18.50	16.25
T158	SRPN	KS	HRW	86.5	80.0	100.0	87.2	60.0	40.0	30.0	6.25	5.00
KS980554-12-~9	SRPN	KS	HRW	78.2	52.5	80.2	62.4	53.9	62.5	45.0	13.10	6.26
KS980512-2-2	SRPN	KS	HWW	66.0	45.0	26.5	44.5	15.6	40.0	40.0	19.40	13.72
TX04M410211	SRPN	TX	HRW	100.0	90.0	95.3	98.0	90.4	60.0	50.0	11.70	9.61
N98L20040-44	NRPN	NE	HRW	100.0	77.5	71.3	93.9	65.0	90.0	55.0	7.85	6.85
NI04420	NRPN	NE	HRW	46.0	37.5	6.1	56.0	16.0	70.0	20.0	9.75	7.56
Duster	PI644016	OK	HRW	90.2	87.5	95.0	96.7	55.5	75.0	40.0	14.85	8.13
OK02522W	SRPN	OK	HWW	55.0	83.8	41.9	82.8	22.0	52.5	45.0	14.10	13.71
Scout 66	Citr13996	NE	HRW	65.1	82.5	19.0	71.3	47.5	45.0	35.0	9.40	8.79
AP04T8211	SRPN	KS	HRW	34.6	45.0	95.8	74.3	72.0	45.0	35.0	5.00	5.09
HV9W96-1271R-1	SRPN	KS	HRW	66.7	62.5	91.6	86.6	79.6	40.0	27.5	7.40	5.13
NE04424	SRPN	NE	HRW	73.6	75.0	31.2	69.5	85.4	50.0	25.0	10.70	6.43
CO02W237	SRPN	CO	HWW	75.3	87.5	54.5	88.3	68.0	20.0	22.5	10.05	8.43
OK03825-5403-6	SRPN	OK	HRW	73.1	90.0	75.3	68.3	75.3	65.0	60.0	5.25	10.27
TX04V075080	SRPN	TX	HRW	77.6	90.0	89.5	85.8	86.7	35.0	25.0	4.15	11.34
SD06165	NRPN	SD	HRW	72.5	70.0	70.8	64.6	60.6	65.0	50.0	9.10	11.57
NX03Y2489	NRPN	NE	HWW	86.1	92.5	95.6	100.0	85.4	85.0	35.0	27.05	7.65
NI04427	NRPN	NE	HRW	60.5	55.0	61.8	76.8	79.7	55.0	15.0	4.40	8.41
Endurance	PI639233	OK	HRW	24.7	20.0	36.9	24.6	12.5	40.0	20.0	5.90	5.00
TAM-107	PI495594	TX	HRW	88.3	47.5	96.8	84.2	38.5	60.0	15.0	7.55	2.90

AP05T2413	SRPN	KS	HRW	63.9	42.5	37.6	20.5	8.3	72.5	40.0	8.40	6.46
HV9W03-539R	SRPN	KS	HRW	69.0	50.0	100.0	72.3	59.4	60.0	35.0	5.05	7.95
CO03064	SRPN	CO	HRW	68.7	47.5	97.2	56.6	43.9	60.0	55.0	9.10	12.93
TX02A0252	SRPN	TX	HRW	85.8	90.0	100.0	100.0	95.5	77.5	55.0	10.45	12.60
Kharkof	NRPN	KS	HRW	56.3	67.5	24.7	70.4	100.0	35.0	25.0	7.70	7.72
SD06173	NRPN	SD	HRW	62.5	35.0	91.7	72.3	64.3	40.0	20.0	5.20	4.11
NX04Y2107	NRPN	NE	HRW	68.4	90.0	94.4	90.0	87.5	45.0	40.0	12.85	17.17
NE05548	NRPN	NE	HRW	44.0	77.5	61.8	80.9	70.3	25.0	30.0	5.30	10.61
Deliver	PI639232	OK	HRW	58.8	85.0	100.0	87.8	94.9	40.0	32.5	8.10	12.63
Trego	PI612576	KS	HWW	64.7	80.0	100.0	100.0	95.8	57.5	40.0	15.35	15.46
HV9W03-696R-1	SRPN	KS	HRW	72.6	50.0	96.9	100.0	66.4	45.0	12.5	4.10	8.25
NE05426	SRPN	NE	HRW	95.6	97.5	86.4	88.7	100.0	65.0	45.0	7.55	12.48
CO03W054	SRPN	CO	HWW	55.3	50.0	18.2	88.2	84.4	50.0	25.0	21.05	10.59
TX03A0148	SRPN	TX	HRW	55.8	55.0	94.4	97.6	68.2	95.0	65.0	5.40	11.57
Antelope	PI633910	NE	HWW	67.6	52.5	85.8	80.1	91.7	60.0	35.0	15.00	13.90
SD03164-1	NRPN	SD	HRW	43.7	18.8	37.3	65.7	83.3	25.0	10.0	5.65	3.73
NW04Y2188	NRPN	NE	HRW	60.3	46.3	61.0	94.9	79.4	80.0	35.0	7.75	7.74
NE05549	NRPN	NE	HRW	52.6	25.0	86.9	83.9	71.8	70.0	40.0	7.20	10.17
OK Bullet	PI642415	OK	HRW	80.5	100.0	80.4	57.4	85.9	40.0	12.5	3.60	5.82
OK03716W	OSU	OK	HRW	80.8	87.5	67.4	43.3	93.3	40.0	40.0	4.25	5.43
OK00514-05806	SRPN	OK	HRW	59.3	65.0	43.2	41.1	100.0	45.0	40.0	4.30	7.50
AP06T3832	SRPN	KS	HRW	80.0	62.5	94.9	38.0	97.5	90.0	50.0	4.80	6.54
HV9W02-942R	SRPN	KS	HRW	20.4	26.3	35.5	34.1	34.2	70.0	30.0	5.30	6.06
NE05430	SRPN	NE	HRW	72.2	52.5	100.0	55.9	84.2	35.0	32.5	6.10	7.64
CO03W139	SRPN	CO	HWW	14.3	30.0	100.0	68.6	41.2	20.0	12.5	5.60	4.99
TX03A0563	SRPN	TX	HRW	86.3	82.5	100.0	96.9	93.7	80.0	30.0	5.25	9.18
Wesley	PI605742	NE	HRW	78.0	40.0	75.2	28.5	75.2	75.0	17.5	7.60	6.94
NE02533	NRPN	NE	HRW	37.9	57.5	60.6	40.8	56.8	45.0	35.0	2.80	5.93
NE05569	NRPN	NE	HRW	48.9	72.5	63.7	53.9	59.4	77.5	25.0	11.45	5.59
Overley	certified	KS	HRW	87.5	80.0	100.0	67.9	89.4	82.5	55.0	9.25	15.07
OK05903C	OSU	OK	HWW	51.9	32.5	83.9	57.7	67.6	72.5	35.0	12.70	7.35

Century	PI502912	OK	HRW	69.4	27.5	8.1	27.2	21.4	42.5	17.5	5.80	3.70
KS05HW15-2	SRPN	KS	HWW	85.1	78.8	79.5	48.1	54.7	50.0	20.0	12.30	6.13
T151	SRPN	KS	HRW	43.1	54.5	90.8	65.9	45.5	20.0	20.0	3.00	3.00
KS970093-8-9-#1	SRPN	KS	HRW	25.3	25.0	5.9	36.1	17.9	17.5	15.0	2.05	10.71
CO03W239	SRPN	CO	HWW	100.0	100.0	100.0	96.9	100.0	100.0	85.0	26.25	7.99
TX04A001246	SRPN	TX	HRW	63.3	65.0	90.8	74.3	58.1	65.0	55.0	4.85	5.69
Jerry	PI632433	ND	HRW	51.0	25.0	41.3	63.6	71.7	60.0	27.5	14.75	9.28
SD05118	NRPN	SD	HRW	75.6	55.0	23.4	11.7	41.7	75.0	32.5	16.80	9.76
NE02558	NRPN	NE	HRW	59.7	67.5	78.3	41.5	81.3	40.0	15.0	6.70	4.86
MT0495	NRPN	MT	HRW	37.7	62.5	40.1	85.6	95.5	77.5	40.0	15.00	9.25
Fuller	certified	KS	HRW	42.5	35.0	74.7	73.5	38.1	55.0	25.0	8.20	5.88
OK03522	SRPN	OK	HRW	67.0	47.5	81.0	57.5	53.4	45.0	27.5	3.60	3.74
KS05HW121-2	SRPN	KS	HWW	90.7	75.0	75.0	53.6	45.3	50.0	35.0	11.05	11.62
T153	SRPN	KS	HRW	31.3	25.0	40.2	15.8	36.9	35.0	17.5	4.20	1.97
KS970187-1-10	SRPN	KS	HRW	32.5	27.5	49.2	53.1	54.9	55.0	35.0	14.65	4.60
CO03W043	SRPN	CO	HWW	53.6	67.5	41.1	93.1	63.1	45.0	27.5	14.20	10.56
TX01V5134RC-3	SRPN	TX	HRW	49.9	52.5	91.4	85.5	54.0	50.0	12.5	4.80	3.83
SD06W117	NRPN	SD	HWW	80.9	75.0	93.1	100.0	96.4	40.0	30.0	12.90	8.54
SD05210	NRPN	SD	HRW	52.2	35.0	10.8	15.8	28.6	55.0	17.5	18.40	7.36
NW03666	NRPN	NE	HRW	58.1	62.5	98.3	83.3	89.9	55.0	30.0	8.10	8.96
MTS0531	NRPN	MT	HWW	59.5	52.5	28.5	18.2	34.8	55.0	17.5	15.80	7.90
Centerfield	PI644017	OK	HRW	72.0	55.0	51.1	32.9	39.5	50.0	25.0	4.95	4.62
OK04525	OSU	OK	HRW	49.4	62.5	100.0	66.5	93.3	35.0	45.0	3.50	5.44
OK03305	SRPN	OK	HRW	87.7	75.0	88.5	100.0	86.1	17.5	10.0	3.40	5.65
MT0552	UN	MT	HRW	67.5	70.0	82.7	89.1	56.2	60.0	22.5	7.85	3.44
T154	SRPN	KS	HRW	13.9	25.0	12.7	15.1	18.8	40.0	12.5	4.75	3.03
NE05496	SRPN	NE	HRW	77.3	95.0	91.1	91.4	60.2	45.0	40.0	5.05	8.66
TX04M410164	SRPN	TX	HRW	91.2	87.5	100.0	48.5	84.9	97.5	40.0	8.45	6.25
SD06069	NRPN	SD	HRW	61.6	45.0	52.3	29.2	14.8	65.0	70.0	14.25	7.37
SD05W030	NRPN	SD	HWW	93.5	72.5	95.6	78.3	28.5	37.5	25.0	11.10	5.77
chisholm	PI486219	OK	HRW	75.8	77.5	74.8	56.8	42.7	45.0	45.0	4.50	4.24

Guymon	PI643133	OK	HWW	98.9	85.0	100.0	99.5	89.3	35.0	45.0	16.00	13.02
OK05830	OSU	OK	HRW	42.7	75.0	100.0	66.3	65.8	60.0	65.0	9.55	9.43
OK02405	RGON	OK	HRW	16.6	25.0	100.0	35.8	52.5	20.0	10.0	3.90	2.11
KS010957K~4	RGON	KS	HRW	47.7	90.0	97.7	90.3	39.0	72.5	65.0	10.90	9.77
NE06619	RGON	NE	HRW	58.1	22.5	73.3	77.1	15.8	70.0	45.0	11.40	5.55
MTS04120	RGON	MT	HRW	81.9	20.0	88.6	59.3	37.9	80.0	10.0	10.20	4.01
TX06A001239	RGON	TX	HRW	75.2	85.0	93.5	82.8	100.0	77.5	50.0	11.45	7.95
TXHT006F8-CS06/472-STA34	RGON	TX	HRW	68.3	65.0	91.1	96.1	66.8	92.5	45.0	34.10	7.78
MO011126	UESRWWN	MO	SRW	24.0	20.0	42.4	40.1	47.9	22.5	7.5	9.95	3.87
OH02-7217	UESRWWN	OH	SRW	47.5	28.8	38.3	25.0	31.3	20.0	15.0	13.25	6.64
MD99W483-06-9	UESRWWN	MD	SRW	44.3	30.0	28.0	56.3	21.4	25.0	20.0	9.10	4.70
OK04507	RGON	OK	HRW	89.6	77.5	98.3	89.7	70.5	87.5	60.0	10.20	7.82
KS020304K~3	RGON	KS	HRW	62.0	72.5	71.9	86.9	27.5	45.0	60.0	7.75	7.83
KS010143K-11	RGON	KS	HRW	84.7	36.3	63.6	65.4	10.2	45.0	15.0	7.30	11.87
TX05A001334	RGON	TX	HRW	77.0	70.0	90.8	88.2	25.0	40.0	22.5	3.55	4.07
TX06A001376	RGON	TX	HRW	36.5	73.8	52.7	55.3	10.0	65.0	80.0	14.15	9.64
VA03W-412	UESRWWN	VA	SRW	75.4	70.0	100.0	87.6	53.4	30.0	22.5	11.95	5.51
OH03-41-45	UESRWWN	OH	SRW	87.0	85.0	65.0	89.3	91.7	25.0	40.0	5.10	3.66
OK05312	OSU	OK	HRW	77.8	50.0	64.6	76.2	32.3	50.0	22.5	7.90	5.08
HV9W05-881R	RGON	KS	HRW	83.5	75.0	88.0	96.1	40.4	60.0	35.0	9.50	7.01
NE06436	RGON	NE	HRW	63.4	62.5	41.5	100.0	52.8	50.0	40.0	7.70	8.67
NW05M6011-6-1	RGON	NE	HWW	42.3	45.0	61.4	49.3	9.3	50.0	35.0	18.05	14.67
TX06A001431	RGON	TX	HRW	90.0	90.0	80.0	100.0	100.0	85.0	75.0	12.85	7.07
TXHT023F7-CS06/607-STA07/40	RGON	TX	HRW	85.7	42.5	100.0	100.0	57.1	100.0	40.0	7.50	4.55
AR97044-10-2	UESRWWN	AR	SRW	73.4	55.0	80.2	59.7	21.5	55.0	22.5	5.70	7.11
P02444A1-23-9	UESRWWN	IN	SRW	12.4	17.5	55.0	33.7	15.9	30.0	10.0	2.00	1.98
VA05W-414	UESRWWN	VA	SRW	52.0	60.0	77.5	71.4	55.0	25.0	20.0	6.70	4.84
OK05511	RGON	OK	HRW	68.0	32.5	91.2	94.8	100.0	40.0	15.0	12.45	8.83
SD07W041	RGON	SD	HWW	80.6	65.0	59.4	93.3	76.4	50.0	35.0	22.85	16.46
SD07204	RGON	SD	HRW	74.8	25.0	73.4	84.0	85.6	82.5	55.0	19.15	18.69
NW05M6015-25-4	RGON	NE	HWW	16.6	27.5	95.8	80.2	35.8	32.5	12.5	11.60	2.26

TXHT001F8-CS06/325-PRE07/75	RGON	TX	HRW	43.9	37.5	69.7	52.1	45.1	77.5	35.0	11.20	5.13
CO04W210	RGON	CO	HWW	52.0	40.0	37.0	22.9	24.1	35.0	32.5	13.85	9.48
KY96C-0769-7-3	UESRWWN	KY	SRW	26.1	25.0	21.2	23.0	15.4	15.0	10.0	4.60	5.15
P03207A1-7	USSRWWN	IN	SRW	76.4	51.3	14.3	22.9	19.3	25.0	17.5	7.55	2.06
LA01*425	UESRWWN	IN	SRW	41.2	60.0	16.6	52.4	88.2	35.0	10.0	6.15	3.93
KS07HW25	RGON	KS	HWW	60.9	70.0	47.9	47.9	28.7	70.0	35.0	21.35	11.52
SD07220	RGON	SD	HRW	24.3	40.0	77.2	51.8	48.3	20.0	35.0	5.50	5.47
KS010379M-2	RGON	KS	HRW	68.3	90.0	83.8	64.9	66.6	70.0	45.0	17.80	12.35
NE06472	RGON	NE	HRW	90.3	87.5	55.1	60.1	66.7	60.0	40.0	7.90	3.30
Roane	PI612958	VA	SRW	27.8	17.5	5.3	12.5	14.3	15.0	7.5	3.50	1.35
OH02-12678	UESRWWN	OH	SRW	52.6	22.5	27.6	29.9	33.8	25.0	10.0	7.45	2.15
LA02-923	UESRWWN	IN	SRW	80.7	72.5	45.1	94.1	91.4	40.0	22.5	12.15	8.04
SD05W148-1	RGON	SD	HWW	42.5	35.0	29.4	58.4	64.1	25.0	7.5	16.50	5.95
KS010514-9TM-10	RGON	KS	HRW	83.3	82.5	64.7	90.4	100.0	80.0	70.0	17.75	15.21
N02Y5117	RGON	NE	HRW	49.6	37.5	29.0	22.2	66.0	70.0	50.0	12.45	6.44
INW0411	UESRWWN	IN	SRW	12.2	18.8	3.1	7.5	7.1	37.5	12.5	2.40	1.47
MO040192	UESRWWN	MO	SRW	66.7	45.0	59.5	93.0	66.8	50.0	15.0	4.50	3.66
KS07HW81	RGON	KS	HWW	80.6	87.5	96.3	70.1	86.5	55.0	45.0	16.95	13.11
U07-698-9	RGON	KS	HWW	21.9	23.8	23.6	57.3	25.4	20.0	10.0	9.85	4.59
TX05V5614	RGON	TX	HRW	93.8	70.0	94.8	61.1	80.8	70.0	40.0	9.60	3.51
Branson	UESRWWN	IN	SRW	54.4	45.0	54.2	48.4	69.4	17.5	10.0	5.85	1.76
IL00-8530	UESRWWN	IL	SRW	36.2	37.5	17.5	35.4	17.8	25.0	5.0	4.60	0.72
IL02-18228	UESRWWN	IL	SRW	7.3	22.5	34.4	44.0	85.6	10.0	5.0	3.00	0.77
KS07HW117	RGON	KS	HWW	78.1	75.0	100.0	71.4	87.6	80.0	50.0	24.95	7.84
NE06549	RGON	NE	HRW	67.3	43.8	51.8	95.6	54.2	87.5	35.0	20.60	9.32
TX06A001084	RGON	TX	HRW	82.0	87.5	100.0	79.4	100.0	62.5	45.0	5.80	3.32
Bess	UESRWWN	MO	SRW	34.3	23.8	16.7	27.6	7.2	7.5	5.0	6.90	3.57
IL02-19463	UESRWWN	IL	SRW	66.3	47.5	83.3	60.1	56.5	22.5	5.0	5.10	0.89
Mocha exp.	UESRWWN	OH	SRW	78.8	40.0	19.4	48.9	67.0	95.0	50.0	6.30	3.75
Pioneer Brand 26R61	USSRWWN	IN	SRW	58.8	55.0	100.0	54.8	34.7	75.0	65.0	14.50	5.17
NC04-15533	USSRWWN	NC	SRW	54.0	35.0	45.0	47.1	65.3	37.5	30.0	4.25	4.81

M03-3616-C	USSRWWN	IN	SRW	25.6	22.5	25.0	19.6	50.0	45.0	17.5	9.80	2.09
W98007V1	USSRWWN	SC	SRW	65.6	60.0	90.0	51.7	59.9	40.0	22.5	3.42	1.85
Arena exp.	UESRWWN	OH	SRW	63.0	40.0	85.7	69.6	93.3	50.0	10.0	4.40	2.91
Coker 9553	USSRWWN	IN	SRW	40.1	40.0	93.7	84.5	82.0	30.0	12.5	7.05	4.40
VA05W-258	USSRWWN	VA	SRW	41.7	35.0	68.2	75.5	61.1	27.5	10.0	3.70	1.85
B030543	USSRWWN	AR	SRW	139.9	27.5	69.0	38.5	20.7	12.5	10.0	3.90	3.54
W98008J1	USSRWWN	SC	SRW	65.0	45.0	79.5	63.9	100.0	35.0	5.0	3.10	1.94
OK05122	OSU	OK	HRW	64.0	70.0	100.0	92.9	79.2	15.0	7.5	7.85	3.68
OK06210	OSU	OK	HRW	100.0	82.5	100.0	100.0	100.0	97.5	45.0	12.05	5.73
India exp.	UESRWWN	OH	SRW	12.2	20.0	24.4	83.8	72.7	20.0	7.5	2.00	2.49
G69202	UESRWWN	IN	SRW	29.3	20.0	7.5	63.6	11.7	40.0	30.0	4.45	2.68
USG 3555	USSRWWN	VA	SRW	26.8	17.5	18.2	25.6	31.8	65.0	15.0	13.20	2.79
LA01138D-52	USSRWWN	LA	SRW	75.1	85.0	86.8	100.0	96.4	95.0	50.0	26.35	11.89
VA05W-78	USSRWWN	VA	SRW	81.3	70.0	96.4	84.8	61.9	50.0	55.0	22.60	9.31
OK05723W	OSU	OK	HRW	59.8	75.0	60.0	14.7	28.1	75.0	17.5	11.00	3.37
OK06319	OSU	OK	HRW	68.1	62.5	38.3	72.1	34.2	60.0	20.0	8.50	4.38
D04*5513	UESRWWN	AR	SRW	70.6	65.0	49.1	38.9	71.5	90.0	55.0	15.40	8.05
M04-4566	UESRWWN	IN	SRW	43.1	78.8	71.7	81.3	47.8	92.5	45.0	9.25	5.71
NC03-6228	USSRWWN	NC	SRW	40.7	65.0	100.0	73.3	70.0	40.0	20.0	4.65	1.28
AR96077-7-2	USSRWWN	AR	SRW	59.3	40.0	21.5	55.8	35.5	60.0	12.5	11.10	2.61
D04-5012	USSRWWN	AR	SRW	82.5	82.5	100.0	97.1	68.2	80.0	45.0	14.10	7.94
G59160	USSRWWN	IN	SRW	24.4	28.8	57.6	41.9	69.5	40.0	5.0	6.95	1.70
OK01420W	OSU	OK	HRW	75.6	62.5	49.5	94.4	37.2	65.0	35.0	8.30	6.02
OK06528	OSU	OK	HRW	69.2	50.0	9.2	26.3	84.4	60.0	17.5	11.20	6.69
OK06518	OSU	OK	HRW	55.5	25.0	93.3	64.5	92.9	25.0	7.5	5.00	1.77
KY97C-0321-02-01	UESRWWN	KY	SRW	80.6	80.0	55.7	62.4	100.0	50.0	5.0	9.50	2.59
M04-4802	UESRWWN	IN	SRW	59.3	42.5	14.2	66.6	91.7	67.5	37.5	5.45	3.39
AR97124-4-3	USSRWWN	AR	SRW	74.4	65.0	34.7	61.4	51.9	55.0	12.5	4.20	2.37
GA991336-6E9	USSRWWN	GA	SRW	77.6	70.0	92.7	100.0	100.0	70.0	42.5	16.00	7.76
G61505	USSRWWN	IN	SRW	24.0	27.5	14.6	20.9	84.4	25.0	10.0	3.70	1.50
OK05134	OSU	OK	HRW	37.5	40.0	11.8	14.8	19.7	60.0	17.5	10.70	3.53

OK06313	OSU	OK	HRW	54.7	67.5	62.6	62.6	17.9	50.0	22.5	4.40	4.46
KY97C-0519-04-07	UESRWWN	KY	SRW	36.9	25.0	12.2	36.9	58.6	40.0	10.0	6.80	3.13
M04*5109	UESRWWN	IN	SRW	37.7	20.0	10.1	29.0	40.6	40.0	7.5	5.50	2.57
VA04W-259	USSRWWN	VA	SRW	71.9	82.5	24.3	68.7	85.6	77.5	27.5	12.10	6.47
MD01W233-06-1	USSRWWN	MD	SRW	28.5	27.5	5.4	25.5	42.8	20.0	5.0	1.80	1.79
GA991209-6E33	USSRWWN	GA	SRW	47.2	25.0	92.2	100.0	31.5	35.0	17.5	6.75	1.93
G41732	USSRWWN	IN	SRW	25.6	21.3	63.8	22.0	40.7	60.0	15.0	7.35	2.23
OK06848W	OSU	OK	HWW	76.1	70.0	100.0	68.8	22.7	50.0	27.5	15.15	6.02
W06-202B	UESRWWN	WI	SRW	45.8	60.0	39.1	50.7	22.6	60.0	45.0	7.40	6.48
TAM 110	PI595757	TX	HRW	27.2	82.5	96.1	94.8	70.3	77.5	50.0	6.10	5.12
LA99005UC-31-3-C	USSRWWN	LA	SRW	77.7	92.5	33.2	100.0	96.1	50.0	70.0	8.90	4.83
P03112A1-7-14	USSRWWN	IN	SRW	46.0	30.0	17.6	67.6	21.5	10.0	20.0	4.60	1.84
TN801	USSRWWN	TN	SRW	94.2	81.3	43.4	60.8	100.0	55.0	32.5	10.85	7.35
GA991371-6E13	USSRWWN	GA	SRW	86.3	100.0	81.1	91.7	100.0	75.0	45.0	21.50	10.06
OK05212	OSU	OK	HRW	38.1	37.5	54.6	62.0	59.8	30.0	25.0	4.55	5.89
OK06336	OSU	OK	HRW	81.8	27.5	40.5	48.2	21.4	72.5	17.5	7.60	3.80
MO040152	UESRWWN	MO	SRW	38.9	27.5	8.5	9.2	12.2	50.0	20.0	11.40	6.83
AGS 2000	USSRWWN	GA	SRW	76.6	67.5	83.7	100.0	100.0	50.0	22.5	16.65	7.27
LA98214D-14-1-2-B	USSRWWN	LA	SRW	95.6	100.0	95.9	91.9	100.0	57.5	30.0	8.30	5.31
P04287A1-10	USSRWWN	IN	SRW	31.6	40.0	50.8	34.2	25.1	20.0	7.5	4.45	3.14
M04-4715	USSRWWN	IN	SRW	31.9	41.3	55.3	23.9	48.1	50.0	17.5	1.95	4.23
GA991227-6A33	USSRWWN	GA	SRW	49.8	80.0	84.6	100.0	94.6	70.0	60.0	11.55	11.51
OK05128	OSU	OK	HRW	34.4	37.5	30.6	40.5	13.8	40.0	30.0	4.35	3.07

*SRPN: Southern Regional Performance Nursery; NRPN: Northern Regional Performance Nursery; RGON: Regional Germplasm Observation Nursery; USSRWWN: Uniform Southern Soft Red Winter Wheat Nursery; UESRWWN: Uniform Eastern Soft Red Winter Wheat Nursery; OSU: Oklahoma State University

** HRW: hard red winter wheat; HWW: hard white winter wheat; SRW: soft red winter wheat

Table 3.3 Significant single nucleotide polymorphisms (SNPs) that associated with percentage of symptomatic spikelets in a spike (PSS), *Fusarium* damaged kernels (FDK) and deoxynivalenol (DON) content evaluated in fall 2009 greenhouse (2009G), spring 2010 greenhouse (2010G), fall 2010 greenhouse (2011G) experiments, 2009-2010 (2010F) , 2010-2011 (2011F) field experiments, and best linear unbiased predictions (BLUPs) values for greenhouse PSS (GH-PSS), field PSS (FD-PSS), FDK, DON.

A. PSS

	Marker infromation			2009G-PSS		2010G-PSS		2011G- PSS		GH-PSS BLUP		2010F-PSS		2011F-PSS		FD-PSS BLUP	
Marker_name	Chr	Position	ResistantAllele	p-value	R^2	p-value	R^2	p-value	R^2	p-value	R^2	p-value	R^2	p-value	R^2	p-value	R^2
BS00107852_51	1A	20980029	C					1.1E-05	9.7					3.5E-04	5.1		
D_F1BEJMU01CYX2V_133	1D	89597560	T							6.5E-04	7.9	7.60E-04	4.5	1.7E-04	5.7	1.2E-04	9.7
Excalibur_c18989_1026	2B	629022659	G	4.30E-04	5.2	2.60E-04	6.2	1.6E-05	9.4	5.5E-06	8.5						
Tdurum_contig63460_144	3A	725841228	G			4.80E-04	5.7	1.0E-04	7.5	2.2E-04	6.4						
Tdurum_contig9738_170	3B	798348368	G			5.90E-04	5.5	4.3E-04	6.1	4.3E-04	6.2						
Excalibur_c24511_1282	5B	696023038	A			9.00E-04	5.1	9.0E-04	5.4	2.0E-04	8.2						

B. For the FDK, DON content

FDK, DON traits	Marker infromation			2010F-FDK		2011F-FDK		FDK BLUP		2010F-DON		2011F-DON		DON BLUP	
Marker_name	Chr	Position	ResistantAllele	p-value	R^2	p-value	R^2	p-value	R^2	p-value	R^2	p-value	R^2	p-value	R^2
Excalibur_c687_886	4A	622237212	G	1.00E-05	8.4	1.20E-04	6.5	1.5E-06	9.4	8.60E-05	7.0			4.3E-04	5.1
Excalibur_c687_907	4A	622237191	A	1.40E-04	6.2	3.50E-04	5.6	1.3E-05	7.6	3.80E-04	5.7				
Excalibur_c687_961	4A	622237137	A	1.50E-04	6.1	5.60E-04	5.2	2.1E-05	7.2	4.50E-04	5.5				
Kukri_c1073_91	4A	622236986	T	9.70E-05	6.5	3.60E-04	5.5	1.1E-05	7.8	3.80E-04	5.7				
CAP12_c5949_104	5B	689851808	C	1.40E-04	6.2	7.80E-04	4.9	2.7E-05	7.0	4.00E-04	5.6				
BS00067308_51	5B	690331053	C	5.50E-06	8.9	4.90E-05	7.2	6.8E-07	9.9	4.70E-05	7.5			1.2E-04	6.2
BS00011469_51	5D	546907573	C	9.30E-05	6.5	1.60E-05	8.2	2.0E-06	9.2	8.20E-05	7.0			1.7E-04	5.9
Excalibur_c14043_548	5D	546910514	C			1.30E-04	6.4	2.4E-05	7.1	9.20E-04	4.9				
BobWhite_c13030_406	5D	546086597	G	2.60E-04	5.8	1.10E-05	8.3	5.4E-06	8.3	1.50E-04	6.5			7.5E-04	4.7
BS00079676_51	5D	546652167	A	8.70E-04	4.8	1.30E-04	6.3	2.7E-05	7.0	8.80E-04	4.9			8.6E-04	4.6
RAC875_c13169_459	5D	546652673	G	3.60E-04	5.5	1.50E-04	6.1	1.5E-05	7.5	3.60E-04	5.7				
D_GA8KES401AL4GG_122	5D	546653435	C			3.50E-04	5.4	7.7E-05	6.2	3.90E-04	5.6				
BS00105939_51	5D	546679816	T	5.90E-04	5.1	2.50E-04	5.7	2.7E-05	7.0	8.60E-04	5.0				
Kukri_c7786_81	5D	546689187	T	8.70E-04	4.8	1.80E-04	6.0	3.6E-05	6.8	8.00E-04	5.0				

wsnp_JD_c4438_5568170	5D	546689337	A	3.50E-04	5.6	2.20E-04	5.8	1.8E-05	7.4	3.60E-04	5.7				
wsnp_JD_c4438_5567972	5D	546689535	A	3.60E-04	5.5	1.50E-04	6.1	1.5E-05	7.5	3.60E-04	5.7				
wsnp_JD_c4438_5567834	5D	546689673	C	7.00E-04	5.0	1.90E-04	5.9	3.0E-05	7.0	3.10E-04	5.8				
BobWhite_c4438_162	5D	546689782	C	5.90E-04	5.1	3.00E-04	5.5	3.6E-05	6.8	9.00E-04	4.9				
IACX10520	5D	546689938	A	4.10E-04	5.4	9.90E-05	6.5	1.2E-05	7.7	2.80E-04	5.9				
BS00088587_51	5D	546690002	G	3.50E-04	5.6	1.40E-04	6.2	1.3E-05	7.6	3.80E-04	5.7				
D_GDS7LZN01CBWNE_99	5D	546700575	A	3.60E-04	5.5	1.50E-04	6.1	1.5E-05	7.5	3.60E-04	5.7				
Kukri_c5528_603	5D	546703066	C	3.60E-04	5.5	9.70E-05	6.5	1.1E-05	7.8	3.80E-04	5.7				
Excalibur_c22724_85	5D	546780221	A	7.00E-04	5.0	1.90E-04	5.9	3.0E-05	7.0	3.10E-04	5.8				
BS00073116_51	5D	546864019	T	8.00E-05	6.8	9.50E-04	4.6	2.3E-05	7.2	4.20E-04	5.6				
Excalibur_c42190_383	5D	546906400	A	8.20E-05	6.8	7.00E-04	4.9	1.9E-05	7.3	4.20E-04	5.6	9.5E-04	4.5		
Excalibur_c28592_377	5D	546910004	A	8.00E-05	6.8	9.50E-04	4.6	2.3E-05	7.2	4.20E-04	5.6	8.6E-04	4.6		
Excalibur_c28592_173	5D	546910433	T	8.20E-05	6.8	7.00E-04	4.9	1.9E-05	7.3	4.20E-04	5.6	9.5E-04	4.5		
CAP8_c145_89	5D	547273468	T	7.50E-06	8.9	3.40E-06	9.4	1.1E-07	12	2.10E-05	8.2	9.0E-05	6.4		
CAP7_rep_c12715_390	5D	547273622	C	2.30E-05	7.9	4.00E-05	7.2	8.2E-07	9.9	8.80E-05	6.9	3.0E-04	5.4		
BS00011794_51	5D	547273657	T	1.70E-05	8.2	7.20E-06	8.7	3.6E-07	11	1.70E-05	8.4	6.5E-05	6.7		
wsnp_CAP11_c209_198671	5D	547273711	T	2.40E-05	7.9	2.80E-05	7.5	7.0E-07	10	8.80E-05	6.9	3.4E-04	5.3		
BS00022036_51	5D	547273861	T	2.40E-05	7.9	2.80E-05	7.5	7.0E-07	10	8.80E-05	6.9				

*2009G-PSS: fall 2009 greenhouse percentage of symptomatic spikelets (PSS); 2010G-PSS: spring 2010 greenhouse PSS; 2011G-PSS: fall 2010 greenhouse PSS; 2010F-PSS: 2009-2010 field PSS; 2011F-PSS: 2010-2011 field PSS; 2010F-FDK: 2009-2010 field *Fusarium* damaged kernels (FDK); 2011F-FDK: 2010-2011 field FDK; 2010F-DON: 2009-2010 field deoxynivalenol (DON) content; 2011F-DON: 2010-2011 field DON content

Table 3.4 The total number of resistant alleles for percentage of symptomatic spikelets in a spike (PSS) quantitative trait locus (QTLs), *Fusarium* damaged kernels (FDK) and deoxynivalenol (DON) QTLs in each accession.

Accessions	FDPSS*	GHPSS	FDK	DON	PSS QTLs**							FDK and DON QTLs			
					1A	1D	2B	3A	3B	5B	Total No.	4A	5B	5D	Total No.
Atlas66	48.4	21.4	42.5	21.71	1	0	0	0	0	1	2	0	0	0	0
OK04505	71.1	84.4	42.5	8.32	1	0	0	0	0	1	2	1	1	1	3
KS05HW136-3	75.7	76.4	37.5	17.38	1	0	0	0	0	1	2	1	1	1	3
T158	83.2	82.4	35.0	5.63	1	0	0	0	0	1	2	1	1	1	3
KS980554-12-~9	65.4	65.5	53.8	9.68	0	0	1	1	1	1	4	1	1	1	3
KS980512-2-2	55.5	28.9	40.0	16.56	1	0	0	0	0	1	2	1	1	1	3
TX04M410211	95.0	94.6	55.0	10.66	1	0	0	0	0	1	2	1	1	1	3
N98L20040-44	88.8	76.7	72.5	7.35	1	0	1	0	0	1	3	0	0	0	0
NI04420	41.8	26.0	45.0	8.66	1	1	1	0	0	1	4	1	1	1	3
Duster	88.9	82.4	57.5	11.49	1	0	0	0	0	1	2	1	1	1	3
OK02522W	69.4	48.9	48.8	13.91	1	0	0	0	0	1	2	1	1	1	3
Scout 66	73.8	45.9	40.0	9.10	1	0	0	0	0	1	2	0	0	0	0
AP04T8211	39.8	80.7	40.0	5.05	1	0	0	0	0	0	1				0
HV9W96-1271R-1	64.6	85.9	33.8	6.27	1	1	1	0	0	1	4	1	1	1	3
NE04424	74.3	62.1	37.5	8.57	1	0	1	0	0	1	3	1	1	1	3
CO02W237	81.4	70.3	21.3	9.24	1	0	0	0	0	1	2	1	1	1	3
OK03825-5403-6	81.6	73.0	62.5	7.76	1	1	0	0	0	1	3	0	0	0	0
TX04V075080	83.8	87.3	30.0	7.75	1	0	0	0	0	1	2	1	1	1	3
SD06165	71.3	65.4	57.5	10.34	1	0	0	0	0	1	2	1	1	1	3
NX03Y2489	89.3	93.7	60.0	17.35	1	0	0	0	0	0	1	0	0	0	0
NI04427	57.8	72.8	35.0	6.41	1	1	0	0	0	1	3	1	1	1	3
Endurance	22.4	24.7	30.0	5.45	1	1		1	1	1	5	1	1	1	3
TAM-107	67.9	73.1	37.5	5.23	1	1	0	0	0	1	3	0	0	0	0
AP05T2413	53.2	22.1	56.3	7.43	1	1	0	0	0	1	3	0	0	0	0
HV9W03-539R	59.5	77.2	47.5	6.50	1	0	0	0	0	1	2	0	0	0	0
CO03064	58.1	65.9	57.5	11.02	1	0	1	1	1	1	5	1	0	0	1

TX02A0252	87.9	98.5	66.3	11.53	0	0	1	0	0	1	2	0	0	0	0
Kharkof	61.9	65.0	30.0	7.71	1	0	0	0	0	1	2	1	0	0	1
SD06173	48.7	76.1	30.0	4.66	1	0	0	0	0	1	2	0	0	0	0
NX04Y2107	79.2	90.7	42.5	15.01	1	0	0	0	0	1	2	0	0	0	0
NE05548	60.7	71.0	27.5	7.96	1	0	0	1	1	1	4	1	1	1	3
Deliver	71.9	94.2	36.3	10.37	1	0	0		1	1	3	1	1	1	3
Trego	72.4	98.6	48.8	15.41	1	0	0	0	0	1	2	1	1	1	3
HV9W03-696R-1	61.3	87.8	28.8	6.18	1	1	0	0	0	1	3	1	1	1	3
NE05426	96.5	91.7	55.0	10.02	1	0	0	0	0	1	2	1	1	1	3
CO03W054	52.7	63.6	37.5	15.82	1	0	0	0	0	1	2	0	0	0	0
TX03A0148	55.4	86.7	80.0	8.49	1	0	0	0	0	1	2	0	0	0	0
Antelope	60.1	85.8	47.5	14.45	1	0	0	0	0	0	1	1	1	1	3
SD03164-1	31.2	62.1	17.5	4.69	1	0		0	0	1	2	1	1	1	3
NW04Y2188	53.3	78.5	57.5	7.75	1	0	0	0	0	0	1	0	0	0	0
NE05549	38.8	80.9	55.0	8.69	1	0	0	0	0	1	2	1	1	1	3
OK Bullet	90.2	74.6	26.3	4.71	1	0	0	0	0	1	2	1	1	1	3
OK03716W	84.2	68.0	40.0	4.84	1	0	0	0	0	1	2	1	1	1	3
OK00514-05806	62.2	61.4	42.5	5.90	1	0	0	0	0	1	2	1	1	1	3
AP06T3832	71.3	76.8	70.0	5.67	1	0	0	0	0	1	2	1	1	1	3
HV9W02-942R	23.4	34.6	50.0	5.68	1	1	0	0	0	1	3	1	1	1	3
NE05430	62.4	80.0	33.8	6.87	1	0		0	0	1	2	1	1	1	3
CO03W139	22.1	70.0	16.3	5.30	1	0		0	0	1	2	1	1	1	3
TX03A0563	84.4	96.8	55.0	7.22	1	0	0	0	0	1	2	1	1	1	3
Wesley	59.0	59.6	46.3	7.27	1	0	0	0	0	1	2	1	1	1	3
NE02533	47.7	52.8	40.0	4.37	1	0	0	0	0	1	2	1	1	1	3
NE05569	60.7	59.0	51.3	8.52	1	0	0	0	0	0	1	1	1	1	3
Overley	83.8	85.8	68.8	12.16	1	0	0	0	0	1	2	1	1	1	3
OK05903C	42.2	69.7	53.8	10.03	1	0	0	1	1	1	4	1	1	1	3
Century	48.4	18.9	30.0	4.75	1	1	1	0	0	1	4	0	0	0	0
KS05HW15-2	81.9	60.8	35.0	9.22	1	0	0	0	0	1	2	1	1	1	3
T151	48.8	67.4	20.0	3.00	1	1	0	0	0	1	3	1	1	1	3

KS970093-8-9-#1	25.1	20.0	16.3	6.38	1	0	0	1	1	1	4	1	1	1	3
CO03W239	100.0	99.0	92.5	17.12	1	0	0	0	0	1	2	1	0	0	1
TX04A001246	64.2	74.4	60.0	5.27	1	1	0			1	3		1	1	2
Jerry	38.0	58.9	43.8	12.02	1	0	1	0	0	1	3	0	0	0	0
SD05118	65.3	25.6	53.8	13.28	1	0	1	0	0	1	3	0	0	0	0
NE02558	63.6	67.1	27.5	5.78	1	0	0	0	0	1	2	1	1	1	3
MT0495	50.1	73.7	58.8	12.13	0	0	0	0	0	1	1	0	0	0	0
Fuller	38.7	62.1	40.0	7.04	1	0	0	0	0	1	2	1	1	1	3
OK03522	57.3	64.0	36.3	3.67	1	0	0	0	0	1	2	1	1	1	3
KS05HW121-2	82.8	58.0	42.5	11.34	1	0	0	0	0	1	2	1	1	1	3
T153	28.1	31.0	26.3	3.09	1	1	1	1	1	1	6	1	1	1	3
KS970187-1-10	30.0	52.4	45.0	9.63	1	0	1	0	0	1	3	1	1	1	3
CO03W043	60.6	65.7	36.3	12.38	0	0	1	0	0	1	2	1	1	1	3
TX01V5134RC-3	51.2	77.0	31.3	4.32	1	1	0	0	0	1	3	1	1	1	3
SD06W117	78.0	96.5	35.0	10.72	1	0	0	0	0	1	2	1	1	1	3
SD05210	43.6	18.4	36.3	12.88	1	0	1	0	0	1	3	1	1	1	3
NW03666	60.3	90.5	42.5	8.53	1	0	0	1	1	1	4	1	0	1	2
MTS0531	56.0	27.2	36.3	11.85	1	0	0	1	1	1	4	0	0	0	0
Centerfield	63.5	41.1	37.5	4.79	1	1	1	0	0	1	4	1	1	1	3
OK04525	55.9	86.6	40.0	4.47	1	0	0	1	1	1	4	1	1	1	3
OK03305	81.3	91.5	13.8	4.53	1	0	0	0	0	1	2	1	1	1	3
MT0552	68.7	76.0	41.3	5.65	1	0	0	1	1	1	4	0	0	0	0
T154	19.5	15.5	26.3	3.89	1	1	1	1	1	1	6	1	1	1	3
NE05496	86.1	80.9	42.5	6.86	1	0		0	0	1	2	1	1	1	3
TX04M410164	89.3	77.8	68.8	7.35	1	0	0	0	0	1	2	0	0	0	0
SD06069	53.3	32.1	67.5	10.81	1	0		0	0	1	2	0	0	0	0
SD05W030	83.0	67.5	31.3	8.44	1	1	0	0	0	1	3	1	1	1	3
chisholm	76.6	58.1	45.0	4.37	1	0	1	1	1	1	5	1	1	1	3
Guymon	92.0	96.3	40.0	14.51	1	0	0	0	0	1	2	1	1	1	3
OK05830	58.8	77.4	62.5	9.49	1	0	0	0	0	1	2	1	1	1	3
OK02405	20.8	62.8	15.0	3.01	1	0	0	0	0	1	2	1	1	1	3

KS010957K~4	68.8	75.7	68.8	10.34	1	0	1	0	0	1	3	1	1	1	3
NE06619	40.3	55.4	57.5	8.48	1	0	0	0	0	1	2	0	0	0	0
MTS04120	50.9	61.9	45.0	7.11	1	0	0	0	0	1	2	0	0	0	0
TX06A001239	80.1	92.1	63.8	9.70	1	0	0	0	0	1	2	1	1	1	3
TXHT006F8-CS06/472-STA34	66.7	84.7	68.8	20.94	1	0		0	0	1	2	0	0	0	0
MO011126	22.0	43.5	15.0	6.91	1	1		0	0	1	3	1	1	1	3
OH02-7217	38.1	31.5	17.5	9.95	1	0	0	1	1	1	4	0	0	0	0
MD99W483-06-9	37.2	35.2	22.5	6.90	1	1	0	1	1	1	5	1	1	1	3
OK04507	83.5	86.2	73.8	9.01	1	0	1	0	0	1	3	1	1	1	3
KS020304K~3	67.3	62.1	52.5	7.79	1	0	0	0	0	1	2	1	1	1	3
KS010143K-11	60.5	46.4	30.0	9.59	1	0	0	0	0	0	1	1		1	2
TX05A001334	73.5	68.0	31.3	3.81	1	0	0	1		1	3	1	1	1	3
TX06A001376	55.1	39.3	72.5	11.90	1	0	1	0	0	1	3	0	0	0	0
VA03W-412	72.7	80.3	26.3	8.73	1	0	0	0	0	0	1	1	1	1	3
OH03-41-45	86.0	82.0	32.5	4.38	0	0	0	0	0	0	0	1	1	1	3
OK05312	63.9	57.7	36.3	6.49	1	0	1	0	0	1	3	1	1	1	3
HV9W05-881R	79.2	74.8	47.5	8.26	1	0	0	0	0	0	1	1		1	2
NE06436	63.0	64.8	45.0	8.19	1	0	0	0	0	1	2	1	1	1	3
NW05M6011-6-1	43.7	40.0	42.5	16.36	1	0	1	1		1	4	0	0	0	0
TX06A001431	90.0	93.3	80.0	9.96	1	0	0	1	1	1	4	0	0	0	0
TXHT023F7-CS06/607-STA07/40	64.1	85.7	70.0	6.03	1	0	0	0	0	1	2				0
AR97044-10-2	64.2	53.8	38.8	6.41	1	0	1	1	1	1	5	1	1	1	3
P02444A1-23-9	14.9	34.9	20.0	1.99	1	0	0	1	1	1	4	0	0	0	0
VA05W-414	56.0	68.0	22.5	5.77	1	0	0	0	0	1	2	1	1	1	3
OK05511	50.3	95.3	27.5	10.64	1	0	0	0	0	1	2	1	1	1	3
SD07W041	72.8	76.4	42.5	19.66	1	0	0	0	0	0	1	1	1	1	3
SD07204	49.9	81.0	68.8	18.92	1	0	0	0	0	0	1	0	0	0	0
NW05M6015-25-4	22.1	70.6	22.5	6.93	1	0	0	1	1	1	4	1	1	1	3
TXHT001F8-CS06/325-PRE07/75	40.7	55.6	56.3	8.17	1	0	0	0	0	1	2		1	1	2
CO04W210	46.0	28.0	33.8	11.67	1	0	0	0	0	1	2	1	1	1	3
KY96C-0769-7-3	25.6	19.9	12.5	4.88	1	1	0	1	1	1	5	1	1	1	3

P03207A1-7	63.8	18.8	21.3	4.81	1	1	0	1	1	1	5	1	1	1	3
LA01*425	50.6	52.4	22.5	5.04	0	1	0	0	0	0	1	0	0	0	0
KS07HW25	65.4	41.5	52.5	16.44	1	0	0	0	0	1	2	0	0	0	0
SD07220	32.1	59.1	27.5	5.49	1	0	1	0	0	1	3	0	0	0	0
KS010379M-2	79.2	71.8	57.5	15.08	1	0	0	0	0	1	2	1	1	1	3
NE06472	88.9	60.6	50.0	5.60	1	0	0	0	0	1	2	0	0	0	0
Roane	22.6	10.7	11.3	2.43	1	1	0	1	1	1	5	1	1	1	3
OH02-12678	37.6	30.5	17.5	4.80	1	1	0	0	0	1	3	1	1	1	3
LA02-923	76.6	76.9	31.3	10.10	0	0	0	0	0	0	0	1	1	1	3
SD05W148-1	38.8	50.6	16.3	11.23	1	1	0	1	1	1	5	0	0	0	0
KS010514-9TM-10	82.9	85.0	75.0	16.48	1	0	0	0	0	1	2	1	1	1	3
N02Y5117	43.5	39.1	60.0	9.45	1	0	0	0	0	1	2	0	0	0	0
INW0411	15.5	5.9	25.0	1.94	1	1	0	1	1	1	5	1	1	1	3
MO040192	55.8	73.1	32.5	4.08	1	0	0	0	0	1	2	1	1	1	3
KS07HW81	84.0	84.3	50.0	15.03	1	0	0	0	0	1	2	1	1	1	3
U07-698-9	22.9	35.4	15.0	7.22	1	0	1	0	0	1	3	1	1	1	3
TX05V5614	81.9	78.9	55.0	6.56	1	0		0	0	1	2	0	0	0	0
Branson	49.7	57.3	13.8	3.81	1	0	0	0	0	1	2	1	1	1	3
IL00-8530	36.8	23.6	15.0	2.66	1	0				1	2	1	1	1	3
IL02-18228	14.9	54.7	7.5	1.89	1	0	0	0	0	1	2	1	1	1	3
KS07HW117	76.5	86.3	65.0	16.40	1	0	0	0	0	1	2	0	0	0	0
NE06549	55.5	67.2	61.3	14.96	1	0	0	0	0	1	2	0	0	0	0
TX06A001084	84.8	93.1	53.8	4.56	1	0	0	0	0	1	2	0	0	0	0
Bess	29.0	17.1	6.3	5.24	1	0	1	0	0	1	3	1	1	1	3
IL02-19463	56.9	66.6	13.8	3.00	1	0	0	0	0	1	2	1	1	1	3
Mocha exp.	59.4	45.1	72.5	5.03	1	0	0	0	0	1	2	0	0	0	0
Pioneer Brand 26R61	56.9	63.1	70.0	9.84	1	1	0	0	0	1	3	1	1	1	3
NC04-15533	44.5	52.4	33.8	4.53	0	0	0	1	1	0	2	1		1	2
M03-3616-C	24.1	31.5	31.3	5.95	1	1	0	0	0	1	3	0	0	0	0
W98007V1	62.8	67.2	31.3	2.64	0	0	0	1	1	1	3	1	1	1	3
Arena exp.	51.5	82.9	30.0	3.66	0	0	1	0	0	0	1	1	1	1	3

Coker 9553	40.0	86.7	21.3	5.73	1	0	0	0	0	0	1	1	1	1	3
VA05W-258	38.3	68.3	18.8	2.78	1	1	0	0	0	1	3	1	1	1	3
B030543	83.7	42.8	11.3	3.72	1	1	0	1	1	1	5	0	0	0	0
W98008J1	55.0	81.1	20.0	2.52	1	0	0	0	0	1	2	1	1	1	3
OK05122	67.0	90.7	11.3	5.77	1	0	0	0	0	1	2	1	1	1	3
OK06210	91.3	100.0	71.3	8.89	1	0	0	0	0	1	2	1	1	1	3
India exp.	16.1	60.3	13.8	2.25	1		0	0	0	1	2	1	1	1	3
G69202	24.7	27.6	35.0	3.57	1	0	0	1	1	1	4	0	0	0	0
USG 3555	22.2	25.2	40.0	8.00	1	1	0	1	1	1	5	1	1	1	3
LA01138D-52	80.1	94.4	72.5	19.12	0	0	0	0	0	1	1	1	1	1	3
VA05W-78	75.6	81.1	52.5	15.96	1	1	0	0	0	1	3	0	0	0	0
OK05723W	67.4	34.3	46.3	7.19	1	0	1	1	1	1	5	1	1	1	3
OK06319	65.3	48.2	40.0	6.44	1	0	1	0	0	1	3	1	1	1	3
D04*5513	67.8	53.2	72.5	11.73	1	0	0	1	1	1	4	0	0	0	0
M04-4566	60.9	66.9	68.8	7.48	1	1	0	0	0	1	3	0	0	0	0
NC03-6228	52.9	81.1	30.0	2.97	1	0	0	1	1	0	3	1		1	2
AR96077-7-2	49.7	37.6	36.3	6.86	1	1	0	1	1	0	4	1		1	2
D04-5012	82.5	88.4	62.5	11.02	1	0	0	0	0	1	2	0	0	0	0
G59160	26.6	56.3	22.5	4.33	1	1	0	0	0	1	3	1	1	1	3
OK01420W	69.1	60.4	50.0	7.16	1	0	0	0	0	1	2	1	1	1	3
OK06528	59.6	39.9	38.8	8.95	1	1	1	0	0	1	4	1	1	1	3
OK06518	40.2	83.6	16.3	3.39	1	1	1	0	0	1	4	1	1	1	3
KY97C-0321-02-01	80.3	72.7	27.5	6.05	1	0	0	0	0	0	1	1		1	2
M04-4802	50.9	57.5	52.5	4.42	1	0	0	1	1	1	4	1	1	1	3
AR97124-4-3	69.7	49.3	33.8	3.29	1	0	0	1	1	1	4	1	1	1	3
GA991336-6E9	73.8	97.6	56.3	11.88	0	0	0	0	0	0	0	0	0	0	0
G61505	25.8	40.0	17.5	2.60	1	0	0	0	0	1	2	1	1	1	3
OK05134	38.8	15.4	38.8	7.12	1	0	1	1	1	1	5	1	1	1	3
OK06313	61.1	47.7	36.3	4.43	1	0	1	1	1	1	5	1	1	1	3
KY97C-0519-04-07	30.9	35.9	25.0	4.97	1	1	0	1	1	1	5	1	1	1	3
M04*5109	28.9	26.6	23.8	4.04	1	1	0	1	1	1	5	1	1	1	3

VA04W-259	77.2	59.5	52.5	9.29	0	0	0	0	0	1	1	1	1	1	3
MD01W233-06-1	28.0	24.6	12.5	1.80		1	0	1	1	1	4	1	1	1	3
GA991209-6E33	36.1	74.6	26.3	4.34	1	0	0	0	0	1	2	0	0	0	0
G41732	23.4	42.2	37.5	4.79	1	0	0	0	0	1	2	0	0	0	0
OK06848W	73.1	63.8	38.8	10.59	1	0	0	0	0	1	2	1	1	1	3
W06-202B	52.9	37.5	52.5	6.94	1	0	1	1	1	1	5	0	0	0	0
TAM 110	54.9	87.1	63.8	5.61	1	0	0	0	0	1	2	1	1	1	3
LA99005UC-31-3-C	85.1	76.4	60.0	6.87	0	0	0	0	0	1	1	0	0	0	0
P03112A1-7-14	38.0	35.6	15.0	3.22	1	0	0	1	1	1	4	1	1	1	3
TN801	87.7	68.1	43.8	9.10	0	0	0	1	1	0	2	0	0	0	0
GA991371-6E13	93.1	90.9	60.0	15.78	0	0	0	0	0	0	0	0	0	0	0
OK05212	37.8	58.8	27.5	5.22	1	0	0	0	0	1	2	1	1	1	3
OK06336	54.6	36.7	45.0	5.70	1	0	1	0	0	1	3	1	1	1	3
MO040152	33.2	10.0	35.0	9.12	1	0	1	0	0	1	3	1	1	1	3
AGS 2000	72.0	94.6	36.3	11.96	0	1	0	0	0	0	1	0	0	0	0
LA98214D-14-1-2-B	97.8	95.9	43.8	6.81	0	0	0	1	1	0	2	1		1	2
P04287A1-10	35.8	36.7	13.8	3.80	1	0	0	1	1	1	4	1	1	1	3
M04-4715	36.6	42.4	33.8	3.09	1	1	0	0	0	1	3	1	1	1	3
GA991227-6A33	64.9	93.1	65.0	11.53	0	1	0	0	0	0	1	1	1	1	3
OK05128	35.9	28.3	35.0	3.71	1	1	1	1	1	1	6	1	1	1	3

*FDPSS: PSS value from the field experiments; GHPSS: PSS value from the greenhouse experiments

** 0 reprsents having the resistant QTLs, and 1 represents no QTLs in the line.

Chapter 4 - Developing an Algorithm for Efficient *Fusarium* Damaged Kernels Evaluation

Introduction

As the sequencing technologies have developed rapidly in recent years, phenotyping methods have become one of the main limitations for accelerating the speed of breeding in the 'omics' era (Schrag et al., 2018; Mwadzingeni et al., 2016; Varshney et al., 2016). One solution is using computer vision and machine learning algorithms to develop accessible and efficient high-throughput technologies for phenotyping. These novel technologies have already been employed in fruits, vegetables, and grain crops for food safety and quality (Bhargava et al., 2018; Patrício et al., 2018; Saini et al., 2012). From these studies, it is clear that high-throughput phenotyping systems can be effectively used for disease detection and evaluation (Sankaran et al., 2010; Maloney et al., 2014; Ghaiwat et al., 2014).

Fusarium head blight (FHB), as one of the most destructive crop diseases in the U.S. and many other countries, not only reduces the grain yield but also lowers the grain quality (Bai et al., 2004). In wheat, when the infection occurs after the flowering, the FHB damage appears in kernels, thus we also called the infected kernels as *Fusarium* damaged kernels (FDK). Compared with the healthy kernels, FDK are typically decolored, some may become pinkish on the bran. Additionally, FDK is commonly shrunk and weighted lighter than healthy kernels (Wiwart et al., 2001). Besides being a parameter for the evaluation of FHB damage, some studies have shown that the FDK had a significant correlation with the content of a hazardous mycotoxin, deoxynivalenol or DON (Jin et al., 2014; Ittu et al., 2008). DON is a vomitoxin that is harmful to both human and animal consumption. Reducing FDK and delimiting DON in wheat grains are two of the primary objectives for wheat breeding and FHB management. However, the systems

for FDK and DON evaluation are usually technically complicated, time-consuming, and costly (Brown-Guedira et al., 2008; Buerstmayr et al., 2009).

To date, the most widely used method for FDK assessment is a visual inspection. To do this, evaluators first set up a series of FDK checks with different percentages of damaged kernels (e.g., 1, 5, 10, 25, … 100%). Each check is prepared by mixing a certain number of FDK with healthy kernels. Then evaluators need to quickly compare each sample with all the checks to identify the most closely matched check to estimate the percentage of FDK in each sample (Jin, 2016).

This method is straightforward, but need to be done by experienced evaluators, or the results may fluctuate with different evaluators. Even trained evaluators can get tired quickly when a larger number of samples need to be evaluated in a short time. Thus, it can be hypothesized that more robust FDK scoring systems with up-to-date technologies will help improve FDK scoring efficiency and accuracy.

Several methods have been developed for this purpose including near-infrared (NIR) (Peiris et al., 2010), computer version (Suchowilska et al., 2006) and deep learning (Nicolau et al., 2018) technologies. However, there is no report on combining the image processing and unsupervised machine learning algorithms to detect FDK. Besides, all these FDK scoring systems need specific devices for data collection and analysis, which may limit the accessibilities to breeders and pathologists. Our objective is to develop an accessible algorithm using unsupervised classification methods which can be applied on multiple platforms for fast evaluation of FDK.

Materials and methods

Plant materials

The kernels from 25 randomly selected recombinant inbred lines were used in this project as the plant materials. They all were from an $F_{5:6}$ mapping population of 186 lines developed from the cross 'Overland' × 'Overley'. The population was planted in the FHB nursery during the 2015-2016 wheat year, Rocky Ford, Manhattan, KS. The inoculation method was the same as field FHB evaluation method described in Chapter 2. All the lines were harvested and threshed manually in July 2016. The threshed grains, including FDK and non-FDK, from each plot, were regarded as one sample. The FDK for each sample was visually evaluated, as described in Chapter 3.

Data collection and devices applied in the experiments

To make the algorithm more practical, the device applied for collecting pictures was an Apple iPhone 8 (Apple Inc, Cupertino, CA). The camera was set using all default settings to generate pictures with 1536 × 2408 pixel resolution. All the pictures were taken without extra light sources in an office room in Kansas State University, Manhattan, KS. Three individual photos per sample were taken as original images for this project. About 22-90 seeds in each picture were randomly selected from a sample seed bag and space spread on a rough black cloth without any seed overlapped. A 3 × 3 cm square white paper cut from regular A4 paper was included in every picture for automatic adjustment of white balance and size reference for the kernel size. Each picture was taken from a distance of around 27 cm from the grains, while the iPhone was placed straight up over the seeds. After a photo was taken, the grains for the picture were visually counted for total FDK and non-FDK that were used as the visual rating for the picture later, with a general repeatability about 0.91. After counting, all the seeds were put back

to the original seed bag and mixed well for another picture. The FDK ratio was calculated per picture using Equation 3.1 described in Chapter 3. The FDK ratios from the three pictures were averaged to represent FDK of a sample for further analysis.

A Windows 10 personal computer (ASUS Zenbook 13 UX333FA DH51, Intel Core i5, 8GB Memory) was used for the image analysis and FDK ratio calculation. The algorithm was written in Python version 3.5 (Python Software Foundation, 2015) using Anaconda distribution (Anaconda Software Distribution, 2016). The image processing tasks were done using the OpenCV python library (Bradski, 2000), and numpy library (Walt et al., 2011). The Scikit-learn python library (Walt et al., 2014) was used for the unsupervised machine learning classification. Two unsupervised learning models, K-Means (Lloyd, 1982) and Gaussian mixture model (GMM) (Rasmussen, 2000), were applied in this project.

Workflow

The workflow of this algorithm was depicted in Figure 4.1. In general, the algorithm consisted of three parts: image processing, unsupervised classification, and the FDK ratio calculation. A picture was input as a red, green blue (RGB) file first and then converted into the binary format for segmentation algorithms to find all the possible contours. According to the area of each contour, the wheat kernel contours were masked. Using the pictures with the kernel contours masked, the average color was extracted from each contour and saved in a data list where each item contained three values representing R, G, B, respectively. Then the data list was used in two different unsupervised learning models (K-means, Gaussian Mixture Models (GMM)) to classify into two groups. After applying the unsupervised model, the centroid value of each cluster from the K-means model, and the mean value from the GMM model were summed up. Since the FDK group should have a lighter color than the non-FDK group, in the K-

Means classification, the cluster with a greater sum of the RGB values was determined as the FDK group while the other one was considered as the non-FDK cluster. For the GMM clustering, the item (with three values represent R, G, B) in the data list whose probability was high than 0.9 as well as in the larger sum value group was determined as the FDK. The total seed number extracted from the picture was used for the FDK ratio calculation in both clustering methods. At last, the algorithm lists the number of FDK, total kernel number, and FDK ratio computed from the two unsupervised classification methods.

Processing steps

Segmentation of a picture

Once the original picture (Figure 4.2) was imported, the processing steps started. To increase the efficiency of the algorithm, the input picture was firstly resized to a smaller one with 800×800 pixels that can be customized by the users to pair with their data collection and picture processing devices. The resized picture was then converted into a binary image (Figure 4.3) that only used 0 and 1 in the computer to process the file for finding the contours. Otsu's Binarization (Otsu, 1979) was applied to set the threshold value for the separation of objects from backgrounds. All the detected contours from the original picture (Figure 4.2) can be seen as the green boundaries in Figure 4.4.

Select wheat kernels

Due to the quality of the original image, not all the contours represent the wheat kernels (Figure 4.4). In an 800×800 pixels resized picture, a typical wheat kernel area in this project is between 60 to 500. According to the area of all the contours, a mask was created to select the contours (Figure 4.5) within this range. These selected contours would be used for the next steps, while the others were masked out.

Determine the average color of each kernel

Once the kernels were masked, the average color of each contour was calculated and extracted out. In Figure 4.6, the kernels were filled with their average color. These average colors were saved as a data list using the RGB format in the algorithm, which would be applied as the input data in the next step for the two unsupervised machine learning classifications. Now, each kernel can be considered a data point with three values, which was available to depict in a space defined by the R, G, B coordinators.

Clustering by unsupervised learning algorithms to separate FDK and non-FDK

All the kernels in the picture should be clustered into two groups, FDK and non-FDK. According to this, the k number in the K-means classification, and the number of the components in the GMM both should be 2. The two unsupervised classification methods used the same data list that was saved earlier as the kernel average mean color in RGB format. For the K-means classification, each kernel would have a label of its clustered group, while for the GMM clustering, the probabilities of each kernel in the two groups were generated. For each group, only the ones with higher than 0.9 possibilities were used for the next step.

FDK ratio calculation

Since the FDK was decolored from healthy kernels, the sum of centroid/mean RGB values of FDK group should be greater than the non-FDK group. Based on the sum value, the FDK cluster was selected from two classification methods. The length of the FDK cluster was considered as the FDK number and used in the ratio calculation. At last, the FDK ratio and number of FDK from each classification method would be listed on the screen to end the algorithm.

Results and discussion

Counting total kernel number

In total, 71 pictures with 3,830 wheat kernels from 25 RILs were analyzed (Table 4.1) with an average of 53.29 kernels per picture. The mean kernel number detected by the algorithm was 52.85 per picture. The actually counted seed number and the estimated seed number from the picture were almost the same with a correlation coefficient of 0.996 (Figure 4.7), suggesting the algorithm worked effectively and accurately for kernel identification when these kernels were well separated. If the kernels are touched, the algorithm may 1) cannot detect the kernel as the touched kernel-combine are too big, and flited out by the size limitations 2) only regard the kernel-combine as one kernel to detect the color and do the classification. In the algorithm, the kernel counts from the picture were lower than the actual kernel counts in general, because we set a relatively higher threshold for the contour area to select kernels. Undeveloped or broken kernels may be smaller in kernel size than the algorithm defined threshold. However, these kernels were not the majority of the samples. To minimize the picture noise and small non-kernel contours, this algorithm would not consider the limited number of tiny or broken kernels. Thus, the algorithm can be further modified for counting kernels, with additional width and length detection to broaden the application of seed phenotyping using digital images.

Classification of kernels on a single picture

For each picture, data from two unsupervised classification methods were analyzed and compared with the single kernel separation and count results (the ground truth). For the sample picture (picture ID 4404), 60 kernels in the picture were used to calculate the FDK ratio (Figure 4.8). The K-means clustering method detected 24 kernels that had a greater centroid sum as FDK group, while only seven kernels were regarded as FDK when the GMM method was used for

clustering. And 10 FDK were visually identified by human eyes. Every single kernel was regarded as a three-dimension point with the R, G, B coordinates (Figure 4.9), and two clustering methods varied at the inter-region. The K-means method tended to cluster all the points in relatively balanced clusters; but the GMM more accurately picked up the FDK. In this project, only the red wheat kernels were tested using the algorithm, other kernel coat wheat FDK will be done in the future.

To determine the accuracy of the two methods, each single kernel was visually rated as the true value in this study. When the confusion matrix and accuracy were calculated from the 71 pictures for each of the two unsupervised clustering methods (Table 4.2), the average accuracy was 0.88 for K-Mean and 0.92 for GMM method, with the minimum accuracy 0.61 for the K-means and 0.69 for GMM methods and the maximum accuracy of 1 for both methods. Both classification methods provided higher accuracy than the RGBH method in which the model was built from the RGB and HSL values of the digital images (Jirsa & Polišenská, 2011). Moreover, the accuracy of the GMM model was similar or better than the hyperspectral image and linear discrimination analysis models from a previous study (Shahin & Symons, 2011). Although the algorithm was not as accurate as a NIR-based device (Peiris et al., 2010), the processing time (0.2 seconds per picture) of the algorithm is much shorter than the NIR-based device. Therefore, quick processing time per sample and acceptable data accuracy make the algorithm more attractive for routine FDK rating.

The pairwise correlation for the FDK of lines

Pairwise Pearson correlations were calculated between actual FDK value and FDK ratings obtained from visual scoring and from the pictures using K-means clustering and GMM methods (Figure 4.10). All three methods were significantly positively correlated with the visual

ratings (single kernel separation and count result for each sample). GMM method had the highest correlation, followed by the visual scoring and the K-Means method. The two unsupervised clustering methods had a significant positive correlation, which maybe because the two clustering methods used the same pictures for every sample.

In this project, we developed an efficient algorithm using python for a fast and accurate evaluation of FDK by two classification methods (K-means and GMM) and computer vision. In total, 71 pictures with 3,830 wheat kernels from 25 RILs were analyzed, revealing that the algorithm can be applied for fast FDK evaluation for the red wheat kernels. The evaluators can use both methods of classification results or choose the most suitable one to fit their own projects. This algorithm can be applied on multiple platforms to build FDK detection devices for breeders to use it in routine breeding to improve the wheat FHB resistance in the future.

References

Anaconda Software Distribution. Computer software. Vers. 2-2.4.0. Anaconda, Nov. 2016. Web. https://anaconda.com.

Bai, G., & Shaner, G. (2004). Management and resistance in wheat and barley to *Fusarium* head blight. Annual Review of Phytopathology, 42, 135-161.

Bhargava, A., & Bansal, A. (2018). Fruits and vegetables quality evaluation using computer vision: A review. Journal of King Saud University-Computer and Information Sciences. https://doi.org/10.1016/j.jksuci.2018.06.002.

Bradski, G. (2000). The opencv library (2000). Dr. Dobb's Journal of Software Tools.

Ghaiwat, S. N., & Arora, P. (2014). Detection and classification of plant leaf diseases using image processing techniques: a review. International Journal of Recent Advances in Engineering & Technology, 2(3), 1-7.

Ittu, M., Cana, L., Tabuc, C., & Taranu, I. (2008). Preliminary evaluation of some factors involved in DON contamination of bread wheat under natural and artificial inoculation. Romanian Agricultural Research, 25, 37-41.

Jirsa, O., & Polišenská, I. (2014). Identification of *Fusarium* damaged wheat kernels using image analysis. Acta Universitatis Agriculturae et Silviculturae Mendelianae Brunensis, 59(5), 125-130.

Jin, F., Bai, G., Zhang, D., Dong, Y., Ma, L., Bockus, W., & Dowell, F. (2014). *Fusarium*-damaged kernels and deoxynivalenol in *Fusarium*-infected US winter wheat. Phytopathology, 104(5), 472-478.

Lloyd, S. (1982). Least squares quantization in PCM. IEEE Transactions on Information Theory,

28(2), 129-137.

Maloney, P. V., Petersen, S., Navarro, R. A., Marshall, D., McKendry, A. L., Costa, J. M., & Murphy, J. P. (2014). Digital image analysis method for estimation of *Fusarium*-damaged kernels in wheat. Crop Science, 54(5), 2077-2083.

Mwadzingeni, L., Shimelis, H., Dube, E., Laing, M. D., & Tsilo, T. J. (2016). Breeding wheat for drought tolerance: Progress and technologies. Journal of Integrative Agriculture, 15(5), 935-943.

Nicolau, M., Pimentel, M. B. M., Tibola, C. S., Fernandes, J. M. C., & Pavan, W. (2018). *Fusarium* damaged kernels detection using transfer learning on Deep neural network architecture. arXiv preprint arXiv:1802.00030.

Otsu, N. (1979). A threshold selection method from gray-level histograms. IEEE Transactions on Systems, Man, and Cybernetics, 9(1), 62-66.

Patrício, D. I., & Rieder, R. (2018). Computer vision and artificial intelligence in precision agriculture for grain crops: A systematic review. Computers and Electronics in Agriculture, 153, 69-81.

Peiris, K. H. S., Pumphrey, M. O., Dong, Y., Maghirang, E. B., Berzonsky, W., & Dowell, F. E. (2010). Near-infrared spectroscopic method for identification of *fusarium* head blight damage and prediction of deoxynivalenol in single wheat kernels. Cereal Chemistry, 87(6), 511-517.

Rasmussen, C. E. (2000). The infinite Gaussian mixture model. In Advances in Neural Information Processing Systems. Pp. 554-560. MIT Press, Cambridge, MA, USA.

Saini, M., Singh, J., & Prakash, N. (2014). Analysis of wheat grain varieties using image

processing–a review. International Journal of Science and Research, 3(6), 490-495.

Sankaran, S., Mishra, A., Ehsani, R., & Davis, C. (2010). A review of advanced techniques for detecting plant diseases. Computers and Electronics in Agriculture, 72(1), 1-13.

Schrag, T. A., Westhues, M., Schipprack, W., Seifert, F., Thiemann, A., Scholten, S., & Melchinger, A. E. (2018). Beyond genomic prediction: combining different types of omics data can improve prediction of hybrid performance in maize. Genetics, 208(4), 1373-1385.

Shahin, M. A., & Symons, S. J. (2011). Detection of *Fusarium* damaged kernels in Canada Western Red Spring wheat using visible/near-infrared hyperspectral imaging and principal component analysis. Computers and Electronics in Agriculture, 75(1), 107-112.

Suchowilska, E., & Wiwart, M. (2006). Multivariate analysis of image descriptors of common wheat (*Triticum aestivum*) and spelt (*T. spelta*) grain infected by *Fusarium culmorum*. International Agrophysics, 20(4), 345-351.

Van Der Walt, S., Colbert, S. C., & Varoquaux, G. (2011). The NumPy array: a structure for efficient numerical computation. Computing in Science & Engineering, 13(2), 22. https://doi.org/10.1109/MCSE.2011.37.

Van der Walt, S., Schönberger, J. L., Nunez-Iglesias, J., Boulogne, F., Warner, J. D., Yager, N., Gouillart, E. & Yu, T. (2014). scikit-image: image processing in Python. PeerJ, 2, e453. DOI: 10.7717/peerj.453.

Varshney, R. K., Singh, V. K., Hickey, J. M., Xun, X., Marshall, D. F., Wang, J., Edwards, D. & Ribaut, J. M. (2016). Analytical and decision support tools for genomics-assisted breeding. Trends in Plant Science, 21(4), 354-363.

Wiwart, M., Koczowska, I., & Borusiewicz, A. (2001, September). Estimation of *Fusarium* head

blight of triticale using digital image analysis of grain. In International Conference on Computer Analysis of Images and Patterns. Pp. 563-569. Springer, Berlin, Heidelberg.

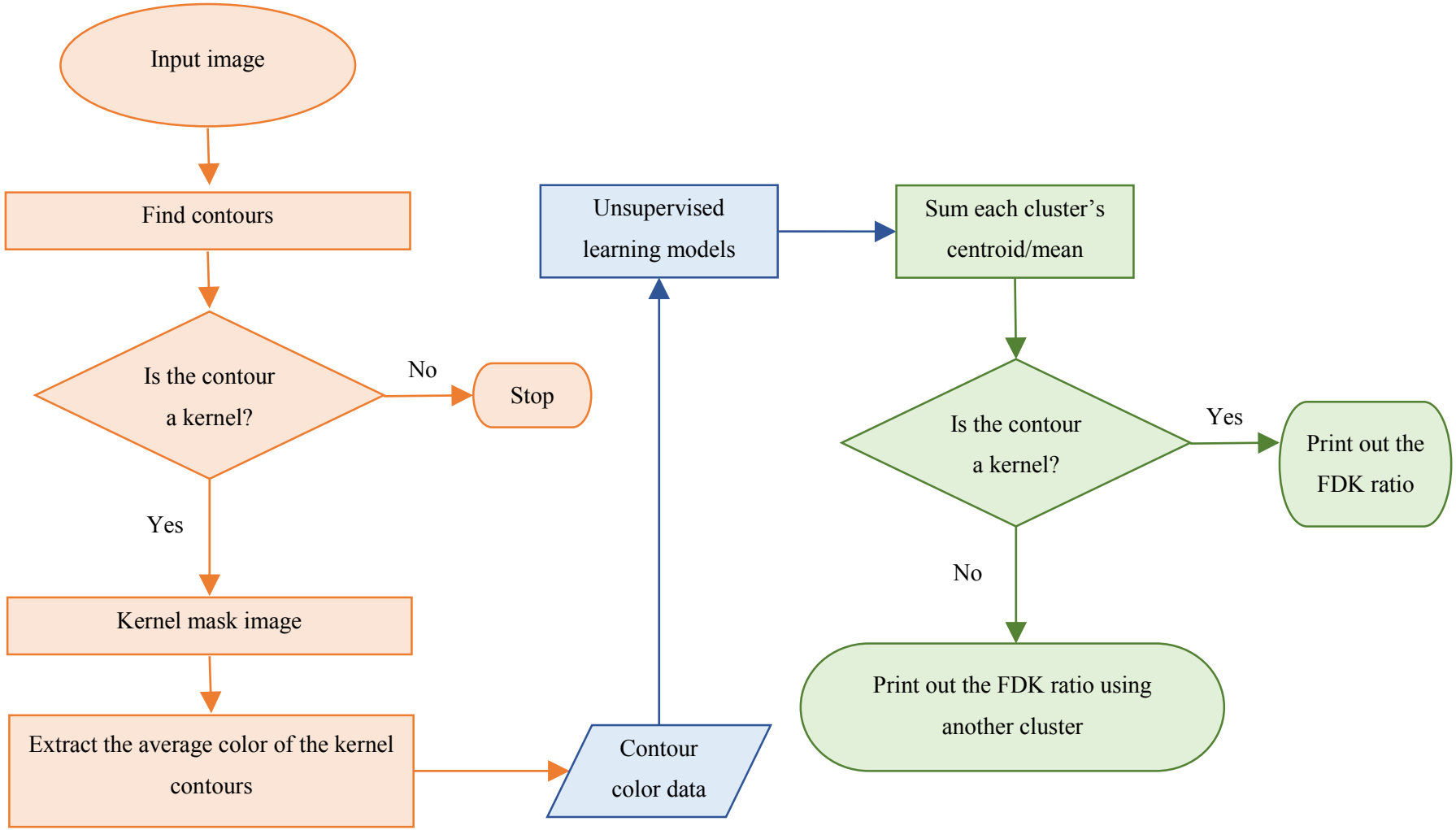

Figure 4.1 The general workflow of the *Fusarium* damaged kernels (FDK) detection algorithm.

This workflow has three main parts: image processing (in red), unsupervised classification (in blue), and *Fusarium* damaged kernels (FDK) ratio calculation (in green).

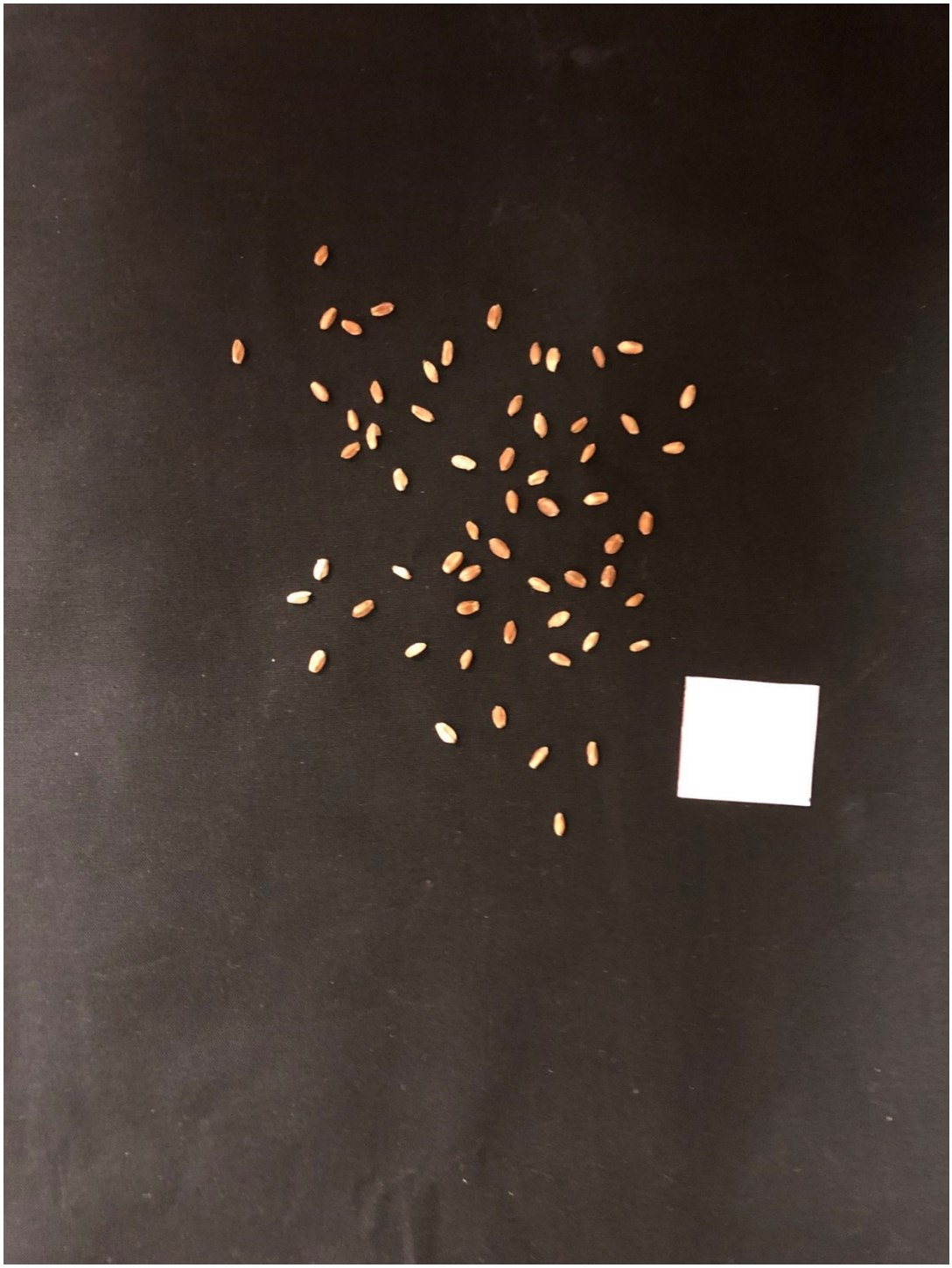

Figure 4.2 The original input picture.

The picture ID is 4404.

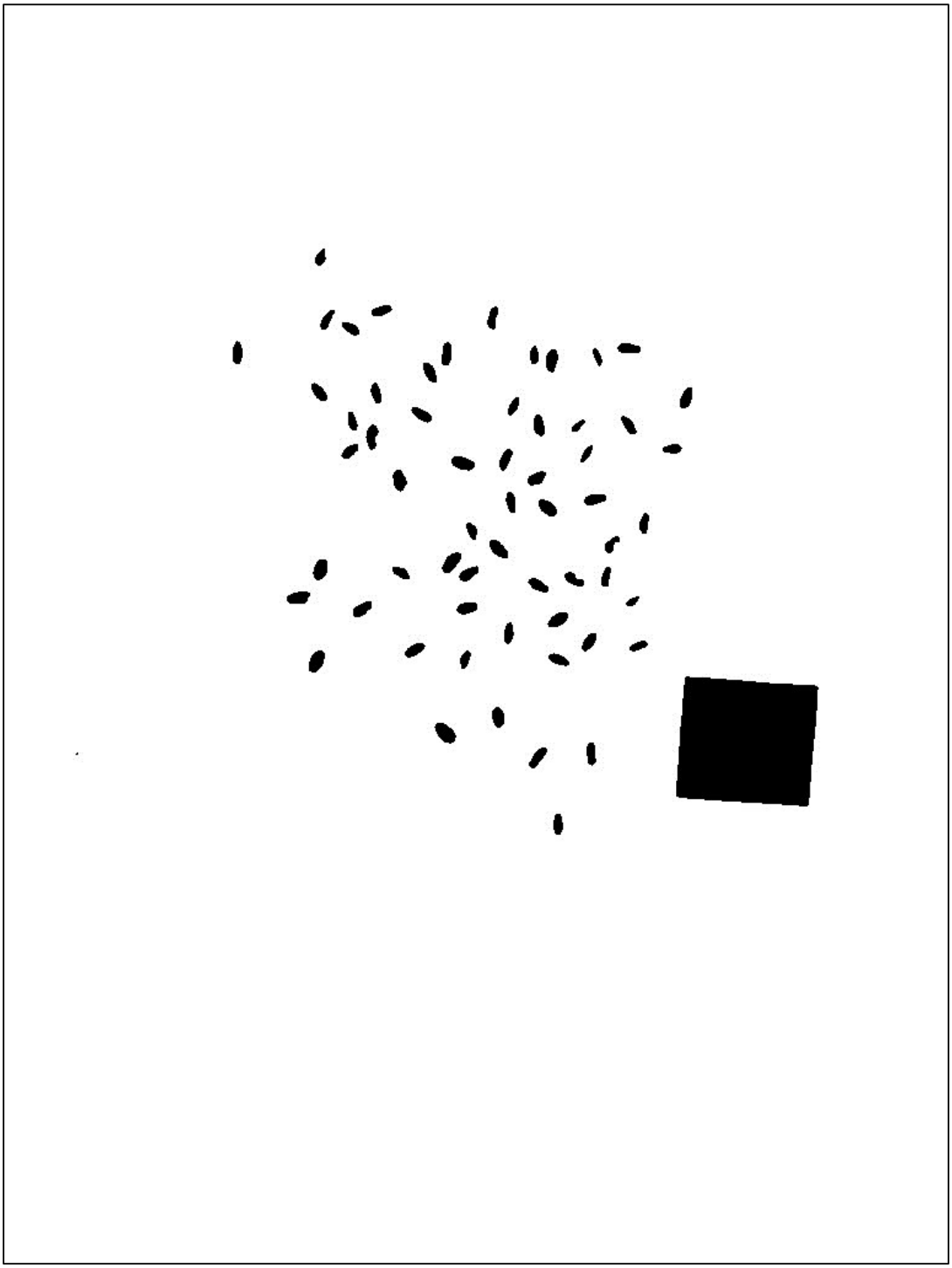

Figure 4.3 The binary picture for finding contours using Otsu's Binarization method. The picture border was added afterward for illustrating the picture boundary. The picture ID is 4404.

Figure 4.4 All the contours found on the picture without the size selection.
The contours were drawn with the green lines. The picture ID is 4404.

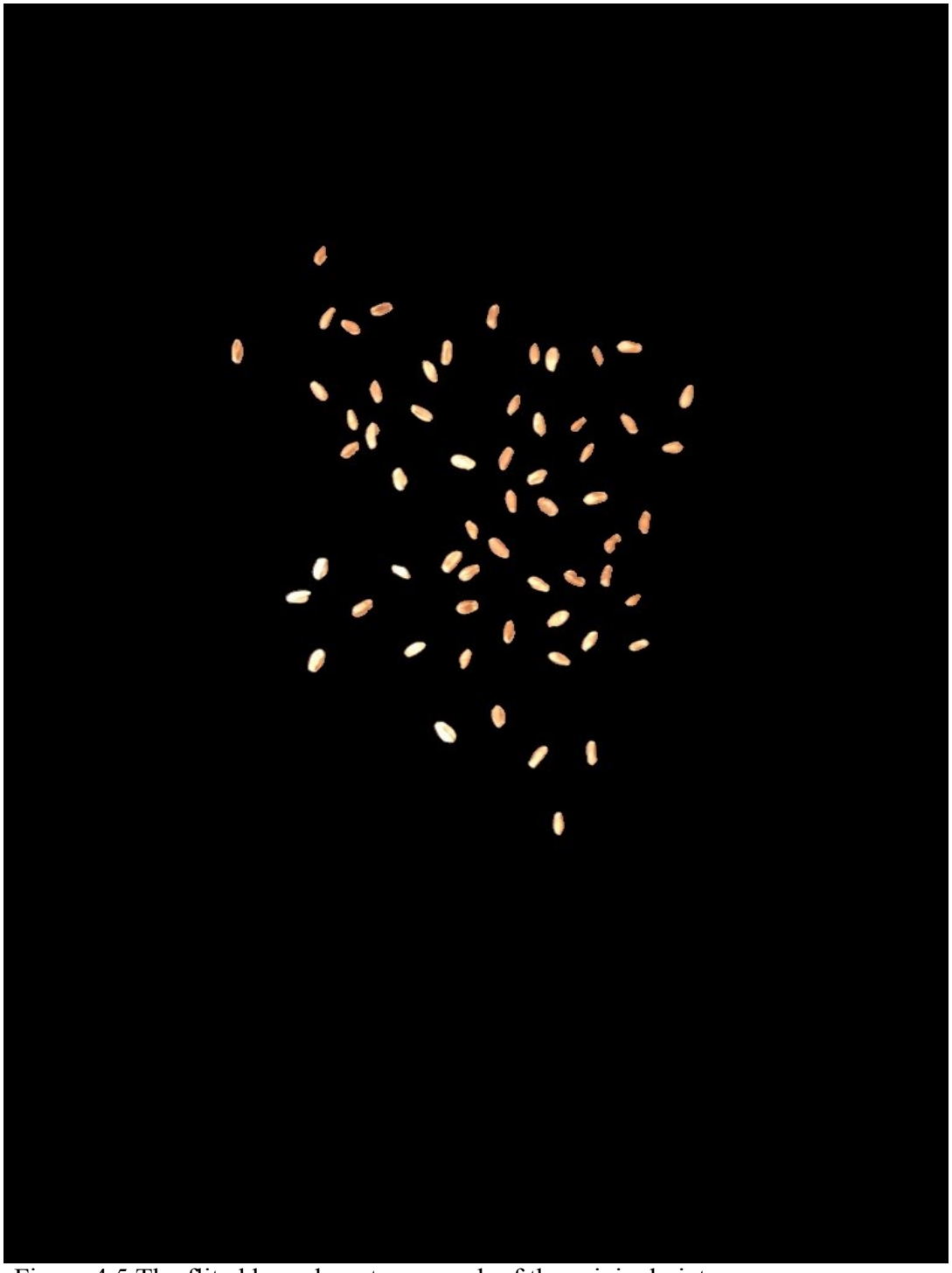

Figure 4.5 The flited kernel contours mask of the original picture.

The picture ID is 4404.

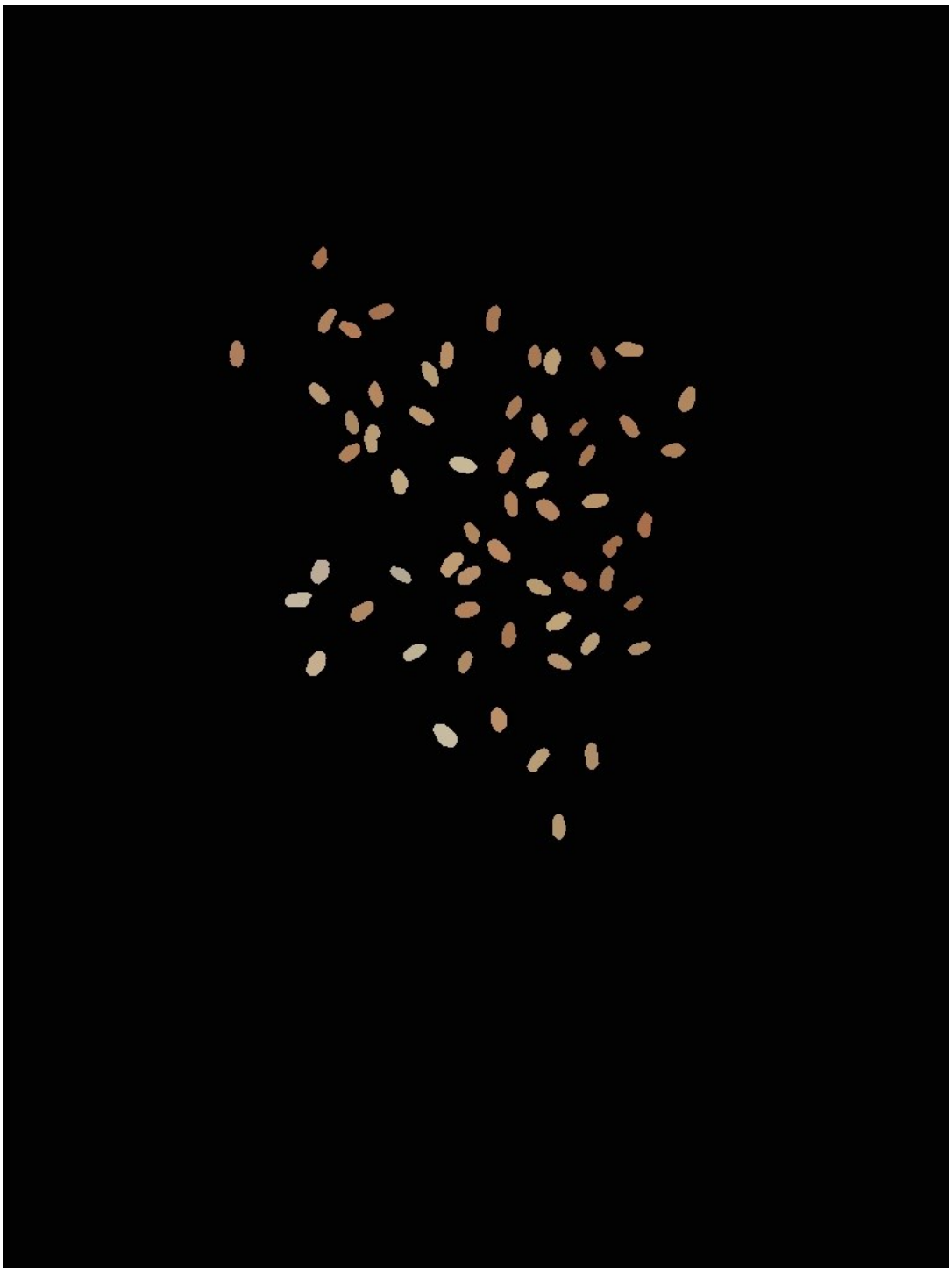

Figure 4.6 The seed contours filed with the average color of the pixels inside the contour. The picture ID is 4404.

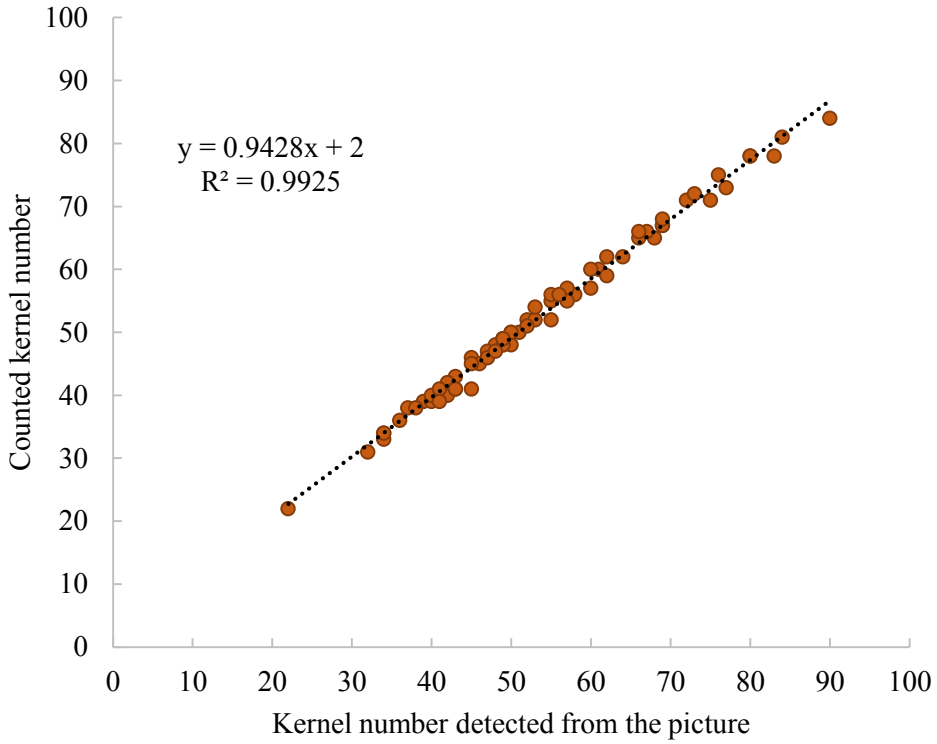

Figure 4.7 The linear regression from the total kernel numbers detected from the pictures and the counted total kernel numbers.

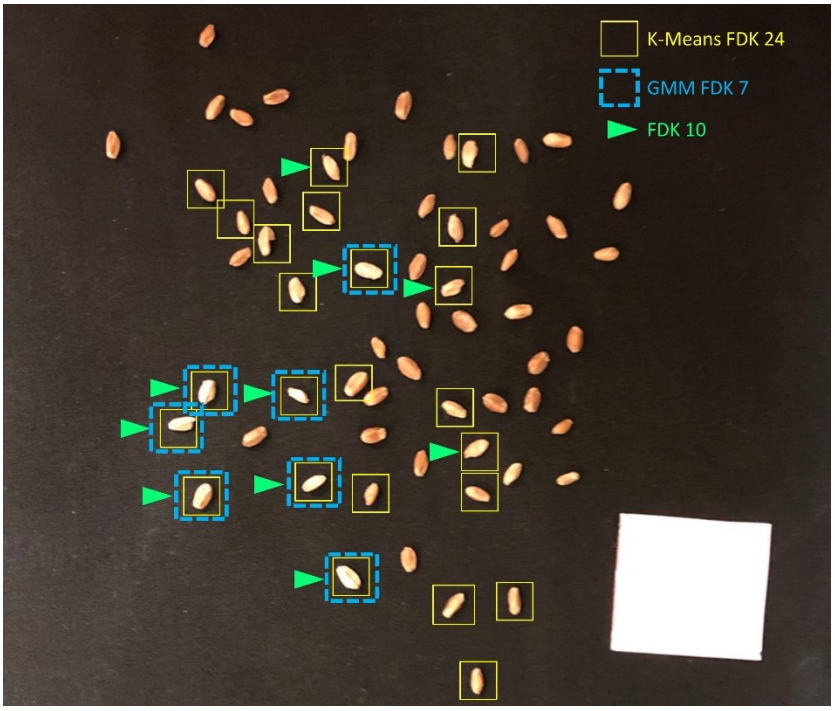

Figure 4.8 The clustering results from K-Means and Gaussian mixture model (GMM) classification and the comparison with the human single kernel classification.

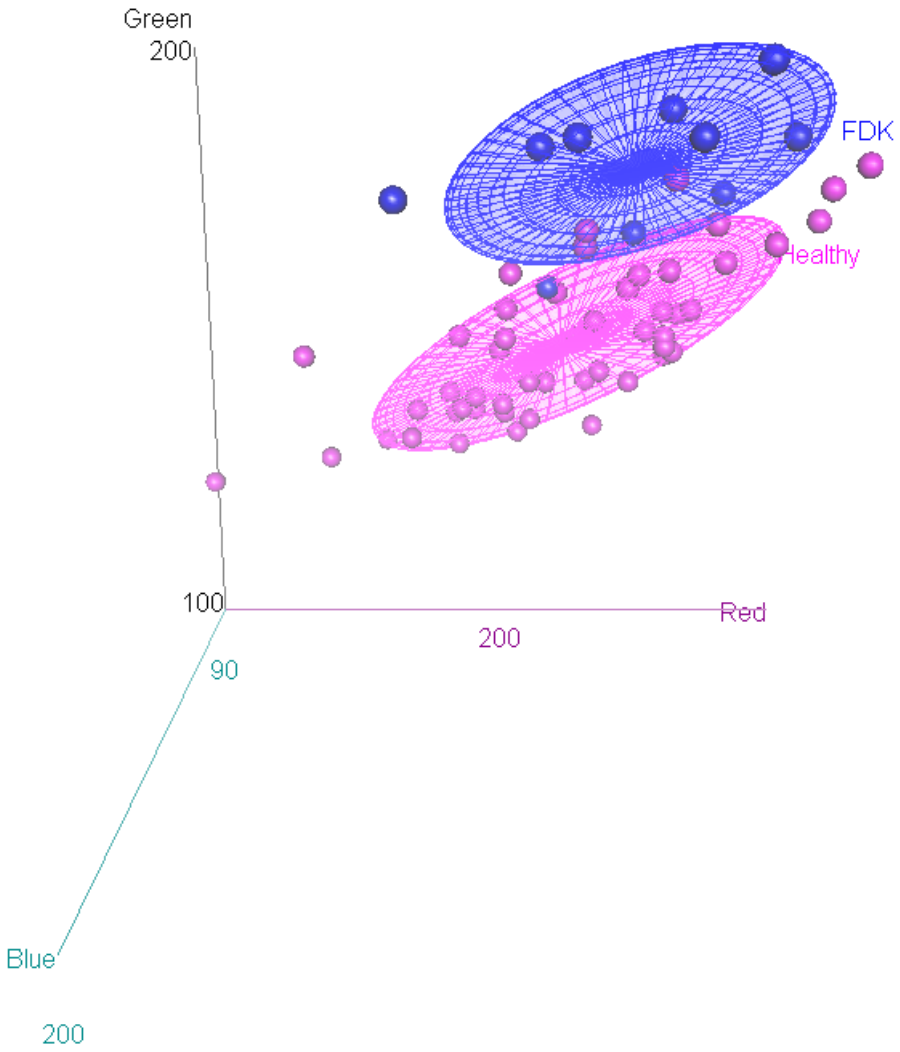

(a) The visually single kernel (ground truth) classification

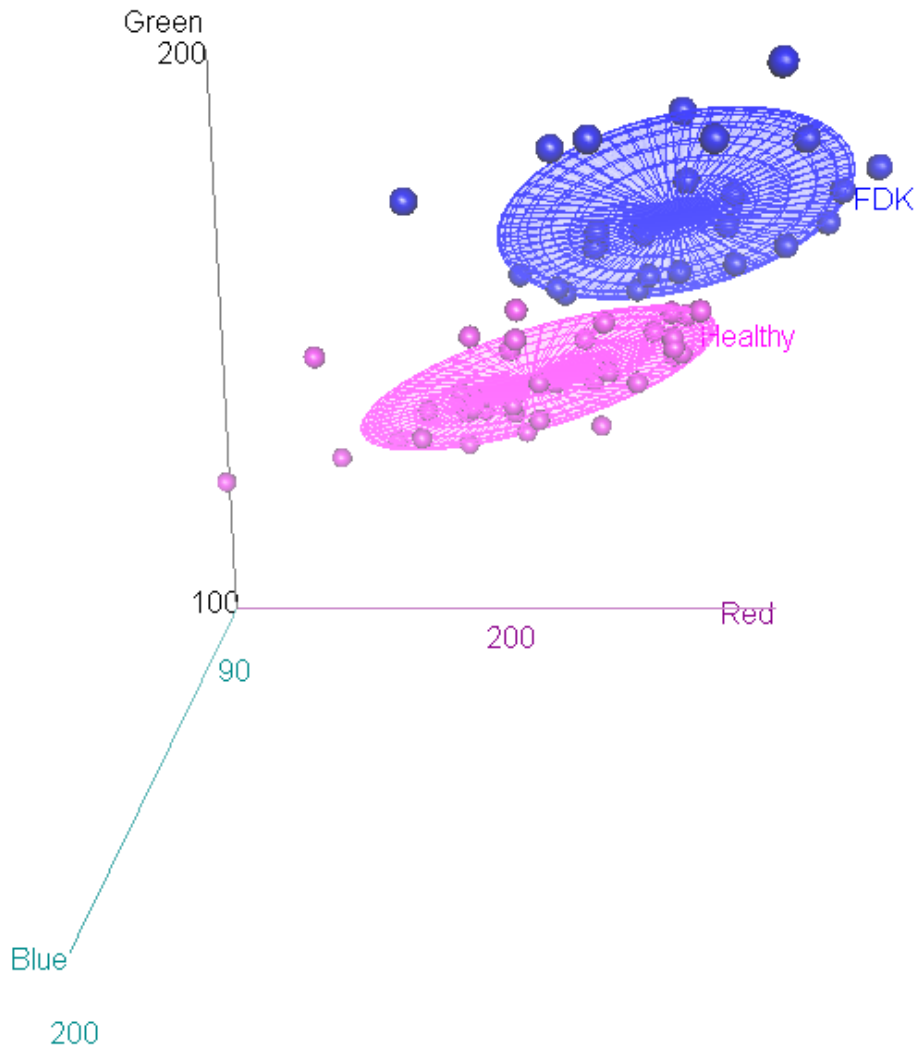

(b) K-Means classification

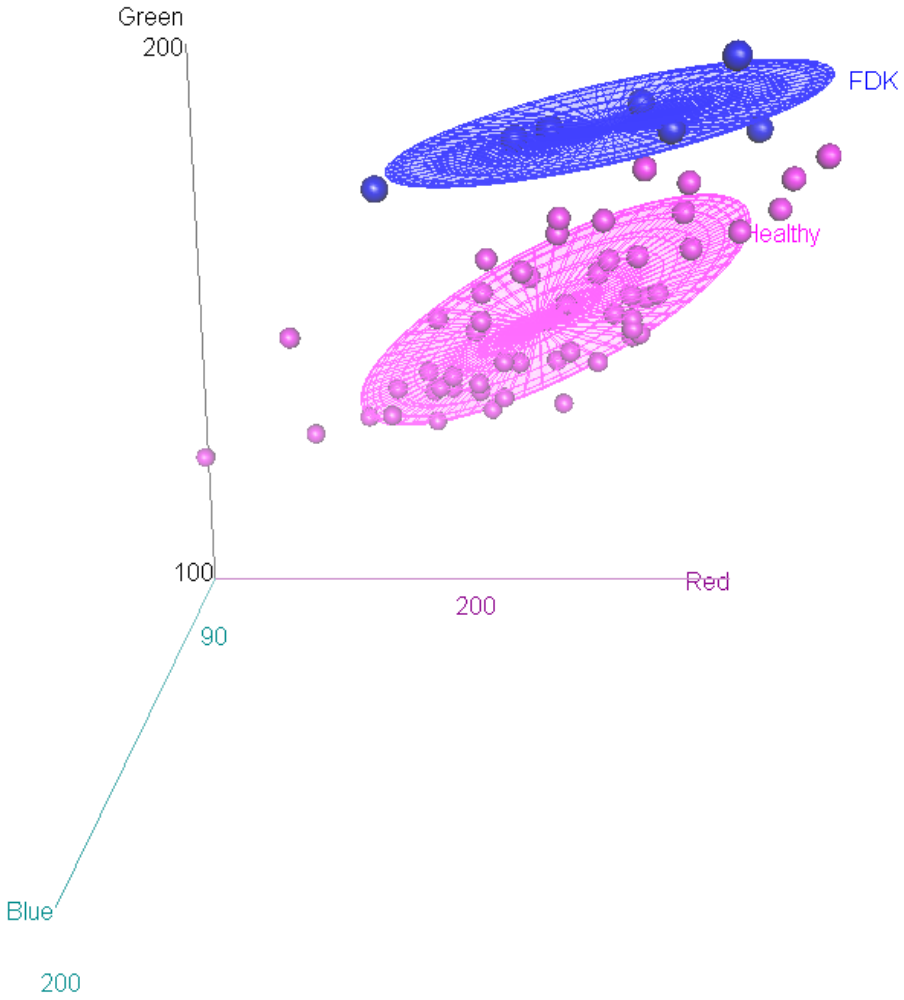

(c) Gaussian mixture model (GMM) classification

Figure 4.9 The classification using the red green blue (RGB) value of the three methods (a) the visually single kernel (b) K-Means (c) Gaussian mixture model (GMM).

Each point represents a kernel on the picture using the average RGB value. The blue points are classified as the *Fusarium* damaged kernels (FDK), while the pink points are the non-FDK, labeled as healthy kernels.

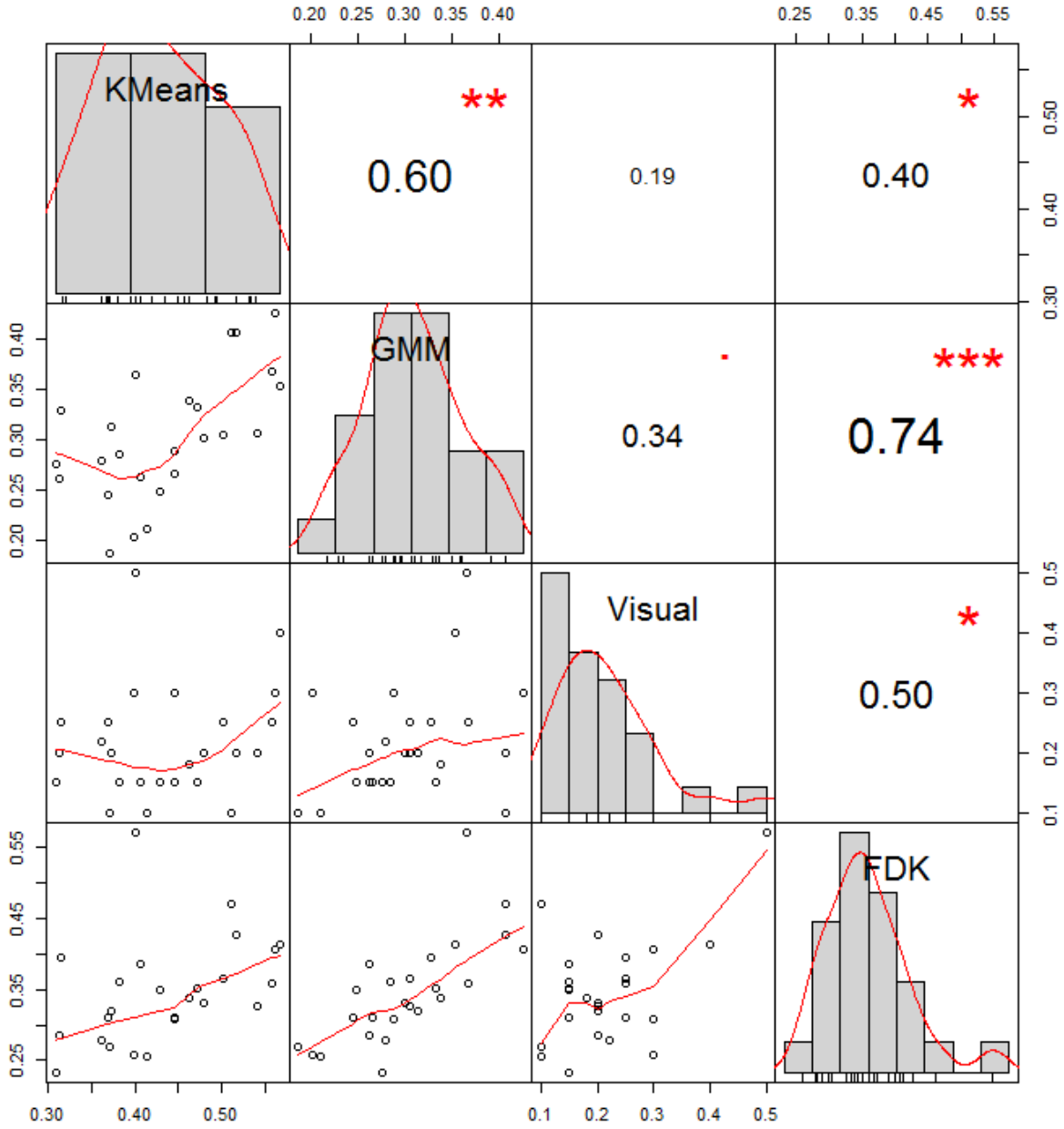

Figure 4.10 The pairwise Pearson correlation between four classification methods.

In the figure, ‘KMeans’ represents for the K-Means classification method; ‘GMM’ is for the Gaussian mixture model clustering; ‘Visual’ is for the visual evaluation methods for many seeds; ‘FDK’ is for the visually single kernel classification method.

Table 4.1 The *Fusarium* damaged kernels (FDK) number and FDK ration results from visually single kernel classification (count) results and K-Means and Gaussian mixture model (GMM) clustering results for each picture.

Picture ID	RIL	Count FDK	Count total	FDK ratio	Picture total	KMeans FDK	KMeans FDK ratio	GMM FDK	GMM FDK ratio
4502	10	15	50	0.30	50	21	0.42	15	0.30
4510	10	16	47	0.34	46	15	0.33	15	0.33
4485	15	13	42	0.31	40	15	0.38	10	0.25
4486	15	14	37	0.38	38	21	0.55	10	0.26
4487	15	18	75	0.24	71	29	0.41	25	0.35
4577	17	23	72	0.32	71	26	0.37	9	0.13
4579	17	13	62	0.21	62	21	0.34	12	0.19
4580	17	19	77	0.25	73	36	0.49	21	0.29
4462	20	30	55	0.55	55	32	0.58	30	0.55
4463	20	13	58	0.22	56	35	0.63	14	0.25
4465	20	15	49	0.31	49	23	0.47	15	0.31
4568	22	8	34	0.24	34	10	0.29	9	0.26
4569	22	14	64	0.22	62	21	0.34	13	0.21
4570	22	12	49	0.24	48	14	0.29	17	0.35
4457	39	14	49	0.29	49	17	0.35	9	0.18
4459	39	15	45	0.33	46	25	0.54	16	0.35
4489	48	13	48	0.27	48	29	0.60	14	0.29
4490	48	23	55	0.42	52	26	0.50	27	0.52
4491	48	22	76	0.29	75	39	0.52	8	0.11
4572	96	19	73	0.26	72	33	0.46	8	0.11
4573	96	19	51	0.37	50	22	0.44	23	0.46
4574	96	25	60	0.42	57	22	0.39	10	0.18
4583	101	29	69	0.42	67	24	0.36	21	0.31
4584	101	35	80	0.44	78	30	0.38	22	0.28
4585	101	24	80	0.30	78	37	0.47	15	0.19
4538	107	12	32	0.38	31	9	0.29	13	0.42
4540	107	15	34	0.44	33	13	0.39	11	0.33
4543	107	16	43	0.37	43	11	0.26	10	0.23
4531	108	23	47	0.49	47	31	0.66	27	0.57
4532	108	9	39	0.23	39	20	0.51	4	0.10
4535	108	23	46	0.50	45	23	0.51	27	0.60
4419	125	15	57	0.26	57	16	0.28	15	0.26
4420	125	15	55	0.27	56	19	0.34	14	0.25
4421	125	7	22	0.32	22	7	0.32	6	0.27
4562	134	14	40	0.35	39	17	0.44	10	0.26
4564	134	21	68	0.31	65	36	0.55	27	0.42

4566	134	22	66	0.33	65	29	0.45	15	0.23
4524	136	13	50	0.26	48	23	0.48	12	0.25
4525	136	24	47	0.51	46	24	0.52	22	0.48
4527	136	12	49	0.24	49	19	0.39	14	0.29
4413	156	27	42	0.64	42	26	0.62	30	0.71
4414	156	18	49	0.37	48	20	0.42	8	0.17
4415	156	20	50	0.40	50	25	0.50	17	0.34
4408	157	18	34	0.53	34	13	0.38	10	0.29
4409	157	35	57	0.61	55	23	0.42	24	0.44
4513	167	12	43	0.28	41	18	0.44	10	0.24
4515	167	19	45	0.42	41	35	0.85	24	0.59
4516	167	30	56	0.54	56	23	0.41	13	0.23
4600	172	32	83	0.39	78	41	0.53	16	0.21
4601	172	33	90	0.37	84	32	0.38	29	0.35
4602	172	18	52	0.35	52	31	0.60	19	0.37
4435	184	20	40	0.50	40	22	0.55	19	0.48
4440	184	15	38	0.39	38	24	0.63	20	0.53
4441	184	16	41	0.39	41	15	0.37	9	0.22
4553	189	10	41	0.24	39	20	0.51	5	0.13
4554	189	8	36	0.22	36	13	0.36	5	0.14
4556	189	16	53	0.30	52	19	0.37	19	0.37
4609	192	14	49	0.29	49	23	0.47	6	0.12
4610	192	10	53	0.19	54	10	0.19	7	0.13
4611	192	28	61	0.46	60	27	0.45	29	0.48
4591	197	33	69	0.48	67	28	0.42	26	0.39
4592	197	20	67	0.30	66	28	0.42	14	0.21
4594	197	19	62	0.31	59	18	0.31	15	0.25
4605	209	12	45	0.27	45	22	0.49	19	0.42
4606	209	14	66	0.21	66	14	0.21	4	0.06
4607	209	17	52	0.33	51	21	0.41	4	0.08
4404	216	10	60	0.17	60	24	0.40	7	0.12
4406	216	27	69	0.39	68	22	0.32	30	0.44
4518	265	35	84	0.42	81	37	0.46	23	0.28
4520	265	14	48	0.29	47	21	0.45	21	0.45
4522	265	15	43	0.35	41	21	0.51	11	0.27

Table 4.2 The confusion matrix and accuracy of each picture from the K-Means and Gaussian mixture model (GMM) clustering methods for *Fusarium* damaged kernels (FDK) classification.

Picture ID	RIL	K-Means					GMM				
		TP*	FP*	FN*	TN*	Accuracy	TP	FP	FN	TN	Accuracy
4502	10	15	6	0	29	0.88	15	0	0	35	1.00
4510	10	15	0	0	31	1.00	15	0	0	31	1.00
4485	15	13	2	0	25	0.95	10	0	1	29	0.98
4486	15	14	7	0	17	0.82	10	0	5	23	0.87
4487	15	18	11	0	42	0.85	18	7	0	46	0.90
4577	17	23	3	0	45	0.96	9	0	13	49	0.82
4579	17	13	8	0	41	0.87	12	0	1	49	0.98
4580	17	19	17	0	37	0.77	19	2	0	52	0.97
4462	20	30	2	0	23	0.96	30	0	0	25	1.00
4463	20	13	22	0	21	0.61	13	1	0	42	0.98
4465	20	15	8	0	26	0.84	15	0	0	34	1.00
4568	22	8	2	0	24	0.94	8	1	0	25	0.97
4569	22	14	7	0	41	0.89	13	0	0	49	1.00
4570	22	12	2	0	34	0.96	12	5	0	31	0.90
4457	39	14	3	0	32	0.94	9	0	5	35	0.90
4459	39	15	10	0	21	0.78	15	1	0	30	0.98
4489	48	13	16	0	19	0.67	13	1	0	34	0.98
4490	48	23	3	0	26	0.94	23	4	0	25	0.92
4491	48	22	17	0	36	0.77	8	0	13	54	0.83
4572	96	19	14	0	39	0.81	8	0	10	54	0.86
4573	96	19	3	0	28	0.94	19	4	0	27	0.92
4574	96	22	0	0	35	1.00	10	0	12	35	0.79
4583	101	24	0	3	40	0.96	21	0	6	40	0.91
4584	101	30	0	3	45	0.96	22	0	11	45	0.86
4585	101	24	13	0	41	0.83	15	0	7	56	0.91
4538	107	9	0	2	20	0.94	12	1	0	18	0.97
4540	107	13	0	1	19	0.97	11	0	3	19	0.91
4543	107	11	0	5	27	0.88	10	0	6	27	0.86
4531	108	23	8	0	16	0.83	23	4	0	20	0.91
4532	108	9	11	0	19	0.72	4	0	5	30	0.87
4535	108	23	0	0	22	1.00	23	4	0	18	0.91
4419	125	15	1	0	41	0.98	15	0	0	42	1.00
4420	125	15	4	0	37	0.93	14	0	2	40	0.96
4421	125	7	0	0	15	1.00	6	0	1	15	0.95
4562	134	14	3	0	22	0.92	10	0	3	26	0.92
4564	134	21	15	0	29	0.77	21	6	0	38	0.91
4566	134	22	7	0	36	0.89	15	0	6	44	0.91

4524	136	13	10	0	25	0.79	12	0	0	36	1.00
4525	136	24	0	0	22	1.00	22	0	1	23	0.98
4527	136	12	7	0	30	0.86	12	2	0	35	0.96
4413	156	26	0	1	15	0.98	27	3	0	12	0.93
4414	156	18	2	0	28	0.96	8	0	9	31	0.81
4415	156	20	5	0	25	0.90	17	0	3	30	0.94
4408	157	13	0	5	16	0.85	10	0	8	16	0.76
4409	157	23	0	10	22	0.82	24	0	9	22	0.84
4513	167	12	6	0	23	0.85	10	0	0	31	1.00
4515	167	19	16	0	6	0.61	19	5	0	17	0.88
4516	167	23	0	7	26	0.88	13	0	17	26	0.70
4600	172	32	9	0	37	0.88	16	0	11	51	0.86
4601	172	32	0	0	52	1.00	29	0	0	55	1.00
4602	172	18	13	0	21	0.75	18	1	0	33	0.98
4435	184	20	2	0	18	0.95	19	0	1	20	0.98
4440	184	15	9	0	14	0.76	15	5	0	18	0.87
4441	184	15	0	1	25	0.98	9	0	7	25	0.83
4553	189	10	10	0	19	0.74	5	0	3	31	0.92
4554	189	8	5	0	23	0.86	5	0	3	28	0.92
4556	189	16	3	0	33	0.94	16	3	0	33	0.94
4609	192	14	9	0	26	0.82	6	0	8	35	0.84
4610	192	10	0	1	43	0.98	7	0	4	43	0.93
4611	192	27	0	0	33	1.00	28	1	0	31	0.98
4591	197	28	0	3	36	0.96	26	0	5	36	0.93
4592	197	20	8	0	38	0.88	14	0	5	47	0.92
4594	197	18	0	0	41	1.00	15	0	1	43	0.98
4605	209	12	10	0	23	0.78	12	7	0	26	0.84
4606	209	14	0	0	52	1.00	4	0	10	52	0.85
4607	209	17	4	0	30	0.92	4	0	12	35	0.76
4404	216	10	14	0	36	0.77	7	0	3	50	0.95
4406	216	22	0	4	42	0.94	27	3	0	38	0.96
4518	265	35	2	0	44	0.98	23	0	9	49	0.89
4520	265	14	7	0	26	0.85	14	7	0	26	0.85
4522	265	15	6	0	20	0.85	11	0	2	28	0.95

*TP: true positive, algorithm rated FDK and single kernel visual rated FDK; TN: true negative, algorithm rated healthy kernel and single kernel visual rated healthy kernel; FP: algorithm rated FDK but single kernel visual rated healthy kernel; FN: algorithm rated healthy kernel but single kernel visual rated FDK.